ON-LINE OPTIMIZATION OF THE TENNESSEE EASTMAN CHALLENGE PROBLEM

by

PHILIP MARSHALL DUVALL, B.S.Ch.E.

A THESIS

IN

CHEMICAL ENGINEERING

Submitted to the Graduate Faculty
of Texas Tech University in
Partial Fulfillment of
the Requirements for
the Degree of

MASTER OF SCIENCE

IN

CHEMICAL ENGINEERING

December, 1996

ACKNOWLEDGMENTS

I would like to thank Dr. J. B. Riggs, chairman of my committee, for his help and guidance through the past few years. His insights into optimization helped guide me through critical parts of my research.

I would also like to thank Dr. R. R. Rhinehart for being on the committee. Dr. Rhinehart has provided me with valuable information on the control aspect of my research.

I would like to thank Dr. N. L. Ricker for his help on implementation of his decentralized control structure to the Tennessee Eastman (TE) process.

I would like to thank my fellow graduate students for their advice on increasing the speed of the optimization algorithm.

I would like to thank the member companies of the Texas Tech Process Control and Optimization Consortium for funding this research.

TABLE OF CONTENTS

LIST OF TABLES

LIST OF FIGURES

NOMENCLATURE

ΔC_p	- Makeup heat capacity model parameter
C_j	- Operating cost for process unit j [$/h]
C_{Mi}	- Cost of component i [$/kgmol]
E_j	- Activation energy for reaction i [cal/gmol]
f_i	- Stripping fraction for component i in Stream 11
F_c	- Flow rate through the compressor [kscm]
F_j	- Molar flow rate for stream j
$F_{j,i}$	- Molar flow rate of component i in stream j
h_j	- Liquid enthalphy for stream j
H_j	- Vapor enthalphy for stream j
k_j	- Pre-exponential constant for reaction j
P_j	- Pressure for process unit j
$P_{j\,i}$	- Partial pressure of component i in stream j
$P_{Vap,i}$	- Vapor pressure for component i
Q_j	- Heat duty for process unit j [Btu/hr]
R_j	- Reaction rate for reaction j
R_{gc}	- Universal gas constant [1.987 cal/gmol/K]
$S_{j,i}$	- Stripping factor for component i in stream j
T_j	- Temperature for process unit j
v_j	- Valve position for stream j [%/100]
V_j	- Vapor volume for process unit j
V_{R_l}	- Liquid volume in the reactor
W_j	- Work for process unit j
$x_{j,i}$	- Mole fraction of component i in stream j

Subscripts

Atm	- Atmosphere
Cmp	- Compressor
Prd	- Product
Prg	- Purge
R	- Reactor
Sep	- Separator
Stm	- Steam
Str	- Stripper
Tot	- Total

Greek Letters

α	- Model parameter for the exponential on component partial pressure in reaction rate
β	- Compressor model parameter
δ	- Linear regression parameter to convert liquid level to liquid volume
ε	- Valve coefficient model parameter
λ	- Latent heat for steam

CHAPTER 1
INTRODUCTION AND LITERATURE SURVEY

At the fall AIChE annual meeting in 1990, Downs and Vogel presented a complex control and optimization problem for continuous chemical processes based on a Tennessee Eastman company recycle reactor process. The abbreviation TE will be used to refer to Tennessee Eastman throughout this thesis. The Tennessee Eastman (TE) process is an open loop unstable process consisting of four process units: an exothermic two-phase reactor, a flash separator, a reboiled stripper, and a recycle compressor. The process is operated either at a fixed production rate or maximum production rate for three different product grades. A number of known and unknown process disturbances affect the feed compositions, feed flows, and reaction properties.

The TE process is open-loop unstable due to the presence of exothermic reactions and a recycle loop. Open loop step tests used for process identification also cause the process to become unstable. Most multivariable process identification techniques require the use of open loop responses. Due to the number of available measurements (41) and manipulated variables (12), a large number of control structures are possible (Banerjee and Arkun, 1995). Thus, a number of control strategies ranging from linear control to nonlinear control to the trendy neural network have been tested on the TE process simulation over the past six years. Testing

the robustness of control strategies was only part of the challenge established by Downs and Vogel in the TE process.

Increased interest in on-line plant operation optimization has been supported by increasing global competition, increasing feed costs, and increasing product quality requirements. However, the field of on-line optimization is relatively new and applications to the TE process have been sparse. This research mainly focuses on the application of steady state, model based, on-line optimization to the TE process.

1.1. Literature Survey on TE Process Control

A number of control strategies have been developed for the TE process. Both decentralized, multi-loop control schemes (i.e., cascaded PI control) and centralized control schemes (MPC) have been successfully applied to the TE control problem. Ricker (1996) used the decentralized approach to apply conventional PI control to the TE process. Decentralized control separates the plant into sub-units with controllers designed for each sub-unit. Ricker used a production rate index in ratio and flow controllers and feedforward/feedback control to maintain production rate and grade even during large feed flow and composition disturbances. Results from the control scheme covered the entire plant operating range for different modes of operation. Disturbance rejection to maintain production rate and grade was robust.

Banerjee and Arkun (1995) applied the theories for identifying good decentralized control configurations to the TE process. While the control design was robust, the design was limited to the base case operation of the TE process. McAvoy and Ye (1994) also applied decentralized PID control to the TE process. The plant-wide control strategy decomposed the control problem into stages based on the relative loop speed. As one proceeded from the inner stages to the outer stages, the speed of the control loops decreased. The flow control loops were the fastest while the product grade and rate loops were the slowest. Unfortunately, McAvoy and Ye (1994) limited the control scheme to the base case for plant operation.

Lyman and Georgakis (1995) proposed four different SISO plant-wide control structures with PID type controllers for the TE process. Three of the control structures were prone to plant shutdown due to high reactor pressure. One structure which used SISO loops and cascade loops was able to meet all of the control objectives established by Downs and Vogel (1993). However, this control structure was not applied to control outside of the base case conditions.

As an outgrowth of the application of nonlinear control techniques to the large-scale processes, Yan and Ricker (1995) applied multi-objective Model Predictive Control (MMPC) to the TE process. The MMPC uses a nonlinear programming goal with multiple control objectives. The MMPC controller was able to tract rapid changes in the production rate versus the slower conventional PI

control loops for the different modes of operation. However, the MMPC control often prone to numerical instabilities in the control algorithm and setpoint off-set, especially when multiple design goals were not attained.

Changes in the reactor temperature and reactor pressure contribute to most of the nonlinearity and instability of the TE process. Kanadibhotla and Riggs (1995) combined a nonlinear process model based reactor temperature controller with conventional SISO control to model the nonlinear behavior of the reactor temperature. A steady state GMC control law was used to control the reactor temperature. Disturbance rejection and setpoint tracking were robust, but Ricker (1996) showed that a conventional PI controller provided similar, robust control for the reactor temperature.

Nonlinear Model Predictive Control (NMPC) has been applied to the TE process by Ricker and Lee (1995a). The NMPC control used a nonlinear, mechanistic, state-variable model. The NMPC controlled eight outputs using eight manipulated variables. Additional SISO loops were required to control the reactor level and reactor pressure when one of the feeds was lost. While the NMPC control results were better than most of the typical SISO application results, the effort required to design the NPMC controller was considerably greater. The control design engineer must balance controller design with controller effectiveness when evaluating linear and nonlinear control strategies.

The use of neural networks for control is an emerging field. A standard backpropagation network was applied to reactor pressure control of the TE process only (Baughman and Liu, 1995). Unfortunately while the control results looked promising, the time and amount of data required to train the network has limited the application of neural networks to the complete plant-wide control of the TE process.

1.2. Literature Survey on TE Optimization

Global competition has been key in spurring interest in on-line optimization of chemical processes. On-line optimization can result in increased plant profit when the following criteria are satisfied (Marlin and Hrymak, 1996).

1. Adjustable optimization variables exist after control priorities have been achieved;
2. Profit changes significantly for changes in the optimization variables;
3. Disturbances occur frequently enough and have a large enough impact on costs to require real-time adjustments;
4. Determining the proper values of the optimization variables is too complex to be achieved using standard operating procedures.

Direct search methods usually are not applicable to complex optimization problems involving multiple optimization variables. For complex optimizations with equality, linear, and/or nonlinear

constraints, a set of optimization methods has evolved (Riggs, 1994).

1. Successive Linear Programming (SLP);
2. Successive Quadratic Programming (SQP);
3. Generalized Reduced Gradient Method (GRG).

SLP converts the nonlinear problem into a linear problem about a starting point. SLP is easy to implement and effective on large problems but suffers from slow convergence when the optima are not on the vertices of constraints. SQP converts the nonlinear problem into a quadratic programming problem. While SQP is the most effective method, SQP is difficult to implement. GRG converts the constrained optimization problem into an unconstrained problem and uses a gradient method to determine the optimal values for the decision variables. GRG is most difficult method to implement. SQP was the optimization method of choice for this research.

Very little work into the application of the above techniques to the on-line optimization of the TE process has been published. Ricker (1995b) determined the optimal operating conditions for the TE process for all six modes of operation. However, Ricker used the full knowledge of the plant states with noise-free measurements, conditions which are never known in practice, to determine the optimal operating conditions. Thus, Ricker's work was used in this research as a benchmark for comparison of the on-line optimization operating conditions to the theoretical, optimal operating conditions.

CHAPTER 2
TE PROCESS DESCRIPTION

At the 1990 AIChE annual meeting in Chicago, Downs and Vogel proposed a industrial control and optimization problem based on a Tennessee Eastman Company process. In 1993, the paper was accepted and published in *Computers and Chemical Engineering*. Even though the process has been simplified and its anonymity protected, the realistic behavior of the dynamics of interest, such as the gas phase dynamics, have been retained in the process simulator. Figure 2.1 is a schematic of the Tennessee Eastman process (Downs and Vogel, 1993).

2.1. Unit Operations

The TE process is open-loop unstable and has five unit operations: a two-phase reactor, a condenser, a vapor/liquid separator, a recycle compressor, and a reboiled stripper. The gaseous reactants, A through E, are fed to the reactor where the reactants undergo irreversible, exothermic, catalytic reactions to form two liquid products, G and H, and one liquid by-product, F. A total of eight components are present in the process. Components A through C are non condensable, and component B is an inert.

Four gas phase reactions occur in the reactor and are catalyzed by a nonvolatile catalyst dissolved in the liquid phase.

(1)	$A_{(g)} + C_{(g)} + D_{(g)} \rightarrow G_{(l)}$	Product 1
(2)	$A_{(g)} + C_{(g)} + E_{(g)} \rightarrow H_{(l)}$	Product 2
(3)	$A_{(g)} + E_{(g)} \rightarrow F_{(l)}$	By-product
(4)	$3D_{(g)} \rightarrow 2F_{(l)}$	By-product

The reaction rates are approximately first-order and are a function of temperature through an Arrhenius expression. The first reaction is more sensitive to temperature due to a higher activation energy.

An internal cooling bundle is used to remove the heat generated from the reactions. The products, due to moderate volatility, are vaporized and leave the reactor with the unreacted gases. The catalyst remains in the reactor. The reactor product stream passes through a cooler and vapor/liquid separator to condense the products. The noncondensed components from the separator are recycled through a centrifugal compressor.

Condensed components from the separator liquid bottom are fed to the stripper. The stripper is used to minimize the loss of D and E in the liquid product. Steam is used to heat the stripper, if necessary. Feed stream 4 is used to remove the remaining reactants from the separator bottom. Liquid products G and H are removed from

the stripper bottom and are separated in a downstream refining section, which is not part of this problem.

The gas overhead from the stripper combines with the compressed overhead from the separator, and the combined stream is recycled back to the reactor feed. The purge is used to prevent buildup of excess reactants, the inert, and the by-product.

2.2. Modes of Operation

Depending on market demand and plant capacity, the process can operate at six different modes based on the mass ratio of G to H in the product and the product rate. Table 2.1 summarizes the six operating modes as defined by Downs and Vogel (1990).

Table 2.1. Modes of Operation for the TE Process

Mode	G/H Mass Ratio	Production Rate (kg/h)
1	50 / 50	14076
2	10 / 90	14076
3	90 / 10	11111
4	50 / 50	Maximum
5	10 / 90	Maximum
6	90 / 10	Maximum

2.3. Control Objectives

The primary objectives for control of the process are to maintain the specified ratio of G/H in the product and maintain the specified product rate during normal operation and process disturbances. The control strategy should also minimize feed flow variability of a

specific frequency content and high frequency valve movement. After disturbances, production rate changes, or product grades changes, the control strategy should recover quickly and smoothly. Low and high alarm violations on process equipment should be kept to a minimum for a given control strategy. The low and high alarm limits for the various process units are listed in Chapter 3.

2.4. Optimization Objectives

An objective function based on operating costs was provided by Downs and Vogel (1990) for optimization. Raw material losses though the purge, product, and by-product side reactions result in high operating costs. Economic costs are determined by summing the costs of raw materials and products in the purge and the costs of raw materials in the product. Costs are also calculated for steam and compressor use. An optimization scheme should be able to determine the optimal operating conditions for the six modes of operation described in section three of this chapter. The optimization cost function is described in more detail in Chapter 3.

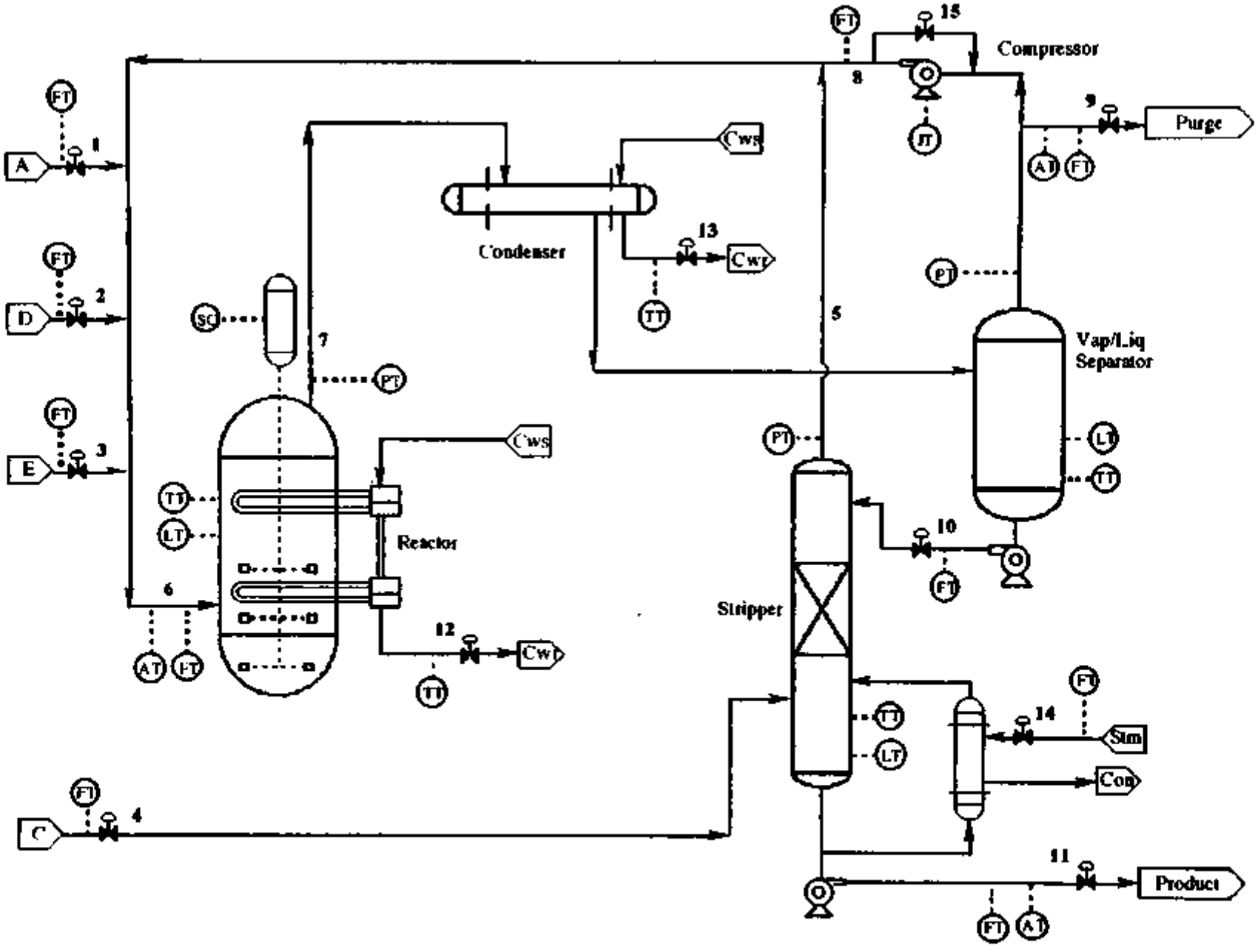

Figure 2.1. TE Process Schematic from Downs and Vogel (1993)

CHAPTER 3
TE PROCESS SIMULATOR DESCRIPTION

The Tennessee Eastman process simulator, a series of FORTRAN subroutines, was presented as a dynamic simulation of an actual process. However, the model represented a compromise between rigor and stiffness due to the gas phase dynamics (Downs and Vogel, 1993). Realistic behavior of the gas phase dynamics has been retained without the system becoming too stiff during integration. Fast dynamics such as transmitter lags were not modeled, but valve lags were included in the model.

The process has 41 measured outputs with Gaussian noise and 12 manipulated variables (11 valves and reactor agitation speed). Three GC analyzers provide delayed measurements of the reactor, purge, and product compositions. Process disturbances, both known and unknown, were also included along with typical control constraints on unit operations. To simplify the model and reduce the stiffness of the dynamic integration, certain process assumptions were used in the process simulator.

3.1. Process Assumptions

The process assumptions used in the simulator as identified by Downs and Vogel (1993) were as follows.

1. The vapors all behave as ideal gases;

2. The pressures are calculated from the Antoine equation where the equation constants have been supplied for components D through H;
3. The vapor/liquid equilibrium follows Raoult's Law;
4. All reactions occur in the vapor phase;
5. Reaction rates are proportional to the vapor volume in the reactor and the partial pressures of each reactant;
6. Components A, B, and C are non condensable while component B is an inert;
7. All reaction rates are approximately first order;
8. All vessels are well mixed with no distributed parameters;
9. All reactions are exothermic, irreversible, and have an Arrhenius dependence on temperature;
10. Flow variables with units such as kscmh or kg/hr are not functions of pressure while flow variables listed as percentage valve position are a function of pressure;
11. While the reactor is agitated, the agitation speed only affects the heat transfer coefficient;
12. The relation between flow through the compressor and inlet-outlet pressure difference follows a typical centrifugal compressor curve;
13. All process measurements include Gaussian noise with a standard deviation typical of the measurement type;
14. An integration step size of one second is sufficient for integration stability.

3.2. Process Constraints

Normal operating constraints as well as shut down constraints have been placed on the reactor, separator, and stripper as shown in Table 3.1.

Table 3.1. Process Operating Constraints

Process Variable	Normal Low Limit	Normal High Limit	Shut Down Low Limit	Shut Down High Limit
Reactor Pressure	none	2895 kPa	none	3000 kPa
Reactor Level	50 % (11.8 m^3)	100 % (21.3 m^3)	2.0 m^3	24.0 m^3
Reactor Temperature	none	150 °C	none	175 °C
Separator Level	30 % (3.3 m^3)	100 % (9.0 m^3)	1.0 m^3	12.0 m^3
Stripper Level	30 % (3.5 m^3)	100 % (6.6 m^3)	1.0 m^3	8.0 m^3

3.3. Process Disturbances

Both known and unknown process disturbances can be introduced at any time into the simulation to test control and optimization schemes. The series of twenty disturbances ranging from steps in stream component compositions to random variations in reaction kinetics can be used separately or simultaneously in the simulator. Table 3.2 lists the disturbances used in the simulator.

Table 3.2. Process Disturbances for the TE Simulation

Number	Process Disturbance	Type
1	A/C Feed Ratio (Stream 4), B Composition Constant	Step
2	B Composition (Stream 4), A/C Ratio Constant	Step
3	D Feed Temperature	Step
4	Reactor Cooling Water Inlet Temperature	Step
5	Condenser Cooling Water Inlet Temperature	Step
6	A Feed Loss (Stream 1)	Step
7	C Header Pressure Loss (Reduced Stream 4)	Step
8	A, B, C Feed Composition (Stream 4)	Random Variation
9	D Feed Temperature (Stream 2)	Random Variation
10	C Feed Temperature (Stream 4)	Random Variation
11	Reactor Cooling Water Inlet Temperature	Random Variation
12	Condenser Cooling Water Inlet Temperature	Random Variation
13	Reaction Kinetics	Slow Drift
14	Reactor Cooling Water Valve	Sticking
15	Condenser Cooling Water Valve	Sticking
16	Unknown	Unknown
17	Unknown	Unknown
18	Unknown	Unknown
19	Unknown	Unknown
20	Unknown	Unknown

3.4. Base Case Description

Downs and Vogel provided a set of steady state material and energy balance data for the process base case operating conditions.

At the base case conditions, the 41 measured outputs were as follows. Table 3.3 lists the base case measurements. For the base case operation, the setpoints for the 12 manipulated variables are listed in Table 3.4.

3.5. Process Operating Costs

Downs and Vogel provided operating cost data for the compressor and steam use as well as reactant and product losses. No cost data was provided for the inert component B. The operating cost data are summarized in Table 3.5. The total operating cost are a summation of the reactant and product losses in the purge, losses of components D to F in the product, steam use, and compressor use.

$$C_{Tot} = C_{Prg} + C_{Prd} + C_{Cmp} + C_{Stm} \tag{4.1}$$

where

$$C_{Prg} = F_9 \sum_{\substack{i=A \\ i=B}}^{H} C_{M,i} x_{9,i} \tag{4.2}$$

$$C_{Prd} = F_{11} \sum_{i=D}^{F} C_{M,i} x_{11,i} \tag{4.3}$$

$$C_{Cmp} = \left(0.0536 \frac{\$}{kW-h}\right) \cdot W_{Cmp} \tag{4.4}$$

$$C_{Stm} = \left(0.0318 \frac{\$}{kg}\right) \cdot F_{Stm} \qquad (4.5)$$

The work of the compressor, W_{Cmp}, is measured variable 20. The stream flow, F_{Stm}, is measured variable 19. At the base case for the simulation provided by Downs and Vogel, the total operating cost of the process was 170.6 \$/h.

Table 3.3. Base Case Measurement Outputs

	Measurements [units]	Base Case
1	A feed [kscmh]	0.251
2	D feed [kg/h]	3664
3	E feed [kg/h]	4509
4	A/C feed [kscmh]	9.35
5	Recycle flow [kscmh]	26.90
6	Reactor feed [kscmh]	42.34
7	Reactor pressure [kPa]	2705
8	Reactor level [%]	75
9	Reactor temp [°C]	120.4
10	Purge rate [kscmh]	0.337
11	Sep temp [°C]	80.1
12	Sep level [%]	50.0
13	Sep press [kPa]	2634
14	Sep underflow [m^3/h]	25.16
15	Stripper level [%]	50.0
16	Stripper press [kPa]	3102
17	Stripper underflow [m^3/h]	22.95
18	Stripper temp [°C]	65.73
19	Steam flow [kg/h]	230.0
20	Comp. work [kW]	341.0
21	Reac. cool temp. [°C]	94.6
22	Cond. cool temp. [°C]	77.3
23	Feed % A [mol%]	32.19
24	Feed % B [mol%]	8.89
25	Feed % C [mol%]	26.38
26	Feed % D [mol%]	6.88
27	Feed % E [mol%]	18.78
28	Feed % F [mol%]	1.66
29	Purge % A [mol%]	32.96
30	Purge % B [mol%]	13.82
31	Purge % C [mol%]	23.98
32	Purge % D [mol%]	1.26
33	Purge % E [mol%]	18.58
34	Purge % F [mol%]	2.26
35	Purge % G [mol%]	4.84
36	Purge % H [mol%]	2.30
37	Prod % D [mol%]	0.02
38	Prod % E [mol%]	0.84
39	Prod % F [mol%]	0.10
40	Prod % G [mol%]	53.72
41	Prod % H [mol%]	43.83

Table 3.4. Base Case Manipulated Variables

	Manipulated Variable [units]	Base Case
1	D Feed [%]	63.053
2	E Feed [%]	53.980
3	A Feed [%]	24.644
4	A+C Feed [%]	61.302
5	Recycle Valve [%]	22.210
6	Purge Valve [%]	40.064
7	Separator Valve [%]	38.100
8	Stripper Valve [%]	46.534
9	Steam Valve [%]	47.446
10	Reactor Coolant [%]	41.106
11	Condenser Coolant [%]	18.113
12	Agitator Speed [%]	50.000

Table 3.5. Process Operating Costs Data

Component	Cost (C_M)	Units
A	2.206	$/kgmol
C	6.177	$/kgmol
D	22.06	$/kgmol
E	14.56	$/kgmol
F	17.89	$/kgmol
G	30.44	$/kgmol
H	22.94	$/kgmol

CHAPTER 4
PROCESS CONTROL STRATEGY

Before model development and optimization were begun on the TE process, the decentralized control scheme proposed by Ricker (1996) was used to stabilize the process. Most of the proposed control strategies from Chapter 1 were able to keep variations in the product grade, product rate, and feed rates within the limits specified by Downs and Vogel for the specified process disturbances. However, the decentralized control scheme proposed by Ricker had one distinct advantage over the other strategies which was ease of implementation.

4.1. Description of Control Strategy

The decentralized control strategy proposed by Ricker partitioned the plant into sub-units for which a cascaded (master to slave) set of PI feedback loops were designed. The design was based around a production-rate control mechanism which was used to control the feed rates, liquid inventory levels, product rate, and product compositions. Only two override loops were required to maintain good process control for all of the process disturbances.

The ratio control for the seven, slave flow controllers used a production rate index, F_p, which has a value of 100% at the base case rate of 23.0 m^3/h (Stream 11). Any changes in setpoint for production rate, F_p, were converted to ramps with a maximum ramp

rate of ±30% in 24 hours. A feedback loop was used to trim F_D to remove steady state offset in the Stream 11 production rate. The feedback loop was disabled when the production rate was constrained (i.e., Modes 4 to 6 or during Disturbance 6).

Inventory control loops were used to control the reactor, separator, and stripper liquid level. By coordinating the levels in the separator and stripper, changes in production rate (Stream 11) were reduced. Variations in Stream 10 only caused minor changes in production rate which allowed for coordination of the stripper and separator levels. The condenser valve and separator temperature were used to control the reactor liquid level. Reactor pressure control was achieved by manipulating the purge valve. Using the purge for reactor pressure control, which represents a major dominating effect on the operating costs, tended to minimize the purge operating cost automatically.

Control of the %G in the product (i.e., the product grade) was achieved using a feedforward/feedback scheme in combination with the production rate control. This combination maintained the correct product grade without upsetting the production rate. If the measurement of %G in the product is too high, the feed rate of D is decreased while the feed rate of E is increased to minimize production rate upsets. The feedback was de-tuned to minimize interactions with the other control loops. However because limits on the allowed rate of change of D and E feed streams were established

by Downs and Vogel (1993), rate of change of %G during setpoint changes was limited to ±50 mol% in 24 hours.

Control of the chemical inventories of the eight components, A to H, was important to prevent the buildup of excess reactants, inert, or by-product. Component B, the inert, was self-regulated through the reactor pressure control loop. The reactor temperature was manipulated to control the by-product F. Higher reactor temperatures favor product G and the formation of the by-product. Thus, Ricker (1995b) suggested that the reactor temperature be controlled between 120-130 °C to minimize the formation of the by-product F. The reactor pressure control loop also helped to automatically regulate the buildup of the by-product in the system. Components G and H are self-regulated through the inventory control loops.

Reactants A to E are recycled in the process to increase conversion rates. The pressure control loop automatically regulated a buildup of the reactants in the process. Ricker proposed to keep reactants A and C in excess in the process so that reactants D and E were always the limiting reactants. The production rate in the process would then be maximized by increasing the use of D or E until a flow constraint on D or E was reached. If arbitrary rates were set to keep excess A and C in the process, the reactants would be self-regulated through the pressure control loop. However, purge operating costs would not be minimized. Ricker used two discrete PI control loops to keep the partial pressures of A and C in the reactor

high enough to maintain D and E as the limiting reactants without causing a large increase in purge operating costs.

A reactor pressure override and reactor level override were included in the control strategy. When the purge valve saturated on the reactor control loop, the production rate, F_p, was decreased which would proportionally decrease the feed rates and would lower the reactor pressure. When the condenser valve saturated on the reactor level control loop, the compressor recycle valve position would be changed. A persistent high reactor liquid level would result in an increase in the recycle valve position (increasing the recycle flow) which would decrease the reactor liquid level. A persistent low reactor liquid level would result in a decrease in the recycle valve position which would increase the reactor liquid level.

Using this control strategy, Ricker obtained excellent control results for the TE process for the first three modes of operation. During disturbances such as loss of A feed, the control scheme was able to maintain initially a higher production rate than other proposed control schemes. Disturbances such as feed compositions variations, drifts in reaction kinetics, or loss of analyzers had minimal, if any, effect on the production rate, product grade, or feed rates.

4.2. Proposed Changes to the Ricker Control Scheme

The control scheme proposed by Ricker (1996) was easy to implement and provided good control of the process over the range of

plant operations. Only one gain and integral time per control loop were required to control the process at the three different modes of operation. Ricker did not suggest the use of gain scheduling for the control loops when operating at different product grades.

Unfortunately, decentralized control schemes have tended to show poor control performance due to the interactions of different control loops. The proposed scheme by Ricker also has problems with control loop interactions. For example when a sudden change in reactor level was corrected by the level control loop, a sudden change in reactor pressure occurred. Changes in the purge valve position to control the reactor pressure resulted in changes in separator and stripper pressure. The changes in separator pressure and stripper pressure caused level oscillations in the separator and stripper which would cause undesired product rate changes and feed rate changes. The control strategy by Ricker tried to remove the interactions between flow control loops by detuning (i.e., overdamped responses) these loops and using maximum rate of change ramps on product grade and product rate changes.

Detuning the flow control loops removed some of the control loop interactions. However, the maximum rate of change ramps limited how fast the process was changed from one product grade to another product grade as well as how fast the production rate was maximized. No information was provided by Downs and Vogel on the frequency of product grade and product rate changes. However in most process operations, steady state operation is desired, and slow

product rate/grade changes result in unsteady state conditions. Various changes in the Ricker control scheme to decrease product grade and product rate ramp times were investigated.

4.2.1. Gain Scheduling for Control Loops

The maximum rate of change ramps provided by Ricker were very conservative to keep control loop interactions to a minimum, especially in the flow control loops. Initially, the product grade and product rate maximum ramp rates were increased until either the product flow or feed flows violated a variability constraint as established by Downs and Vogel (1993). From this test, the new maximum ramp rate for the production rate changes was set as 30% in 16 hours. The new rate for the product grade changes was set as 50% in 16 hours. Thus without modifying the control scheme, the times required for rate and grade changes were decreased by eight hours (i.e., rates were conservative to begin with). To further reduce the ramp times, a reduction in the variability of the feed stream control was required. Fast changes in product grade tended to result in high flow rate variability in Streams 1 and 4.

Process control problems usually require on-line tuning of the controller settings (i.e., gain and integral time) to maintain good process control (Seborg et al., 1989). Depending on the frequency of the re-tuning, an adaptive control system can be implemented to adjust controller parameters for changing process conditions. Two common situations requiring adaptive control are

1. Unknown process changes;
2. Known or anticipated process changes.

Known process changes are an easier problem for designing an adaptive control system (Seborg et al., 1989). In the case of the TE process (excluding disturbances), the product grade and product rate changes are known process changes.

One of the simplest forms of an adaptive control system implementation is the ramped, gain scheduling technique. Controller gain and integral time are calculated for different process conditions. As the process is ramped to the new process conditions, the controller gain and integral time are ramped to the new controller values. Gain scheduling was applied to the control scheme proposed by Ricker.

From the 50/50 base case steady state conditions, 10/90 and 90/10 base case startup, steady state conditions were determined. From the base case, the %G in the product was decreased for the 10/90 and increased for the 90/10 product grades. The process was lined out at steady state, and the steady state process conditions determined by storing the state and manipulated variable vectors from the TE simulation. The TE process simulation was then used to converge the derivatives of the states to zero as suggested by Downs and Vogel (1993).

At the 50/50 base case, Ricker tuned the flow control loops for slightly overdamped responses for the slave control loops and slightly underdamped responses for the master control loops.

However, these controller gain and integral times gave very different responses at 10/90 and 90/10 base cases ranging from approximately quarter damped to severely overdamped. Using step changes in the various flow control loops at the 10/90 and 90/10 product grades, the flow controllers were retuned to have responses similar to the 50/50 controller tuning. Table 4.1 shows the new controller gain and integral time used at the three different modes of operation. The other control loops were not re-tuned.

Table 4.1. Modified Controller Gains and Integral Times

Loop	50 / 50		10 / 90		90 / 10	
	Gain	Integral Time [min]	Gain	Integral Time [min]	Gain	Integral Time [min]
1	0.01	0.001	0.02	0.001	0.01	0.001
3	1.8×10^{-6}	0.001	1.8×10^{-6}	0.001	1.4×10^{-4}	0.001
4	0.002	0.001	0.002	0.001	0.001	0.001
14	1.4×10^{-4}	120.0	1.0×10^{-4}	100.0	1.0×10^{-4}	100.0
15	4.5×10^{-4}	100.0	2.0×10^{-4}	120.0	4.5×10^{-4}	110.0

Gain scheduling was used to update the control loops in Table 4.1 during product grade changes. The ramp times for gain scheduling were synchronized with the ramp times required to move the process from one product grade to another. The maximum ramp rates for product grade and product rate changes were recalculated with the controller gain scheduling implemented. The new maximum rate

of change ramp for product rate changes was set to 30% in 14 hours while the new rate of change ramp for product grade changes was set to 50% in 14 hours. The two hour decrease in production rate and grade change times was significant enough to show importance of consistent, good flow control loop tuning.

4.2.2. Decoupling Product Grade Changes

The new controller tuning parameters removed some of the variability in Stream 4, which was associated with product grade changes. During product grade changes, Stream 1 (A feed) flow rate would often deviate by ±5% before returning back to setpoint, even with the slower product grade ramp rates. A temporary decrease in the amount of A entering the reactor during product grade changes was responsible for the temporary increase in Stream 1 flow rate. Regardless of the mode of operation during normal operation, Ricker (1995b) has shown that the feed to the reactor should remain 50% A+C and 50% D+E with A making up 50% of the A+C feed.

The interaction (coupling) of the control loops was creating an undesired, temporary flow deviation in Stream 1 during the product grade change. Thus, a decoupler was developed to remove the interaction of the product grade change ($\hat{G}$ the Laplace transformed - in deviation variables) and the Stream 1 flow rate ($\hat{v}_3$ the Laplace transform - in deviation variables).

$$\hat{v}_3 = D \cdot \hat{G} \tag{4.1}$$

where $\hat{v}_3$ was added to the Loop 1 control action during product grade changes. The final form of the Laplace transfer function of the decoupler, D, was

$$D = -K \cdot s \cdot \frac{(\tau_{lead} s + 1)}{(\tau_{lag} s + 1)} \qquad (4.2)$$

where K is the gain, τ_{lead} is the lead time, and τ_{lag} is the lag time. The gain, lead time, and lag time were calculated from open loop responses on the amount of A and C entering the reactor due to changes in product grade and Stream 1 valve position.

$$K = -4.78 \times 10^{-2} \ \frac{\%}{\%G}$$

$$\tau_{lead} = 780 \ \text{min}$$

$$\tau_{lag} = 90 \ \text{min}$$

Equations 4.1 and 4.2 were used to determine the change required in the control valve position for Loop 1 (Ricker's scheme) to off-set the changes due to product grade changes. Unfortunately, the use of the decoupler during product grade changes resulted in amplification of the Stream 1 flow deviations due to process-model mismatch. Even with changes to the decoupler model and detuning of the decoupler, the flow deviations in Stream 1 could not be reduced. A seemingly good idea, the decoupler was eventually removed from the control scheme used in this work.

CHAPTER 5
STEADY STATE PROCESS MODEL DESCRIPTION

Model based optimization was chosen for this process because the process involved a number of optimization variables for a highly interactive process (Forbes and Marlin, 1996). To perform a steady state, model based, on-line optimization analysis of the TE process, a steady state model of the process had to be developed. The complex, dynamic, simulation model provided by Downs and Vogel (1993) could not be used as the optimization model because the simulation model was supposed to represent the actual process. The simulation model was treated as a black-box function which could only be used to obtain process measurements for different process operating conditions.

The steady state model should accurately reflect the steady state conditions and operating costs of the process over the six modes of operation. Complex steady state models may provide highly accurate representations of the process but suffer in the computational time required to converge the model for different operating conditions in the plant. A simple steady state model may provide an accurate representation of the process without the computational overhead. In either case, the model can be used in an optimization routine to determine the optimal operating conditions for the process over the six modes of operation. Simplified steady state models which accurately describe the plant conditions at the six different modes

of operation were developed for the reactor, separator, stripper, and compressor. The abbreviation SS will be used throughout the thesis to represent the term steady state.

5.1. SS Reactor Model

The feeds to the reactor consist of five, well-mixed streams: Stream 1, Stream 2, Stream 3, Stream 5, and Stream 8. Streams 1, 2, and 3 are nearly pure A, D, E, respectively, with a small amount of inert B. Stream 5 is the overhead from the stripper, and Stream 8 is the recycle stream from the separator overhead. The product stream, Stream 7, from the reactor is a gas phase flow containing all eight components. A cooling bundle is present in the reactor to remove excess heat generated by the four exothermic reactions. The agitator insures a well-mixed reactor but only affects the heat transfer coefficients in the reactor in the process simulation.

The steady state model of the reactor consists of eight component molar flow, material balances and four reaction rate equations. Previous work by Kanadibholta and Riggs (1995) established the functional form of the material balances as

$$0 = F_6 x_{6,A} - F_7 x_{7,A} - R_1 - R_2 - R_3 \tag{5.1}$$

$$0 = F_6 x_{6,B} - F_7 x_{7,B} \tag{5.2}$$

$$0 = F_6 x_{6,C} - F_7 x_{7,C} - R_1 - R_2 \tag{5.3}$$

$$0 = F_6x_{6,D} - F_7x_{7,D} - R_1 - 1.5R_4 \tag{5.4}$$

$$0 = F_6x_{6,E} - F_7x_{7,E} - R_2 - R_3 \tag{5.5}$$

$$0 = F_6x_{6,F} - F_7x_{7,F} + R_3 + R_4 \tag{5.6}$$

$$0 = F_6x_{6,G} - F_7x_{7,G} + R_1 \tag{5.7}$$

$$0 = F_6x_{6,H} - F_7x_{7,H} + R_2 \tag{5.8}$$

where the reaction rates are in units of lbmol/hr. From the process assumptions, the reaction rates are known to be functions of temperature, reactant partial pressures, and reactor gas volume. The Arrhenius expression provides the relationship between the reaction rates and temperature. The four reaction rates for the process were modeled as follows (Kanadibholta and Riggs, 1995).

$$R_1 = e^{\left(k_1 - \frac{E_1}{R_{gc}T_R}\right)} V_R P_{7,A}^{\alpha_1} P_{7,C}^{\alpha_2} P_{7,D}^{\alpha_3} \tag{5.9}$$

$$R_2 = e^{\left(k_2 - \frac{E_2}{R_{gc}T_R}\right)} V_R P_{7,A}^{\alpha_4} P_{7,C}^{\alpha_5} P_{7,E}^{\alpha_6} \tag{5.10}$$

$$R_3 = e^{\left(k_3 - \frac{E_3}{R_{gc}T_R}\right)} V_R P_{7,A}^{\alpha_7} P_{7,E}^{\alpha_8} \tag{5.11}$$

$$R_4 = e^{\left(k_4 - \frac{E_4}{R_{gc} T_R}\right)} V_R P_{7,A}^{a_9} P_{7,D}^{a_{10}} \qquad (5.12)$$

The reaction volume, V_R, is the gas phase volume in the reactor in ft^3. The reactor temperature, T_R, has units of Kelvin while the partial pressures units are absolute Torr.

The reaction volume can be calculated by subtracting the volume of liquid in the reactor from the total volume of the reactor, 1300 ft^3.

$$V_R = 1300 - V_{R_l} \qquad (5.13)$$

The partial pressures of the components A to H in the gas phase are related to the total pressure (in absolute Torr) in the reactor and molar compositions of each component in Stream 7 as follows.

$$P_{7,i} = x_{7,i} P_R \qquad (i = A...H) \qquad (5.14)$$

The products from the reactor pass through a partial condenser, which was not modeled, and then to the vapor/liquid separator. No pressure drop losses due to friction in the pipes or in the condenser were model for the reactor product flow to the separator. Also, the effects of the agitator speed on reactor heat transfer coefficients were not model.

5.2. SS Separator Model

The separator was model as a single stage flash of the reactor product, Stream 7, into a vapor flow, Stream 10, and liquid flow, Stream (8+9). For a given flash temperature and pressure, the feed to the separator must have a set enthalpy. The partial condenser is used to remove any excess heat in the reactor products prior to the flash separation. The eight component material balances for the separator model were derived as follows.

$$0 = x_{7,i}F_7 - x_{89,i}F_{89} - x_{10,i}F_{10} \qquad (i = A...H) \qquad (5.15)$$

Since components A through C are non condensable, the molar compositions of these components in Stream 10 are zero.

$$x_{10,i} = 0 \qquad (i = A...C) \qquad (5.16)$$

Using Raoult's Law the molar compositions of components D to H in Stream 10 can be calculated as

$$x_{10,i} = x_{89,i}\frac{P_{Sep}}{P_{Vap,i}} \qquad (i = D...H) \qquad (5.17)$$

where the vapor pressures in units of absolute Pa for components D through H are calculated using the Antoine equation with coefficients supplied by Downs and Vogel (1993). The units on separator pressure are also in absolute Pa.

$$P_{Vap,i} = e^{\left(A_i + \frac{B_i}{C_i + T}\right)} \qquad (i = D...H) \qquad (5.18)$$

The temperature in Equation 5.18 is the separator temperature, T_{Sep}, in °C.

After the flash separation, the vapor flow is recycled back to the front of the plant to reuse the unreacted reactants. A purge stream prevents an excess buildup of the inert component, B, and the by-product, F. The liquid flow from the separator is pumped to the stripper for further removal of the reactants A through E and the by-product, F. No model was included for temperature and/or pressure changes in the separator underflow when passed through a pump.

5.3. SS Compressor Model

The compressor is used to increase the pressure of the recycled overhead from the separator to the pressure of the overhead stream from the stripper. An accurate compressor model is required due to the inclusion of compressor work in the optimization objective function. Ideally for a isentropic compression, the work done by the compressor, $W_{Com,isen}$, is

$$W_{Com,isen} = C_p(T_{out} - T_{in})F_{Com} \qquad (5.19)$$

where C_p is the heat capacity of the stream being compressed, F_C is the flow rate of the stream through the compressor, T_{in} is the inlet

temperature of the stream to the compressor, and T_{out} is the outlet temperature of the stream from the compressor. For an isentropic compression, the inlet temperature and outlet temperature are related to inlet and outlet pressures as follows (Smith and Van Ness, 1987).

$$T_{out} = T_{in}\left(\frac{P_{out}}{P_{in}}\right)^{\frac{R}{C_p}} \tag{5.20}$$

where P_{out} is the outlet pressure, P_{in} is the inlet pressure, and R is the universal gas constant.

Since compressors are not 100% efficient, the actual work, W_{Com}, done by the compressor is determined as

$$W_{Com} = \frac{W_{Com,isen}}{\eta_{eff}} \tag{5.21}$$

where η_{eff} is the compressor efficiency. Combining Equations 5.19 to 5.21 results in the compressor model relationship of actual work to pressure changes.

$$W_{Com} = eff \cdot C_p T_{in} F_{Com}\left[\left(\frac{P_{out}}{P_{in}}\right)^{\frac{R}{C_p}} - 1\right] \tag{5.22}$$

Since the efficiency of the compressor is unknown and good heat capacity data is unavailable, model parameters are used to replace these variables.

$$W_{Com} = \beta_1 T_{in} F_{Com} \left[\left(\frac{P_{out}}{P_{in}} \right)^{\beta_2} - 1 \right] \tag{5.23}$$

From Bernoulli's equation for flow, the flow through the compressor, F_{Com}, can be related to the recycle stream, Stream 8, and the recycle valve stream, Stream 15.

$$F_{Com} = F_8 + v_{15} \beta_6 \sqrt{P_{out} - P_{in}} \tag{5.24}$$

Combining Equations 5.23 and 5.24 with substitutions of variables for the process streams into and out of the compressor, the final form of the relationship between compressor work and pressure changes was determined.

$$W_{Com} = \beta_1 T_{Sep} F_{Com} \left[\left(\frac{P_{Str}}{P_{Sep}} \right)^{\beta_2} - 1 \right] \tag{5.25}$$

where

$$F_{Com} = F_8 + v_{15} \beta_6 \sqrt{P_{Str} - P_{Sep}} \quad . \tag{5.26}$$

The separator temperature has units of Kelvin, and separator and stripper pressures have units of absolute kPa. Stream 8 flow has units of kscmh, and work is in units of kW. Valve position, v15, has units of %/100.

Downs and Vogel described the compressor as a centrifugal compressor which follows a typical centrifugal compressor curve (Downs and Vogel, 1993). In general equation format, the relationship between compressor flow, F_{Com}, and pressure changes for a centrifugal compressor is as follows.

$$F_{Com} = \beta_3 + \beta_4 \left[1 - \left(\frac{P_{out}}{P_{in}} \right)^{\beta_5} \right] \qquad (5.27)$$

Or, when rewritten to reflect the pressure increase in the separator overhead from the separator pressure to the stripper pressure, Equation 5.27 is

$$F_{Com} = \beta_3 + \beta_4 \left[1 - \left(\frac{P_{Str}}{P_{Sep}} \right)^{\beta_5} \right] \qquad (5.28)$$

Equations 5.25 with Equation 5.26 or 5.28 can be used to determine the work done by the compressor.

5.4. SS Stripper Model

Stripping is accomplished by lowering the partial pressures of the solutes absorbed in the solvent over the solution by heating the solvent, lowering the total pressure, or using non-condensable gases. (Hines and Maddox, 1985). The stripper uses non-condensable Stream 4, A+C feed, to strip the unreacted reactants and by-products from the separator underflow, Stream 10. Steam is provided to maintain the temperature of the stripper. The liquid products G and H are sent downstream to be refined while the overhead from the stripper joins the compressed recycle stream from the separator overhead.

Consider a simple single component, countercurrent stripping process as shown in the Figure 5.1. Here, L_1 and L_{n+1} represent the liquid streams leaving and entering the stripper, respectively. V_n and V_0 represent the vapor streams leaving and entering the stripper, respectively. Liquid mole fraction is represented by x while y is the vapor mole fraction.

For a given stage, n, the stripping factor is defined as

$$S_n = \frac{K_n V_n}{L_n} \tag{5.29}$$

where K_n is the equilibrium constant. An overall material balance yields the following equation.

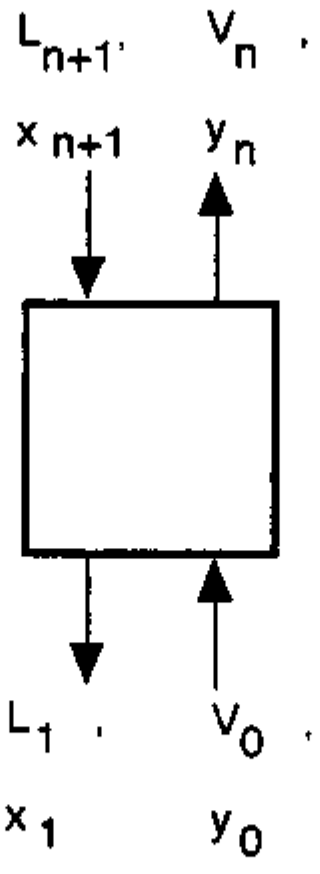

Figure 5.1. Countercurrent Stripping Process (Hines and Maddox, 1985)

$$x_{n+1}L_{n+1} + y_0V_0 = x_1L_{n+1} + y_nV_n \qquad (5.30)$$

Generally, all vapor stream compositions are based on the feed gas to the stripper, and all the liquid stream compositions are based on the rich solvent entering the stripper (Hines and Maddox, 1985). Rewriting Equation 5.30 results in the following overall material balance.

$$X'_{n+1}L_{n+1} + Y'_0V_0 = X'_1L_{n+1} + Y'_nV_0 \qquad (5.31)$$

where

$$X'_n = x_n \frac{L_n}{L_{n+1}} \qquad \text{and} \qquad Y'_n = y_n \frac{V_n}{V_0} \quad . \tag{5.32a,b}$$

At equilibrium,

$$Y'_n = X'_n S_n \frac{L_{n+1}}{V_0} \tag{5.33}$$

Substituting Equation 5.33 into Equation 5.31 and rearranging yields

$$X'_n = \frac{X'_{n+1} + X'_{n-1} S_{n-1}}{1 + S_n} \tag{5.34}$$

For a single component, single stage stripper after back-substitution of Equations 5.32a and 5.32b, Equation 5.34 can be rewritten as follows.

$$x_1 L_1 = \frac{x_2 L_2 + y_0 V_0}{1 + S_1} \quad . \tag{5.35}$$

in terms of a multi-component, single stage stripper as used in the TE process for the streams entering and leaving the stripper, Equation 5.35 is applied as follows.

$$x_{11,i}F_{11} = \frac{x_{10,i}F_{10} + x_{4,i}F_4}{1 + S_{11,i}} \qquad (i = A...H) \qquad (5.36)$$

Since components D to H only enter the stripper in Stream 10 and components A to C only enter the stripper in Stream 4, the stripping model equations used for these components are reduced to

$$x_{11,i}F_{11} = \frac{x_{4,i}F_4}{1 + S_{11,i}} \qquad (i = A...C) \qquad (5.37)$$

$$x_{11,i}F_{11} = \frac{x_{10,i}F_{10}}{1 + S_{11,i}} \qquad (i = D...H) \qquad (5.38)$$

If f_i for components A through H is defined as the fraction of component i in Stream 10 stripped into Stream 5, the eight, steady state stripper material balances can be written as follows.

$$F_{11,i} = x_{4,i}F_4(1 - f_i) \qquad (i = A...C) \qquad (5.39)$$

$$F_{11,i} = x_{10,i}F_{10}(1 - f_i) \qquad (i = D...H) \qquad (5.40)$$

By combining Equations 5.37 and 5.39 as well as 5.38 and 5.40, the relationship between stripping factor and fraction stripper can be calculated as

$$f_i = \frac{S_{11,i}}{1 + S_{11,i}} \qquad (i = A...H) \qquad (5.41)$$

The stripping factor, $S_{11,i}$, is a function of temperature due to the dependence on the equilibrium constant and is a function of the entering gas to entering liquid ratio, as shown in Equation 5.29. If the relationship between stripping factor, stripper temperature, and gas/liquid ratio is known, the fraction stripped can be determined from Equation 5.41. The eight, steady state material balances can be solved using Equations 5.39 and 5.40.

The steady state energy balance around the stripper is used to determine the amount of steam required to heat the stripper.

$$Q_{Str} = F_5H_5 + F_{11}H_{11} - F_4h_4 - F_{10}h_{10} \qquad (5.42)$$

Knowing the latent heat of the steam and the heat requirement of the stripper, Q_{Str}, the required steam flow is calculated as follows.

$$F_{14} = \frac{Q_{Str}}{\lambda_{Stm}} \qquad (5.43)$$

An accurate knowledge of the steam requirement is needed due to the inclusion of steam use in the optimization objective function.

5.5. Mixing of Feed and Recycle Streams

The overheads of the stripper and separator are combined with Streams 1, 2 and 3. The well-mixed stream, Stream 6, then enters the reactor. At steady state, the Stream 6 material balances are

$$0 = x_{6,i}F_6 - x_{5,i}F_5 - x_{8,i}F_8 - x_{1,i}F_1 - x_{2,i}F_2 - x_{3,i}F_3 \tag{5.44}$$

for components i = A...H.

5.6. Overall Component Material Balances

The steady state overall component material balances for the process can be used to check how accurately the steady state model has calculated the amount and flow of components in the process streams. Large errors in the overall component material balances will result in poor approximations of the optimization objective function. The overall component material balances are as follows.

$$0 = x_{1,A}F_1 + x_{4,A}F_4 - x_{9,A}F_9 - x_{11,A}F_{11} - R_1 - R_2 - R_3 \tag{5.45}$$

$$0 = x_{1,B}F_1 + x_{4,B}F_4 - x_{9,B}F_9 - x_{11,B}F_{11} \tag{5.46}$$

$$0 = x_{4,C}F_4 - x_{9,C}F_9 - x_{11,C}F_{11} - R_1 - R_2 \tag{5.47}$$

$$0 = x_{2,D}F_2 - x_{9,D}F_9 - x_{11,D}F_{11} - R_1 - 1.5R_4 \tag{5.48}$$

$$0 = x_{3,E}F_E - x_{9,E}F_9 - x_{11,E}F_{11} - R_2 - R_3 \tag{5.49}$$

$$0 = x_{3,F}F_3 - x_{9,F}F_9 - x_{11,F}F_{11} + R_3 + R_4 \tag{5.50}$$

$$0 = -x_{9,G}F_9 - x_{11,G}F_{11} + R_1 \tag{5.51}$$

$$0 = -x_{9,H}F_9 - x_{11,H}F_{11} + R_2 \tag{5.52}$$

5.7. Flow Valve Model

Most of the valves in the TE process are linear valves as stated in the information provided by Downs and Vogel (1993). However, the compressor recycle stream valve (v15) and the purge valve (v9) are proportional valves. The flow through these two valves is a function of pressure. The description of the compressor recycle stream valve is given in the compressor model section of this chapter. For the purge valve, Bernoulli's equation for flow was applied to determine the relationship of purge flow to valve position and system pressure.

$$F_9 = \varepsilon_1 v_9 \sqrt{P_{Sep} - P_{Atm}} \tag{5.53}$$

Flow is in lbmol/h, and pressure is in absolute kPa. Valve position, v9, is in %/100. The valve coefficient, ε_1, has the units which make Equation 5.53 dimensionally correct.

CHAPTER 6
MODEL PARAMETER APPROXIMATIONS

Only in very simple, and usually artificial, processes can the model exactly match the true process behavior. For more complex processes, simplifications in the model are made to decrease the complexity of the model and increase the speed of calculations while minimizing process-model mismatch. Often, simplified models of a complex system can accurately approximate the process conditions over the entire range of operation of the process. The steady state model equations introduced in Chapter 5 contain a number of simplifications which ease the computational impact of the calculations. Most of the process assumptions were listed in Chapter 3.

Other assumptions for the TE process were made based on the available data for the process from Downs and Vogel. Downs and Vogel only provided one heat capacity data point, enthalpy data point, and liquid density data point for the components in the process (Downs and Vogel, 1993). Because the exact nature of the components was unknown (i.e., their identity given as components A to H), properties such as liquid density or heat capacity could not be calculated using known correlations one would find for many components in books such as *Properties of Gases and Liquids* by Reid, Prausnitz, and Poling. Thus, either the single data point for the above properties would have to be used in calculations, or a

parameterization technique would have to be used to update the component properties at different process conditions.

Steady state model parameters from the first principal models in Chapter 5, such as the reaction rate pre-exponential, activation energy, and partial pressure exponential, must be fit to the non-linear process model over the range of process operation to be able to accurately predict what plant conditions yield a minimization of the optimization objective function. By using a series of numerical techniques, the model parameters for the reactor, stripper, and compressor were determined and validated over the six modes of operation of the TE process.

6.1. Reactor Model Parameters

The steady state reactor material balance equations were presented in Chapter 5. The equations contained a series of parameters specific to the TE process:

1. Pre-exponentials k_1, k_2, k_3, and k_4;
2. Activation energies E_1, E_2, E_3, and E_4;
3. Partial pressure exponentials $\alpha_{i(i=1..10)}$.

Each of these parameters were fitted to the process using process data and the steady state reactor model equations. Five steps were required to regress and validate the model parameters for the steady state reactor component material balances.

First, a linear approximation was made for the relationship of percent reactor liquid level to volumetric (ft^3) reactor liquid level

using steady state data provided by Downs and Vogel (1993). The linear model approximation was as follows.

$$V_{R_1} = \delta_1 V_{R_{\%1}} + \delta_2 \tag{6.1}$$

From the linear regression using two data points given in the process constraints (Downs and Vogel, 1993), the constants were as follows.

$$\delta_1 = 6.7098 \frac{ft^3}{\%}$$

$$\delta_2 = 81.2237 ft^3$$

Thus, Equation 5.13 was rewritten.

$$V_R = 1300 - \left[6.7098 V_{R_{\%1}} + 81.2273\right] \tag{6.2}$$

Second, the steady state reactor material balance equations for reactants A to E and four reaction rate equations were rewritten in a molar flow form for Stream 7 which helped determine what data was required for the parameter regressions. The modified forms of Equations 5.1 through 5.5 and Equations 5.9 through 5.12 used were as follows.

$$F_{7,A} = F_6 x_{6,A} - R_1 - R_2 - R_3 \tag{6.3}$$

$$F_{7,B} = F_6 x_{6,B} \tag{6.4}$$

$$F_{7,C} = F_6 x_{6,C} - R_1 - R_2 \tag{6.5}$$

$$F_{7,D} = F_6 x_{6,D} - R_1 - 1.5R_4 \tag{6.6}$$

$$F_{7,E} = F_6 x_{6,E} - R_2 - R_3 \tag{6.7}$$

$$R_1 = e^{\left(k_1 - \frac{E_1}{R_{gc} T_R}\right)} V_R P_R^{(\alpha_1+\alpha_2+\alpha_3)} \frac{F_{7,A}^{\alpha_1} F_{7,C}^{\alpha_2} F_{7,D}^{\alpha_3}}{F_7^{(\alpha_1+\alpha_2+\alpha_3)}} \tag{6.8}$$

$$R_2 = e^{\left(k_2 - \frac{E_2}{R_{gc} T_R}\right)} V_R P_R^{(\alpha_4+\alpha_5+\alpha_6)} \frac{F_{7,A}^{\alpha_4} F_{7,C}^{\alpha_5} F_{7,E}^{\alpha_6}}{F_7^{(\alpha_4+\alpha_5+\alpha_6)}} \tag{6.9}$$

$$R_3 = e^{\left(k_3 - \frac{E_3}{R_{gc} T_R}\right)} V_R P_R^{(\alpha_7+\alpha_8)} \frac{F_{7,A}^{\alpha_7} F_{7,E}^{\alpha_8}}{F_7^{(\alpha_7+\alpha_8)}} \tag{6.10}$$

$$R_4 = e^{\left(k_4 - \frac{E_4}{R_{gc} T_R}\right)} V_R P_R^{(\alpha_9+\alpha_{10})} \frac{F_{7,A}^{\alpha_9} F_{7,D}^{\alpha_{10}}}{F_7^{(\alpha_9+\alpha_{10})}} \tag{6.11}$$

where R_{gc} is 1.987 cal/gmol/K.

Third, data was collected from the steady state operation of the process simulation over the first three modes of operation. The reactor level, reactor temperature, and reactor pressure were varied between the reactor process constraints to cover the entire range of

operation for Modes 1 through 3. The data points collected were all passed through a first-order filter to remove process noise and measurement changes due to controller adjustments. Reaction rates 1 through 4 were calculated using the overall material balances on components G, H, D, and E listed in Equations 5.51, 5.52, 5.48, and 5.49, respectively. Reactor gas phase volume was determined from Equation 6.2. The reactor temperature and reactor feed compositions were obtained from process measurements. Tables A.1 and A.2 in the Appendix list a portion of the steady state data sets for Mode 1 to Mode 3 collected from the process simulation.

Fourth, a non-linear regression technique, based on the Nelder-Mead pattern search and minimization of the sum of the squared of the errors as the objective function as described by Riggs (1994), was used to regress the model parameters for the reactor models. For each set of model parameters in the four reaction rates, a regression was performed to determine the pre-exponential, activation energy, and partial pressure exponents.

Finally, the model parameter values were validated by comparing the error in the reaction rates calculated from the overall material balances and the reaction rates calculated from the reaction rate models using data from the process simulator, which was not used in the data regression. The data used for model validation was taken from Mode 1 to Mode 3 operation with a higher production rate than the previous data sets. Again, data was collected over the range of

unit process constraints for model validation. The final values of the reactor model regressed parameters used are listed in Table 6.1.

6.2. Compressor Model Parameters

Six compressor model parameters were regressed using the same techniques which were used to regress the reactor model parameters. Steady state compressor data was collected using the TE process simulator. Using Equations 5.25, 5.26, and 5.28 and the Nelder-Mead regression technique, the six compressor model parameters were calculated. The values predicted by the compressor model for compressor work were compared to steady state compressor work from the TE process simulator at conditions different than the model design data. Table A.3 in the appendix lists a portion of the steady state data used to regress the compressor model parameters. Table 6.2 shows the final values of the regressed parameters for the compressor model.

Table 6.1. Regressed Reaction Rate Parameters

Parameter	Regressed Value
k_1	31.681
k_2	3.322
k_3	53.814
k_4	53.333
E_1	40,000
E_2	20,000
E_3	60,000
E_4	60,000
α_1	1.077
α_2	0.442
α_3	1.0
α_4	1.016
α_5	0.478
α_6	1.0
α_7	0.995
α_8	1.0
α_9	0.997
α_{10}	1.0

Table 6.2. Regressed Compressor Model Parameters

Parameter	Regressed Value
β_1	0.1026
β_2	1.0
β_3	116.5599
β_4	115.2820
β_5	2.7027
β_6	5.9086

6.3. Stripper Model Parameters

6.3.1. Stripping Factor

To calculate the fraction of Stream 10 stripped into Stream 5, the stripping factor must be calculated. The stripping factor as shown in Chapter 5 is a function of stripper temperature and the entering gas/liquid ratio. A series of steps were employed to determine the functional relationship (i.e., linear, quadratic, etc.) of stripping factor to stripper temperature and entering gas/liquid ratio.

First, steady state data around the stripper was collected for all of the components A to H to determine the effect of changes in the stripper temperature on stripping fraction, f_j. The stripper temperature was varied from 40 °C to 80 °C (i.e., steam valve full closed to full open) for Mode 1 to Mode 3 operation. The steady state data for components D to F are listed in Table A.4 and Table A.5 in

the Appendix. The stripping fractions for components A through C and G to H did not show a recognizable dependence on stripper temperature and entering gas/liquid ratio, so data for these components was not listed in the table. The stripping fractions, f_i, for components A to C were taken to be constant in Equation 5.39. The stripping fractions, f_i, for G and H were taken to be constant for Equation 5.40. The G and H stripping fractions were updated on-line using parameter model updating techniques discussed in a later chapter.

Second, the stripping factor for components D to F were calculated using Equations 5.40 and 5.41. Plots of stripping factor, $S_{11,i}$, divided by entering gas/liquid ratio versus stripper temperature, T_{Str}, for components D to F were made to determine the functional relationship between stripping fraction and stripper temperature. Components D to F stripping fraction showed a linear dependence on stripper temperature as shown in Figures 6.1 to 6.3.

Finally, the linear relationship of the stripping factor to stripper temperature was verified using stripper steady state data collected from Mode 2 and Mode 3 operation. The linear relationship for components D to F of stripping factor to stripper temperature over the operational range of 50°C to 80°C are shown in the equations below.

$$S_{11D} = \frac{F_4}{F_{10}}(0.2058T_{Str} - 4.6011) \qquad (6.12)$$

$$S_{1LE} = \frac{F_4}{F_{10}}(0.2767T_{Str} - 6.2147) \tag{6.13}$$

$$S_{1LF} = \frac{F_4}{F_{10}}(0.2863T_{Str} - 6.4336) \tag{6.14}$$

where the stripper temperature is in degrees Celsius.

6.3.2. Heat Capacity for Stripper Energy Balance

As mentioned earlier, the heat capacity data and enthalpy data provided for the eight components are only for one temperature (i.e., 100 °C). Since no correlations are available to determine the enthalpies or heat capacities, using Equation 5.42 to determine the energy requirements of the stripper will result in a significant error (i.e., >±25%) when the process is moved away from the base case. Thus, a model parameter, ΔC_p, was introduced to correct Equation 5.42 for changes in the energy requirements when the process deviates from the base case conditions. Equation 5.42 was modified as follows.

$$Q_{Str} = F_5H_5 + F_{11}H_{11} - F_4h_4 - F_{10}h_{10} + \Delta C_p(F_5 + F_{11} - F_{10})(T_{Sep} - T_{Str}) \tag{6.15}$$

where temperatures are in degrees Celsius and flows in lbmol/h. The make-up heat capacity parameter, ΔC_p, is updated on-line using model parameter updating techniques discussed in a later chapter.

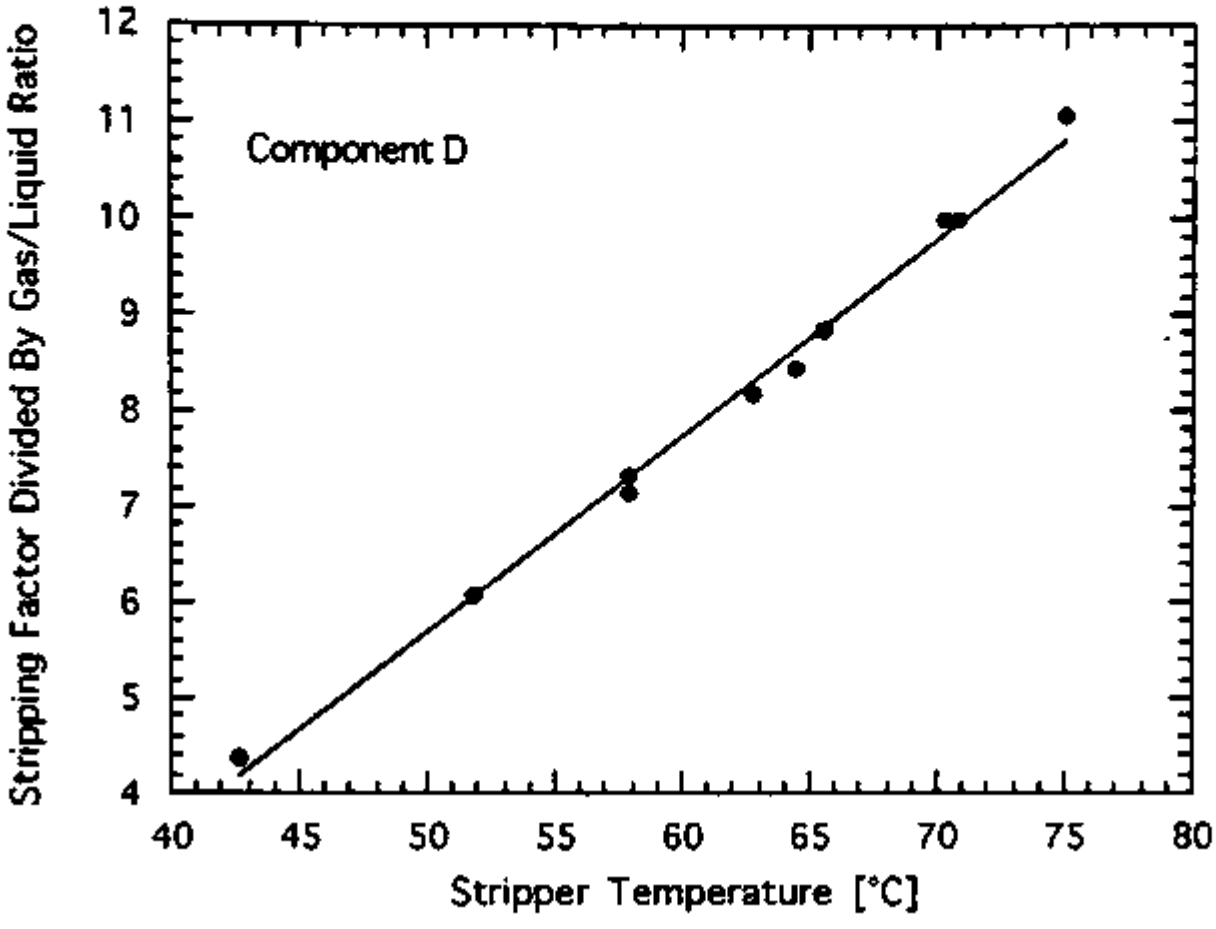

Figure 6.1. Stripping Factor versus Stripper Temperature for Component D

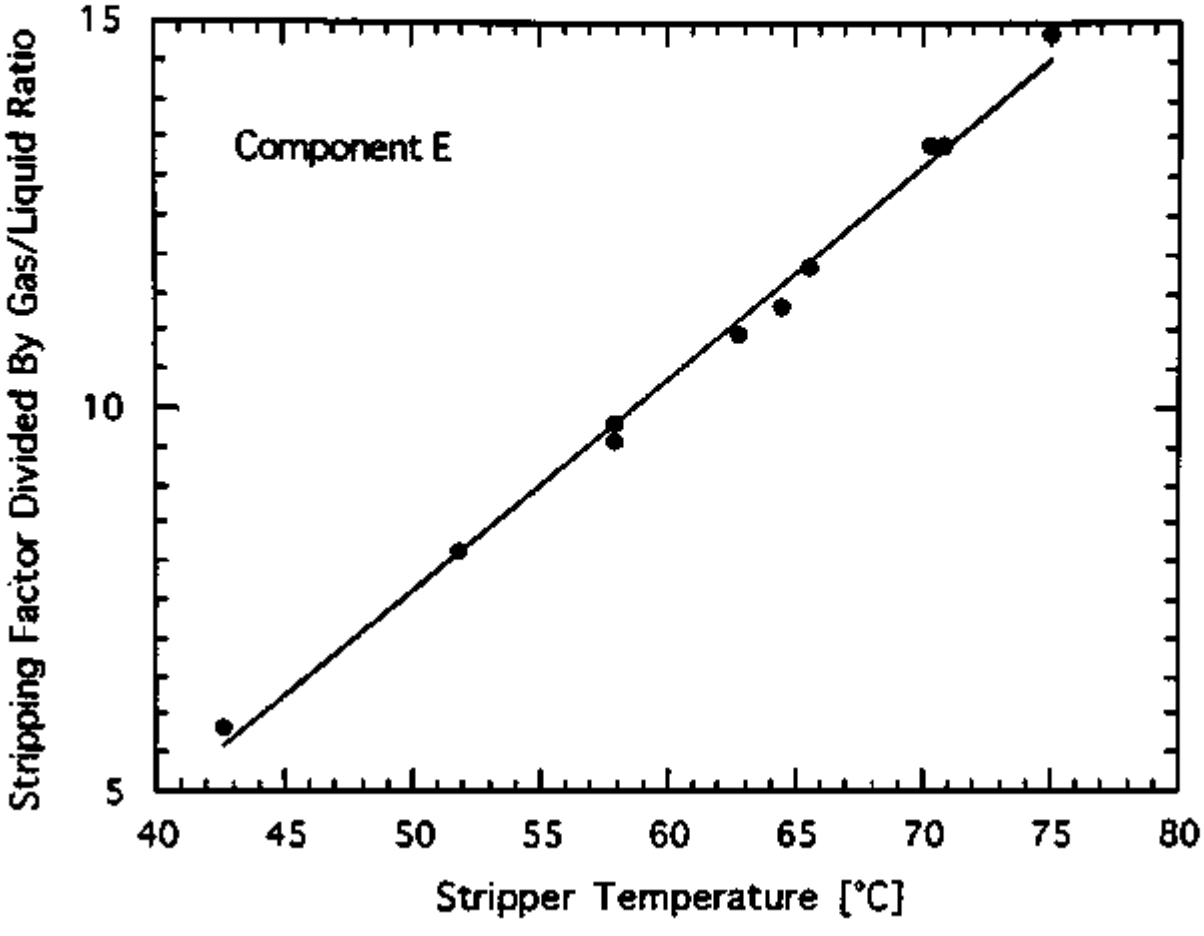

Figure 6.2. Stripping Factor versus Stripper Temperature for Component E

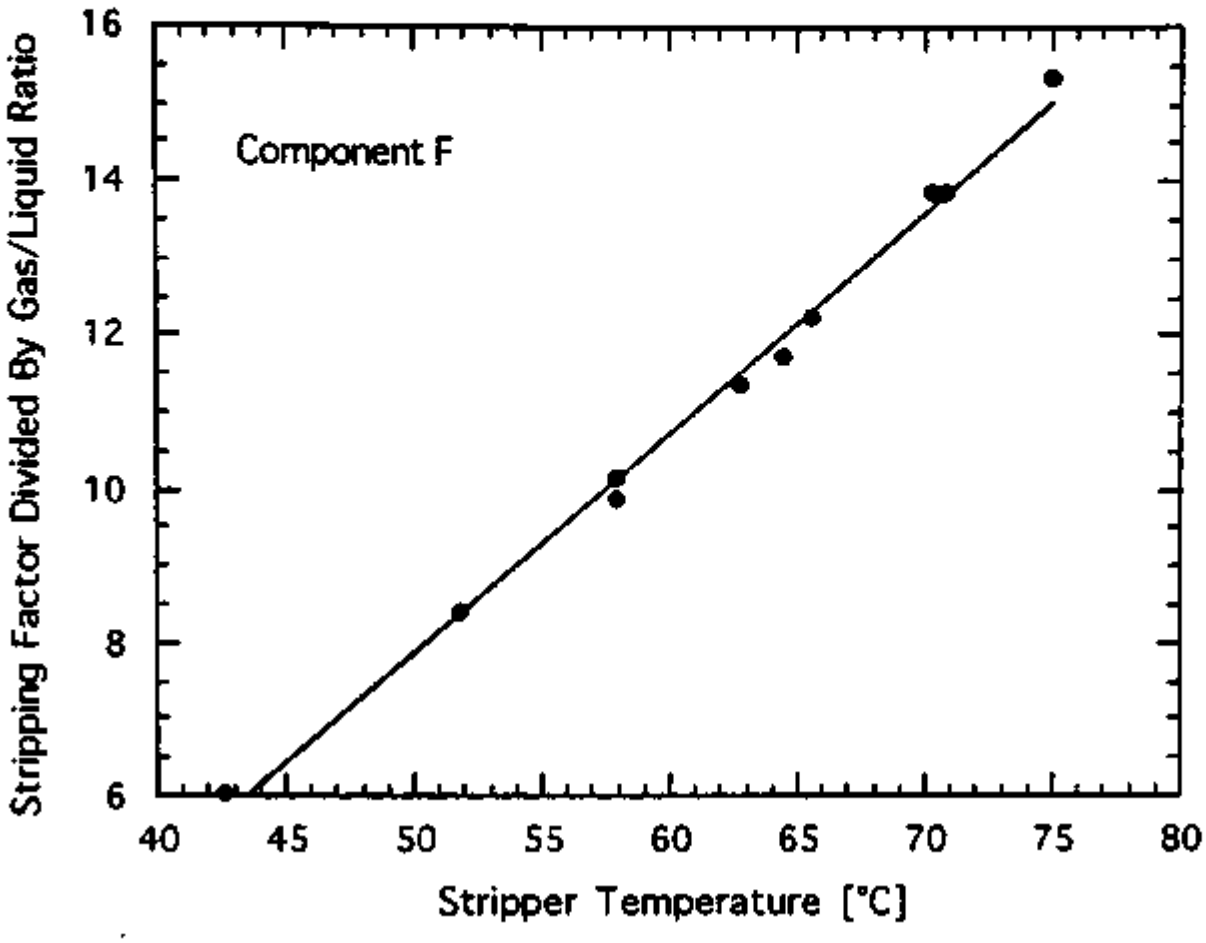

Figure 6.3. Stripping Factor versus Stripper Temperature for Component F

From the steady state data provided by Downs and Vogel (1993), the latent heat of the steam used to heat the stripper was determined.

$$\lambda_{Stm} = 962.279 \frac{Btu}{lb} \tag{6.16}$$

This value for the latent heat corresponds to 20 psia steam at 110 °C. The latent heat value can be used with Equations 5.43 and 6.15 to determine the required steam use for the stripper.

6.4. Flow Valve Dynamics

The purge valve is a proportional valve as discussed in Chapter 5. Steady state data provided by Downs and Vogel was used to determine the value of the valve coefficient parameter in Equation 5.53. The valve coefficient was calculated as follows.

$$\varepsilon_1 = 1.6396 \times 10^{-2} \tag{6.17}$$

CHAPTER 7
STEADY STATE MODEL SOLUTION PATH

Once the models for the process were developed, a solution path had to be developed to determine in which order the model equations for each unit would be solved so that an accurate process description at steady state could be calculated. The final steady state model solution path would have to be robust enough to provide a steady state solution at all six modes of operation, which had conditions far different from the base case conditions provided by Downs and Vogel. The solution path used to solve the for the steady state process conditions is shown in Figure 7 and described in detail below.

7.1. Reactor Model Solution

In Chapter 5, eight material balance equations which include the four reaction rate equations were derived. Equations 5.1 through 5.12 were rewritten in molar flow notation as follows to reduce the number of unknowns in the model equations.

$$0 = F_{6,A} - F_{7,A} - R_1 - R_2 - R_3 \tag{7.1}$$

$$0 = F_{6,B} - F_{7,B} \tag{7.2}$$

$$0 = F_{6,C} - F_{7,C} - R_1 - R_2 \tag{7.3}$$

$$0 = F_{6,D} - F_{7,D} - R_1 - 1.5R_4 \tag{7.4}$$

$$0 = F_{6,E} - F_{7,E} - R_2 - R_3 \tag{7.5}$$

$$0 = F_{6,F} - F_{7,F} + R_3 + R_4 \tag{7.6}$$

$$0 = F_{6,G} - F_{7,G} + R_1 \tag{7.7}$$

$$0 = F_{6,H} - F_{7,H} + R_2 \tag{7.8}$$

where the reaction rates are as follows.

$$R_1 = e^{\left(k_1 - \frac{E_1}{R_{gc}T_R}\right)} V_R P_R^{(\alpha_1+\alpha_2+\alpha_3)} \frac{F_{7,A}^{\alpha_1} F_{7,C}^{\alpha_2} F_{7,D}^{\alpha_3}}{F_7^{(\alpha_1+\alpha_2+\alpha_3)}} \tag{7.9}$$

$$R_2 = e^{\left(k_2 - \frac{E_2}{R_{gc}T_R}\right)} V_R P_R^{(\alpha_4+\alpha_5+\alpha_6)} \frac{F_{7,A}^{\alpha_4} F_{7,C}^{\alpha_5} F_{7,E}^{\alpha_6}}{F_7^{(\alpha_4+\alpha_5+\alpha_6)}} \tag{7.10}$$

$$R_3 = e^{\left(k_3 \frac{E_3}{R_{gc}T_R}\right)} V_R P_R^{(\alpha_7+\alpha_8)} \frac{F_{7,A}^{\alpha_7} F_{7,E}^{\alpha_8}}{F_7^{(\alpha_7+\alpha_8)}} \tag{7.11}$$

$$R_4 = e^{\left(k_4 - \frac{E_4}{R_{gc}T_R}\right)} V_R P_R^{(\alpha_9+\alpha_{10})} \frac{F_{7,A}^{\alpha_9} F_{7,D}^{\alpha_{10}}}{F_7^{(\alpha_9+\alpha_{10})}} \tag{7.12}$$

$$F_7 = \sum_{i=A}^{H} F_{7,i} \qquad (7.13)$$

The material balance equations contain nineteen unknowns.

1. 8 molar reactor inlet flows (Stream 6);
2. 8 molar reactor outlet flows (Stream 7);
3. Reactor temperature;
4. Reactor pressure;
5. Reactor level.

Thus, eleven decision variables can be assigned to the reactor. Reactor temperature, reactor pressure, and reactor level have known process bounds which were given by Downs and Vogel (1993) and represent good bounded decision variables for an optimizer to manipulate to determine optimal operating conditions. If reactor temperature, reactor pressure, reactor level, and the 8 molar outlet flows are taken as the decision variables, Equations 5.1 to 5.12 can be used to directly solve for the reactor inlet compositions. However, correctly guessing the outlet molar flow compositions, as well as upper and lower bounds on the molar flows, of Stream 7 would be very difficult because the reactor exit compositions can vary greatly over the six modes of operation.

Alternately, if the reactor temperature, reactor pressure, reactor level, and 8 molar inlet flows are taken as the decision variables, Equations 5.1 to 5.12 can be used to iteratively solve for the reactor outlet molar flows. From experience running the process simulator at different product grades and product rates, the compositions of

Stream 6 and flow of Stream 6 can be easily bounded to be used as decision variables in an optimization routine. At steady state, the reactor inlet compositions can be determined using process material balances and the Stream 6 analyzer data. Initial guesses for Stream 7 are required for the iterative procedure and can be directly obtained from the analyzer on Stream 6. To iteratively solve a set of nonlinear equations, a number of techniques are available.

Newton's method for sets of nonlinear equations as described in Riggs (1994) was initially used to try to converge the eight reactor model equations. Newton's method provides quadratic converge near the solution. Newton's method proved to be a poor solution method due to continual divergence from ill-conditioning even when the initial guesses for Stream 7 were close to the solution.

Instead, Singular Value Decomposition (SVD) was applied to solve the set of nonlinear reactor model equations replacing Newton's method. Using SVD the condition number which is the ratio of the largest singular value in magnitude to the smallest singular value in magnitude can be calculated during each iteration. An infinity condition number indicates singularity while large condition numbers indicate ill-conditioning. For process conditions where the small singular values become so small as to cause ill-conditioning, SVD was used to zero out the singular value causing the ill-conditioning which in turn throws away one combination of the set of equations being solved. The combination of equations being thrown out is that combination which is causing the solution to

diverge (Press et al., 1992). Thus, SVD was used to avoid ill-conditioning while solving the set of nonlinear reactor equations.

7.2. Separator Model Solution

Equations 5.15, 5.17, and 5.18 were combined and rewritten as eight molar flow material balance equations to reduce the number of unknowns to eighteen.

$$0 = F_{7,i} - F_{89,i} \qquad (i = A...C) \qquad (7.14)$$

$$0 = F_{7,i} - F_{89,i} - F_{10}\frac{P_{Sep}}{P_{Vap,i}}\frac{F_{89,i}}{F_{89}} \qquad (i = D...H) \qquad (7.15)$$

$$P_{Vap,i} = e^{\left(A_i + \frac{B_i}{C_i + T_{Sep}}\right)} \qquad (i = D...H) \qquad (7.16)$$

$$F_{89} = \sum_{i=A}^{H} F_{89,i} \qquad (7.17)$$

Once the reactor material balance equations are solved, the reactor product stream is known. Thus, the final number of unknowns for the separator model was ten.

1. 8 molar overhead flows (Stream 8+9);
2. Separator temperature;
3. Separator pressure.

Using separator temperature and separator pressure as the decision variables, an iterative technique was required to solve the

modified equations for the separator model overhead flow and compositions. Separator temperature and pressure have implied process upper and lower bounds which would make them good choices as decision variables for an optimization routine.

Again, SVD was used to solve the set of nonlinear equations because of the ill-conditioning which could occur due to large changes in process conditions from the base case. Initial guesses for separator overhead molar flows was based on process measurements from the analyzer located on Stream 9 and flow transmitters located on Streams 8 and 9.

7.3. Compressor Model Solution

Equations 5.25, 5.26, and 5.28 for the compressor model contained five unknowns. However, using the choice of degrees of freedom of separator pressure and temperature from the separator model solution, the number of unknowns was reduced to three.

1. Stripper pressure;
2. Work of the compressor;
3. Recycle valve position.

The recycle valve position has normal operational limits of 0% to 100%. The stripper pressure has implied upper and lower bounds due to the use of the process recycle stream. The compressor work has a lower bound of zero, but the upper bound is unknown. Therefore, recycle valve position and stripper pressure represent better choices for decision variables for optimization. For a given change in

stripper pressure or recycle valve position, the stripper pressure created the largest change in compressor work. Thus, stripper pressure represented a better decision variable for an optimizer than recycle valve position when seeking an optimum. Stripper pressure was used as the last decision variables for the compressor model solution.

With stripper pressure known, the compressor flow rate was calculated using Equation 5.28. From Equation 5.26, the recycle valve position was calculated.

7.4. Stripper Model Solution

7.4.1. Stripper Material Balances

The eight material balance equations for the stripper contained nineteen unknowns due to the stripping factors dependence on stripper temperature and the entering gas/liquid ratio for the stripper. Once the separator material balances are solved, Stream 10 molar flow rate and compositions were known which reduced the number of unknowns to thirteen.

1. Stripper temperature;
2. Stream 4 feed;
3. 8 molar flows for Stream 11 components;
4. 3 compositions for components A to C in Stream 4.

While the Stream 4 feed is supposed to be of constant flow and composition, disturbances affect the amount of B in Stream 4 as well as the ratio of A to C in Stream 4. However, the compositions

of A to C in Stream 4 can be easily estimated and updated for process disturbances as shown in a later chapter. Stream 4 compositions for A to C were used as decision variables for the stripper model solution.

The Stream 4 feed has a set upper and lower bound which is important when choosing decision variables for model-based optimization. Even though Downs and Vogel specify the weight production rate of G and H in the product, process simulation experience shows that the specified rates on G and H can not be met for Mode 3 due to plant capacity limitations, even though the specified ratio of G to H can be met. Thus, specification of G and H production rates can lead to infeasible optimization solutions and represent poor decision variables.

When the steam valve is fully closed, the lowest temperature achieved in the stripper over Modes 1 to 3 of operation was 40 °C. With the steam valve fully open, the highest temperature achieved in the stripper was 100 °C. Thus, the stripper temperature seemed to be a good decision variable due to its bounded nature. Using Equations 6.12 to 6.14 and Equations 5.39 and 5.40 with fixed stripping fractions for components A through C and G to H, the stripper material balances were used to solve for the product molar flows and the stripper overhead molar flows.

7.4.2. Energy Balance Model Solution

Using the modified Equation 6.15 for the stripper energy balance, the required heat duty of the stripper was calculated. From Equation 5.43, the required steam flow was then calculated.

7.5. Mixing of Reactor Feed Stream

When the process is at steady state, the reactor feed compositions and flow rate can be calculated using the Stream 6 analyzer data and process material balances. All of the stream compositions and flows for the current steady state conditions can be calculated using the steady state model solution path shown in Figure 7.1.

Initially, the reactor feed compositions and flow were not considered to be decision variables for optimization. Because a recycle stream is used in the process, the model solution path described above can not be used to correctly evaluate the new steady state process conditions arising from changes in the process (i.e., an increase in reactor temperature). When the process changes, the recycle composition changes resulting in a change in the reactor feed compositions.

Initially, an iterative procedure was used to converge the steady state model reactor feed material balances to new steady state conditions. Initial guesses were made for the reactor feed compositions and flow rate, and the steady state model solution path was evaluated. The new reactor feed compositions and flow

rate were calculated from Equation 5.44. Newton's method was then used to converge the reactor feed compositions and flow rate.

Due to severe ill-conditioning in the reactor feed mixing material balance equations during iteration, Newton's method continually diverged even for small changes in the process from current steady state conditions. When applied, SVD also continually diverged when trying to converge the reactor feed material balances. Since a robust model was required to determine the optimal operating conditions for the process over the six modes of operation, an iterative approach for convergence of the reactor feed material balances was abandoned in favor of a more robust technique.

Instead of using an iterative approach such as Newton's method or SVD to converge Equation 5.44, the eight reactor feed material balance equations were eventually treated as open equations and used as nonlinear constraints in the optimization algorithm. The reactor feed compositions and flow rate were then taken to be decision variables for optimization. While adjusting the optimization decision variables to determine operating conditions which minimizes operating costs, the optimization algorithm was simultaneously converging the eight reactor feed material balances. Thus, the optimization routine was used as an open equation solver and optimizer.

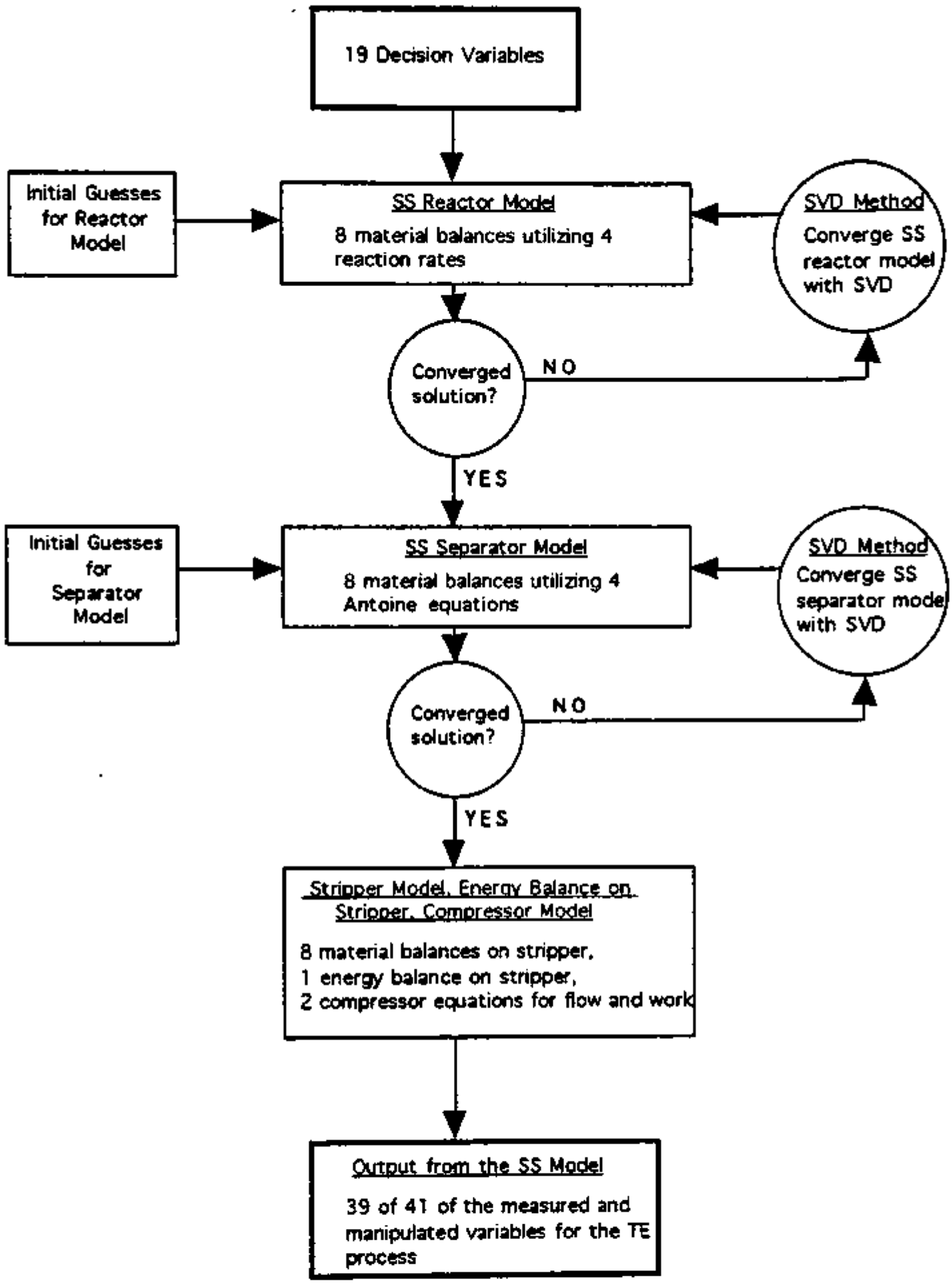

Figure 7.1. Steady State Model Solution Path

CHAPTER 8
MODEL PARAMETER UPDATING

Real-time optimization (i.e., on-line optimization) requires an accurate model to predict the optimal operating conditions of a process. Even for rigorously designed models of simple or complex processes, process-model mismatch occurs. Most models, especially in complex processes, are based on steady state assumptions which can lead to process-model mismatch. A number of techniques exist to estimate model parameters on-line. When updating a steady state model from on-line process measurements, the model updating must be done at or near steady state (Marlin and Hrymak, 1996). Mathematical tests for steady state identification are becoming more prevalent in the engineering field as well as tests to determine the validity of the measurements used to update model parameters. In general, all reliable measurements which have passed validity checks can be used in model parameter updating (Marlin and Hrymak, 1996).

Model parameter updating can prove invaluable when the updated model parameters are properly selected. Usually, only a small percentage of the model parameters are updated to remove process model mismatch. When choosing which parameters to update, the updated model parameters should be observable in the process, represent actual changes in the process, and contribute to removing process-model mismatch (Marlin and Hrymak, 1996). For example,

updating a tank diameter to eliminate model-mismatch in liquid holdup would represent a poor parameter choice because the tank diameter typically does not change in the process. However, updating density properties would represent a possible model parameter to update since the change in liquid density relates to actual changes which occur in a process. A number of tests have been developed to determine parameter observability. Forbes and Marlin (1996) describe a method for checking for parameter observability.

For the steady state model shown in Chapter 7, process-model mismatch occurred when the process conditions were moved away from the base case conditions, especially after a product grade change. To minimize the process-model mismatch, certain model parameters were continuously updated using the current process measurements.

8.1. Reactor Model Parameters

Two reaction rate pre-exponential model parameters, k_1 and k_2, were updated to remove process-model mismatch in the reactor. Based on the above criteria, these parameters, when updated, effectively removed process model mismatch in reaction rates and represented actual changes in the process such as slow deactivation of the catalyst. Reaction rate pre-exponentials k_3 and k_4 were not updated because even the filtered process measurements during minor upsets from steady state resulted in poorly estimated parameters (i.e., large, negative pre-exponentials).

Using the overall material balance equations at steady state process conditions and process measurements, the four reaction rates were calculated. Reactor material balances, Equations 5.1 to 5.8, and Stream 6 analyzer measurements were used to determine the composition of the reactor product stream. By rearranging Equations 5.9 and 5.10, the pre-exponentials k_1 and k_2 were continuously calculated. Using a first-order filter with a long time constant, the pre-exponential model parameters were filtered.

8.2. Compressor Model Parameters

When the recycle valve position was set at either fully closed or fully open, the compressor model underestimated the work required by the compressor. For large pressure differences in the stripper and separator pressures which were outside the data range used to model the compressor, the compressor model also underestimated the required compressor work. Model parameter, β_6, in Equation 5.26 and model parameter, β_4, in Equation 5.24 were determined to be the parameters which most effectively removed the process-model mismatch for the conditions described above.

β_6, which represents the valve coefficient in the recycle stream valve, was continuously calculated from Equation 5.26 after the flow through the compressor, F_{Com}, was calculated using Equation 5.25 and process data. Model parameter β_4 was determined from Equation 5.24 using F_{Com} and process data. The two model parameters were also passed though a first-order filter.

8.3. Stripper Model Parameters

8.3.1. Material Balance Parameters

Disturbances to the process change the composition of B and/or the ratio of A to C in Stream 4 as shown in Chapter 3. No composition analyzer was available for Stream 4. Unfortunately, during disturbances to Stream 4, the stripper model incorrectly predicted the compositions of A to C in the stripper overheads and bottoms (error was ±15% or greater). From process modeling in Chapter 5, the stripping fractions, f_i, for components A to C were determined to be independent of stripper temperature and stripper entering gas/liquid ratio and were taken as a constant value, which was calculated from steady state data provided by Downs and Vogel.

To remove the process-model mismatch in the stripper model, either the compositions of Stream 4 or stripping fractions for components A to C could have been updated. Since the feed disturbances more directly reflected a change in feed compositions, the compositions of A to C were updated using stripper model equations and on-line process data. Since components A to C are not measured by the analyzer on Stream 11, the stripper model Equation 5.39 was modified for components A to B to use Stream 5 compositions which could be back-calculated using the analyzer data on Stream 6 and Stream 9. The composition of C in Stream 4 was determined from the summation of mole fractions.

$$F_{5,i} = x_{4,i} F_4 f_i \qquad (i = A...B) \qquad (8.1)$$

and

$$1 = \sum_{i=A}^{C} x_{4,i} \qquad (8.2)$$

However, process-model mismatch was still prevalent in the stripper model predictions of the overhead and underflow for component C. Equation 8.1, when applied for component C, was used to update the stripping fraction for component C. The updated composition of C in the feed is used in Equation 8.3 below.

$$F_{5,C} = x_{4,C} F_4 f_C \qquad (8.3)$$

The Stream 4 updated compositions for components A to C and the updated stripping fraction for component C were passed through a first-order filter with a long time constant to prevent noise and minor controller adjustments from adversely affecting the updated parameter values.

In Chapter 5, the stripping fractions for components G and H were determined to be weak functions of stripper temperature and gas/liquid ratio which made modeling the functionality of stripper temperature and stripping pressure. Thus, the stripping fractions for G and H were taken as a constant value which was calculated from steady state data provided by Downs and Vogel. The constant

stripping fraction proved to be a poor assumption when process-model mismatch occurred in the predicted product compositions of G and H. Accurate product compositions of G and H were required for setpoints to controllers to maintain plant operation at the specified G/H product ratio.

Errors in the calculated stripper product composition of G and H were removed by updating the stripping fractions for these components. Using the separator and stripper model material balance equations for G and H, the stripping fractions were back-calculated from current process data. A long time constant, first-order filters were used on the G and H stripping fraction parameters.

8.3.2. Energy Balance Model Parameters

Process-model mismatch in the calculated steam rate for the stripper was removed by updating the modified heat capacity parameter, ΔC_p, in the stripper energy balance equation. The model parameter was back-calculated from Equation 6.15. Again the model parameter was filtered with a long time constant, first-order filter.

8.4. Steady State Model Validation

A good steady state model with model parameter updating should closely track the true steady state process conditions over the range of operation of the process. However, model parameter updating to remove process-model mismatch does not guarantee that a model used in conjunction with an optimization algorithm will accurately

predict the gradients which drive the process conditions to optimal operation. Most optimization algorithms use the objective function gradients (i.e., the partial derivatives of the objective function with respect to the decision variables) to determine the magnitude and direction of the changes in the decision variables required to reach the minimum in the objective function. By comparing the model objective function gradients used by an optimization algorithm to the actual process objective function gradients, errors in the model can be easily detected and corrected. Large relative errors (i.e., >50%) in the comparison of the model objective function gradients to the process objective gradients would indicate gross modeling or model parameterization errors.

To determine whether the steady state model would accurately move the optimization algorithm along the path required to reach the optimal operating conditions, the model objective function gradients were compared to the process objective function gradients for the choosen model decision variables. For example, a change in reactor pressure was used in the TE simulation to determine the resulting change in the total operating cost objective function at the new steady state operating conditions. The same change in reactor pressure was used in the steady state model of the process to determine the predicted change in the total operating costs. The objective function gradient (i.e., the partial of the total operating costs with respect to reactor pressure) was then determined.

The base case 50/50 conditions from Downs and Vogel were used to determine base case conditions for the 10/90 and 90/10 operating modes. From the 50/50 base case conditions, the %G in Stream 11 was increased to 90.09% for the 90/10 and decreased to 11.66% for the 10/90 product grade cases. The process was lined out at steady state to obtain the base case start-up state conditions for the 90/10 and 10/90 product grade operation modes. No other control setpoints were changed from the 50/50 base case conditions.

Table 8.1 shows the comparison of the process objective function gradients to the model objective function gradients for the reactor decision variables for different process operating conditions. In all cases for the decision variables for the steady state model, the relative percent difference in the model objective function gradients compared to the process objective function gradients was 25% or less. The model and process gradients showed similiar magnitude and direction for the different process operating conditions. Thus, no gross errors objective function prediction from the steady state model were detected using the process/model objective function gradient comparison test.

Table 8.1. Process/Model Objective Function Gradient Comparison

Operating Condition	Decision Variable	Process (P), Model (M) Gradient	Change in Decision Variable	Change in Total Operating Costs [$/h]	Objective Function Gradient	Relative Percent Difference [%]
Base Case (50/50)	Reactor Pressure [kPa]	P	50.0	-5.81	-0.120 $/h/kPa	
		M	50.0	-7.00	-0.140 $/h/kPa	16.67
	Reactor Pressure [kPa]	P	-50.0	23.39	0.468 $/h/kPa	
		M	-50.0	23.84	0.477 $/h/kPa	2.00
	Reactor Temp [°C]	P	2.6	-2.39	-0.919 $/h/°C	
		M	2.6	-1.80	-0.692 $/h/°C	24.70
	Reactor Temp [°C]	P	-3.4	53.23	-15.66 $/h/°C	
		M	-3.4	47.78	-14.05 $/h/°C	10.28
	Reactor Level [%]	P	5.0	17.26	3.45 $/h/%	
		M	5.0	16.61	3.32 $/h/%	3.77
	Reactor Level [%]	P	-5.0	-3.47	0.694 $/h/%	
		M	-5.0	-4.12	0.824 $/h/%	18.73
Base Case (10/90)	Reactor Temp [°C]	P	2.6	24.07	9.258 $/h/°C	
		M	2.6	21.16	8.138 $/h/°C	12.10
	Reactor Level [%]	P	-5.0	18.67	-3.73 $/h/%	
		M	-5.0	13.95	-2.79 $/h/%	25.20
Base Case (90/10)	Reactor Temp [°C]	P	2.6	-95.36	-36.68 $/h/°C	
		M	2.6	-91.46	-35.18 $/h/°C	4.09
	Reactor Level [%]	P	-5.0	-38.42	7.68 $/h/%	
		M	-5.0	-39.66	7.93 $/h/%	3.22

CHAPTER 9
OPTIMIZATION SOLUTION PATH

A well developed model along with a well defined optimization algorithm is the basis for any successful on-line optimization. Well defined optimization algorithms have known process constraints for the decision variables and calculated variables, account for the type of control strategy being used in the process, and determine optimal operating conditions over the entire range of process operation.

A number of nonlinear programming algorithms are available for optimization problems including augmented lagrangian methods and successive quadratic programming, SQP. The SQP algorithms tend to be better suited for well defined problems which have few decision variables compared to total number of variables in the problem (Marlin and Hrymak, 1996). NPSOL, a successive quadratic programming technique which uses a reduced Hessian gradient search technique (Gill et al., 1986), was used as the optimization algorithm in this research for determining the optimal operating conditions of the TE process over the six modes of operation. Two optimization solution paths were developed for the TE process.

Path 1. Minimize costs for Modes 1 to 3 with fixed production;

Path 2. Minimize costs for Modes 4 to 6 with maximum production.

For Modes 1 to 3, the production rate is fixed. Thus, an optimization algorithm was required to reduce the total operating

cost only. For Modes 4 to 6, the production rate was first maximized. At the maximum production rate, optimization was required to minimize the total operating cost. All six modes of operation required the minimization of the objective function for total operating cost as described by Downs and Vogel (1993).

9.1. Constrained Decision Variables

As shown in the model solution path developed in Chapter 7, nineteen decision variables were chosen to solve the steady state model of the process for all six modes of operation. The nineteen decision variables represented the variables which were adjusted by the optimization algorithm to determine the optimal operating conditions of the process.

1. Reactor temperature;
2. Reactor pressure;
3. Reactor level;
4. Separator temperature;
5. Separator pressure;
6. Stripper temperature;
7. Stripper pressure;
8. Stream 4 valve position;
9. Stream 9 valve position;
10. Stream 10 valve position;
11. Stream 6 molar flow rate;
12. - 19. Stream 6 mole fraction compositions for A to H.

Each of these decision variables had upper and lower process constraints which could be inferred or taken directly from the process description given by Downs and Vogel. A poor choice for the decision variable constraints often resulted in no minimization of the objective function or infeasbile operating setpoints for controllers. For the units operation pressures, levels, and temperatures, the lower and upper bounds were set close to the low and high alarm limits while leaving room for normal process control without continually crossing the low and high alarm limits. Table 9.1 lists the nineteen decision variables with the upper and lower bounds used in the optimization algorithm.

9.2. Nonlinear Constraints

The optimization algorithm was used to determine the optimal operating condition subject to a number of process control constraints, material balance constraints, and product rate and grade constraints. The process control constraints were typical valve operational limits of 1% to 99%. The steady state model was set-up to use the optimization algorithm to solve the reactor feed material balances at the optimal plant operating conditions. Using the optimizer to converge six of the reactor feed material balances for components A to C and F to H increased the robustness of the steady state model and optimization algorithm. The reactor feed material balances for components D and E were used to calculate Stream 2 and Stream 3 flow rates to determine their respective

valve positions. These two valve positions are included as non-linear constraints in the optimization algorithm. The product grade and product rate constraints were obtained from the process description given by Downs and Vogel. For Modes 1 to 3, the product grade and product rate were both fixed constraints. For Modes 4 to 6, the product grade was fixed, and the product rate was first maximized.

Through careful examination of the model and process, fifteen nonlinear constraints were identified for the optimization algorithm for all six modes of operation. Six constraints were derived from the reactor feed material balances. Two constraints were derived from the summation of mole fractions in Streams 6 and 10. Two constraints were based on production rate and product G mole fraction which corresponded to the different product grades. The remaining constraints were based on valve operational limits of 1% to 99%.

Table 9.2 lists the nonlinear constraints with upper and lower bounds. The mathematical formulation for the constraints were set equal to zero and calculated as shown in Equation 9.1 for the production rate, product G mole fraction, reactor material balances, and mole fraction summations.

Table 9.1. Constraints on Decision Variables for Modes 1 to 6

	Decision Variable	Lower Bound	Upper Bound
1	Reactor Temperature [°C]	115.0	140.0
2	Reactor Pressure [kPa]	2600.0	2800.0
3	Reactor Level [%]	50.0	90.0
4	Separator Pressure [kPa]	2625.0	2775.0
5	Separator Temperature [°C]	75.0	95.0
6	Stripper Pressure [kPa]	2825.0	3400.0
7	Stripper Temperature [°C]	50.0	80.0
8	Stream 4 Valve [%]	1.0	99.0
9	Stream 9 Valve [%]	1.0	99.0
10	Stream 10 Valve [%]	1.0	99.0
11	Stream 6 Flow [lbmol/h]	1.0×10^{-4}	5900.0
12	Stream 6 A Mole Fraction [%]	1.0×10^{-4}	50.0
13	Stream 6 B Mole Fraction [%]	1.0×10^{-4}	50.0
14	Stream 6 C Mole Fraction [%]	1.0×10^{-4}	50.0
15	Stream 6 D Mole Fraction [%]	1.0×10^{-4}	50.0
16	Stream 6 E Mole Fraction [%]	1.0×10^{-4}	50.0
17	Stream 6 F Mole Fraction [%]	1.0×10^{-4}	50.0
18	Stream 6 G Mole Fraction [%]	1.0×10^{-4}	50.0
19	Stream 6 H Mole Fraction [%]	1.0×10^{-4}	50.0

Table 9.2. Nonlinear Constraints for Modes 1 to 6

	Nonlinear Constraint	Lower Bound	Upper Bound
1	Production Rate [%]	-1.0×10^{-2}	1.0×10^{-2}
2	Product G Mole Fraction [%]	-1.0×10^{-2}	1.0×10^{-2}
3	Stream 2 Valve [%]	1.0	99.0
4	Stream 3 Valve [%]	1.0	99.0
5	Stream 11 Valve [%]	1.0	99.0
6	Stream 14 Valve [%]	1.0	99.0
7	Stream 15 Valve [%]	1.0	99.0
8	A Reactor Feed Balance [lbmol/h]	-1.0×10^{-4}	1.0×10^{-4}
9	B Reactor Feed Balance [lbmol/h]	-1.0×10^{-4}	1.0×10^{-4}
10	C Reactor Feed Balance [lbmol/h]	-1.0×10^{-4}	1.0×10^{-4}
11	F Reactor Feed Balance [lbmol/h]	-1.0×10^{-4}	1.0×10^{-4}
12	G Reactor Feed Balance [lbmol/h]	-1.0×10^{-4}	1.0×10^{-4}
13	H Reactor Feed Balance [lbmol/h]	-1.0×10^{-4}	1.0×10^{-4}
14	Stream 6 Sum of Mole Fraction	-1.0×10^{-4}	1.0×10^{-4}
15	Stream 10 Sum of Mole Fraction	-1.0×10^{-4}	1.0×10^{-4}

$$0 = C_{i,Desired} - C_{i,Calculated} \qquad (i = 1,2,8...15) \qquad (9.1)$$

The production rate constraint in Table 9.2 was listed as a percentage because the control strategy defined by Ricker (1996) related nominal production rate of 23.0 m^3/h to 100% production rate. The conversion between product rate in m^3/h and product rate in % is given by the following equation.

$$F_{11,\%} = F_{11,\frac{m^3}{h}}\left(\frac{100}{23.0}\right) \qquad (9.2)$$

9.3. Other Manipulated Variables

The separator and stripper levels were determined to have no effect on the total operating cost objective function. Thus, these levels are not included in the decision variables or nonlinear constraints for the optimization algorithm. The level controls on the separator and stripper were set to 50%, which was well in between the alarm limits. The level setpoints were implemented after the optimizer determined the optimal operating setpoints for the applied control strategy.

The agitator speed only affected the heat transfer coefficients in the reactor as mentioned in the process assumptions by Downs and Vogel (1993). The effect of agitator speed on heat transfer coefficients was not modeled. The agitator speed does not affect the total cost objective function. However from process observations, when the agitator speed was maximized, the required reactor coolant rate was reduced. The reactor coolant rate does not affect the total operating costs. Thus to maximize the reactor coolant rate cooling capacity, the agitator speed was set to 100% after the optimization algorithm determined the optimal operating conditions.

9.4 .Optimization Solution Path for Modes 1 to 3

A optimization solution path was developed to determine the optimal operating conditions for the process for Modes 1 to 3. Figure 9.1 shows the path used for Modes 1 to 3. The fixed product G

mole fraction (i.e., product grade) and fixed production rate were specified before the optimization algorithm was used to minimize the total operating costs. The fixed production rate was specified as 100%, 99%, and 79% for Modes 1 to 3, respectively. The fixed mole fraction of component G specified was 53.83%, 11.66%, and 90.09% for Modes 1 to 3, respectively.

When at steady state, the current steady state process conditions were used to initialize the nineteen decision variables for NPSOL. NPSOL used a successive quadratic programming technique to determine the gradient search paths to follow to minimize the total operating costs. Subroutine calls made by NPSOL to evaluate the objective function, the nonlinear constraints, the objective gradients, and the nonlinear constraint gradients required the use of the steady state model solution path described in Chapter 7 and shown in Figure 7.1. When NPSOL determined an optimal solution for minimizing total operating costs, the optimal setpoints were calculated and implemented as described in a later section of this chapter.

9.5. Optimization Solution Path for Modes 4 to 6

For Modes 4 to 6, the production rate was to be maximized. Since the plant operator would not know the maximum production rate of the plant for the current operating conditions, a second optimization (i.e., a maximization) for production rate had to be performed on top of the optimization to minimize the total operating costs. From

observation of the process, component D was determined to be the limiting reactant for Mode 4 and Mode 6 while component E was the limiting reactant for Mode 5.

Initially, Stream 3 flow rate for Mode 4 and Mode 6 and Stream 4 flow rate for Mode 5 in the steady state model were set to the maximum value as determined by the data from Downs and Vogel (1993). Nonlinear constraint 3, for Mode 4 and Mode 6, and nonlinear constraint 4, for Mode 5, were replaced with the reactor feed material balances for components D and E, respectively. The production rate constraint, nonlinear constraint 1, was removed. However, convergence for this algorithm was unreliable often resulting no optimized solution and no increase in production rate.

A different approach was finally employed to determine the optimal operating conditions at a maximized production rate using NPSOL. A step-size doubling method was used to increase the production rate from the current production rate until NPSOL was unable to determine a converged solution for the given production rate. Initially, $\Delta F_{11,\%,j}$ in Equation 5.3 was set equal to 0.5%.

$$F_{11,\%,j} = F_{11,\%,j-1} + \Delta F_{11,\%,j} \tag{9.3}$$

where

$$\Delta F_{11,\%,j} = 2.0 \Delta F_{11,\%,j-1} \tag{9.4}$$

The step-size doubling method was used to effectively bound the maximum production rate for the current process conditions. However, the upper bound on production rate often represented an infeasible maximum production rate (i.e., NPSOL did not obtain a feasible, converged solution). The change made to $F_{11,\%}$ in the latest iterative step was too large to properly determine the true maximum production rate.

Using an interval halving technique, $F_{11,\%}$ (from the last step-size doubling iteration) was decreased until NPSOL determined a feasible, converged solution for the given production rate.

$$F_{11\%,j} = F_{11\%,j-1} - \Delta F_{11\%,j} \tag{9.4}$$

where

$$\Delta F_{11,\%,j} = 0.5\Delta F_{11,\%,j-1} \quad . \tag{9.5}$$

The step-size doubling method and integral halving method were then repeated again (with $\Delta F_{11,\%,j}$ reset back to 0.5%) starting with the new, feasible production rate as the lower bound on production rate. If NPSOL failed to determine an minimum in operating costs for a given production rate when the interval halving method was used and $\Delta F_{11,\%,j}$ was less than or equal to 0.25%, the entire optimization routine was stopped. The last production rate which produce a feasible, converged optimum from NPSOL was taken to be

the maximum production rate for the current process conditions. The optimal setpoints for the control strategy were then calculated and implemented as described in a later section of this chapter.

The final optimization solution path for Modes 4 to 6 was very similar to the optimization solution path for Mode 1 to Mode 3. Figure 9.2 shows the optimization solution path for Modes 4 to 6. At steady state, an initial production rate based the current process conditions started the step-size doubling/ interval halving algorithm. The fixed product grade for G/H was specified before entering NPSOL. The current, steady state process conditions were used to initialize the nineteen decision variables for optimization. NSPOL and the steady state model were used to determine the operating conditions which minimized the total operating costs for the maximized production rate.

9.6. Implementing the Optimal Setpoints

Once NPSOL determined the steady state process conditions for optimal operation of the process at the different modes of operation, the optimization information was used to calculate the new controller setpoints. When implementing an optimized solution for the controller setpoints, the entire setpoint solution set must be used. Implementing only part of the setpoint solutions can result increased operation costs or infeasible process operation (Marlin and Hrymak, 1996). Also, the new setpoints must be evaluated to determine whether the changes in the process represent a

meaningful change from the current process conditions. Only when the change is significant enough to offset upsetting the steady state operation of the plant should the process setpoint change be implemented.

Even with the robust control strategy designed by Ricker (1996), the new master controller setpoints could not be introduced into the system instantly because sudden, large changes in the controller setpoints would result in large deviations in the flow rates of Streams 1 to 4 and sometimes Stream 11. Downs and Vogel limited the maximum allowable changes in stream flows to ±5% during product rate changes and disturbances (Downs and Vogel, 1993). Therefore, maximum ramp rates for each master controller, which did not cause deviations in the stream flow rates greater than ±5%, were calculated through a series of setpoint tests using the TE simulation. Each change in controller setpoint was converted to a ramp with a ramp time determined from a maximized ramp rate. Table 9.3 lists the maximum ramp rates used for the master controller setpoint changes in the Ricker (1996) control scheme.

Table 9.3. Maximum Ramp Rates for Controller Setpoints

Loop	Controlled Variable	Maximum Ramp Rate
8	Production Rate	30% /14 hr
9	Stripper Liquid Level	10 % / 5 hr
11	Reactor Liquid Level	10 % /5 hr
12	Reactor Pressure	100 kPa / 5 hr
13	Mol %G in Stream 11	50 % / 14 hr
14	y_A	1 % / 2 hr
15	y_{A+C}	1 % / 2 hr
16	Reactor Temperature	1 °C / 2 hr
	Steam Valve	5 % / 1 hr
	Agitator Speed	5 % / 1 hr
	Recycle Valve	5 % / 1 hr

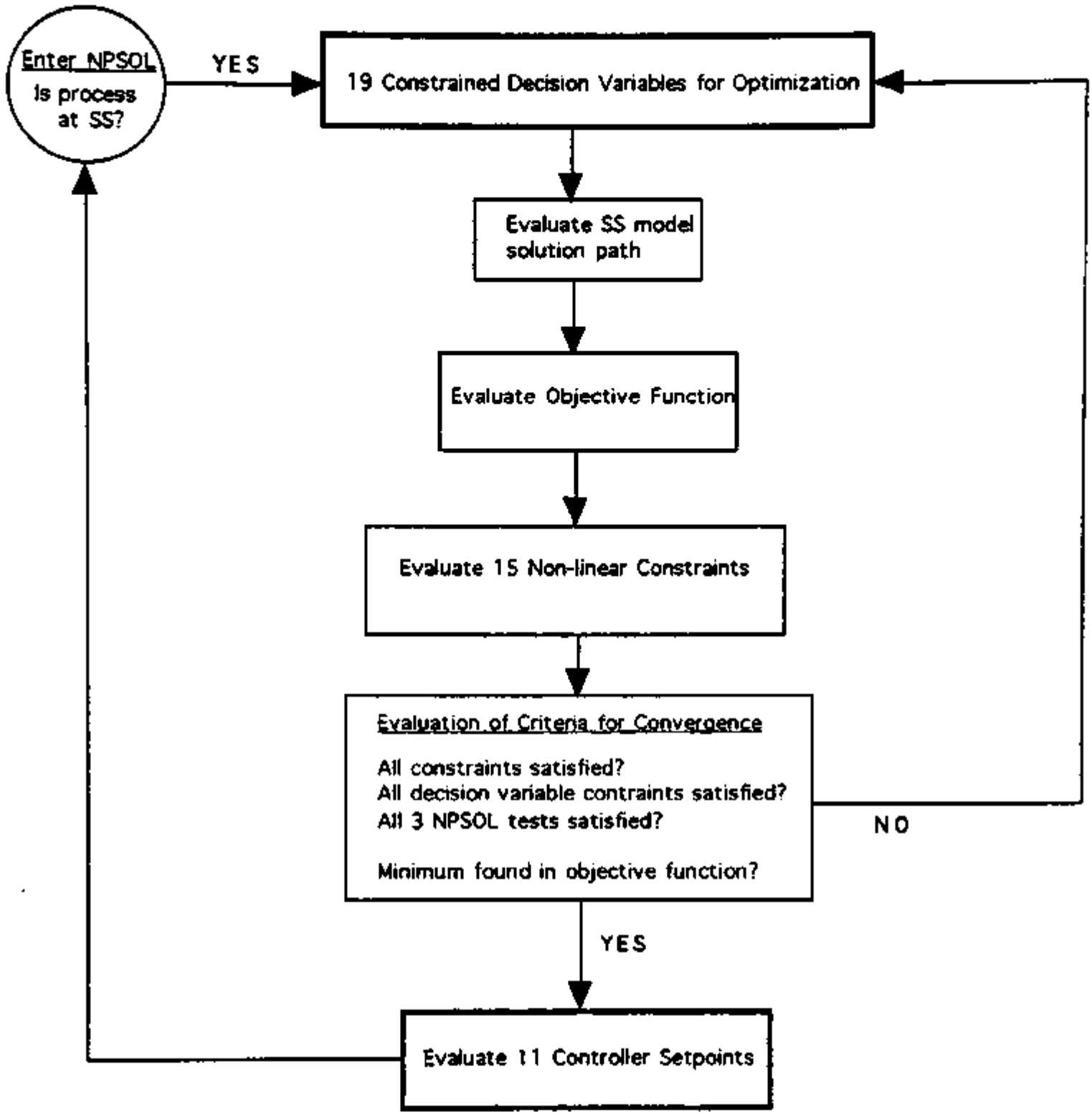

Figure 9.1. Modes 1 to 3 Optimization Path

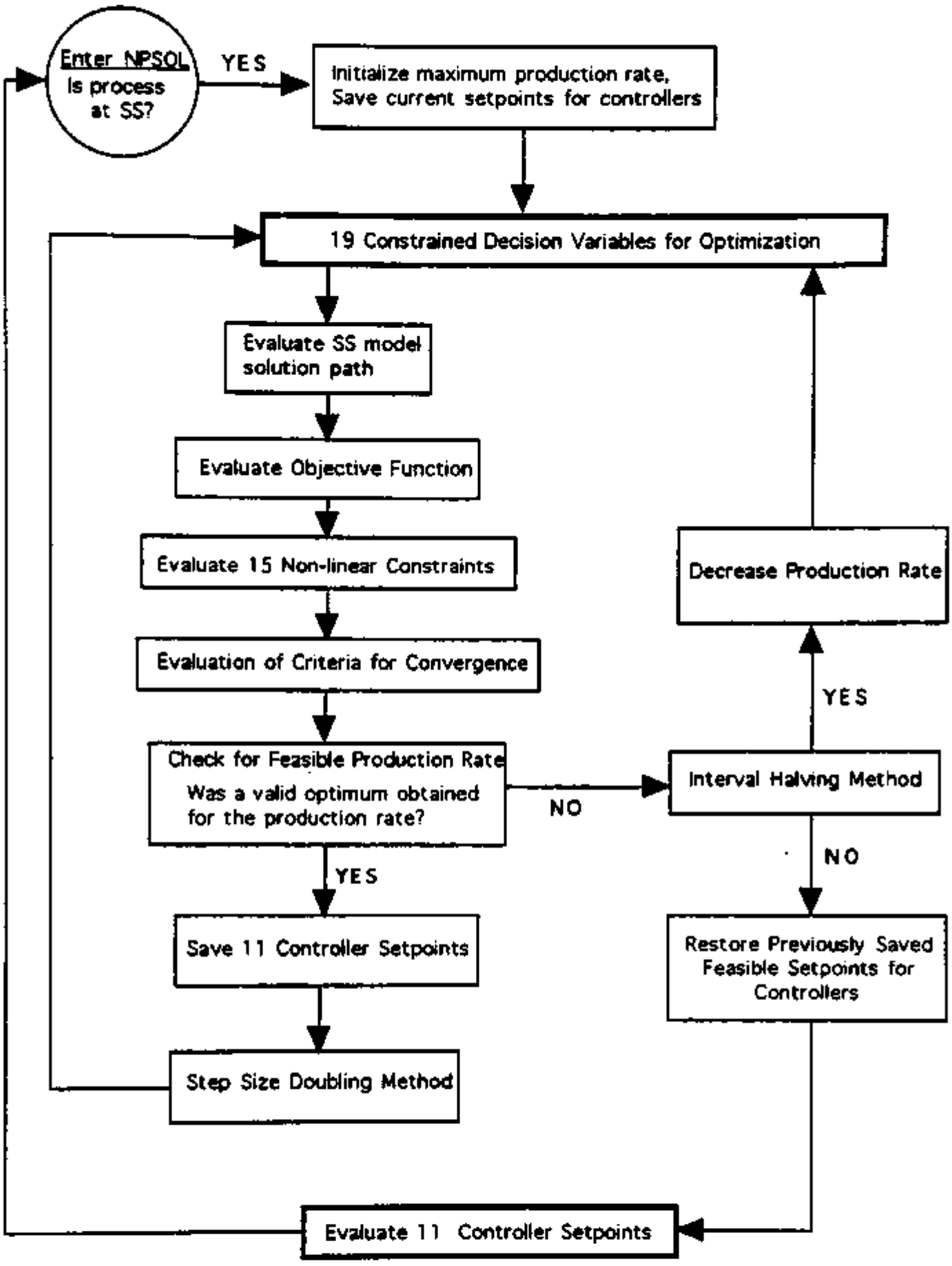

Figure 9.2. Modes 4 to 6 Optimization Path

CHAPTER 10
RESULTS AND DISCUSSION

The control scheme proposed by Ricker (1996) was implemented on the TE process for control during optimization. The modifications to the control scheme detailed in Chapter 4 were also implemented. The results for the on-line, model based, steady state optimization of the TE process have been separated into two different cases based on what optimization results were being compared.

Case I. Comparison of operating costs for on-line optimization to off-line optimization for the six modes of operation;

Case II. Comparison of profits and costs for on-line optimization to operator optimization.

10.1. Case I. Comparison of Off-line to On-line Results

Ricker (1995b) used the exact process states and derivatives with noiseless measurements from the TE simulator provided by Downs and Vogel (1993) to determine the theoretical, optimal steady state operating conditions for the TE process for the six different modes of operation. However, full knowledge of the process states and derivatives with noiseless measurements are conditions which are never satisfied in real processes. The results from Ricker's work were used as a benchmark when analyzing the on-line optimization results of this reasearch. Ricker's optimization

results are referred to as 'off-line' optimization results for remainder the of results discussion.

Using the model-based optimization routine described in Chapter 9, the optimal operating conditions for Mode 1 to Mode 6 were determined. The initial conditions for the optimization of Modes 1 and 4 were the base case conditions from Downs and Vogel (1993). The initial conditions for the optimization of Modes 2 and 5 were taken from the base case conditions given by Downs and Vogel as well. The %G setpoint in Stream 11 was moved to 11.66 mol% while the other operating setpoints for the modified Ricker control scheme remained fixed. For the initial conditions for Modes 3 and 6, the base case conditions were used with a setpoint of 90.09 mol% for %G in Stream 11. The agitator speed was set to 100% to maximize the cooling capacity of the reactor coolant. The separator and stripper levels were set to 50%. These last three setpoints do not influence the total operating cost objective function.

In Modes 1 to 3 of operation, the production rate was specified. In Modes 4 to 6 of operation, the production rate was maximized. While the production rates differed slightly in Modes 1 to 6 of operation when compared to the rates described by Ricker (1995b), the rates are close enough to make a direct comparison to Ricker's optimal results to determine how well the model predicts optimal operating conditions.

Table 10.1 to Table 10.9 summarize the steady state process operating conditions, manipulated variables, and costs for the

optimal operating conditions. These tables compare the on-line optimization results of this research to the theoretical, off-line optimization results by Ricker (1995a). Values for the on-line optimization results are based on two hour averages of the filtered measurements.

In all six modes of operation, the feed composition for components A to F was approximately the same as the base case. For all six modes of operation, the optimal reactor pressure was at the upper bound of 2800 kPa while the optimal reactor level was at the lower bound of 65.0 %. A lower liquid level resulted in a large reaction volume in the vapor phase which increased the reaction rates. From the model equations for the reactor in Chapter 5, higher partial pressures (i.e., higher reactor pressure) combined with a large vapor reaction volume tend to maximize production of G and H in the reactor for a constant composition feed stream. Overall, purge losses tended to dominate the over operating costs while steam use in the stripper was set to 1% (i.e., the lower bound).

For Modes 1 to 3, the compressor costs tended to be higher due to the use of the compressor recycle valve (i.e., always greater then 1%). However for Modes 4 to 6, the optimizer discontinued use of

Table 10.1. Steady State Measured Variables for On-Line and Off-Line Optimization of Mode 1 and Mode 4

Measurements	Error	On-line Mode 1 (Duvall)	Off-line Mode 1 (Ricker)	On-line Mode 4 (Duvall)	Off-line Mode 4 (Ricker)
A feed [kscmh]	±0.002	0.269	0.267	0.432	0.503
D feed [kg/h]	±20.	3680.	3660.	5710.	5810.
E feed [kg/h]	±20.	4460.	4440.	6950.	7240.
A/C feed [kscmh]	±0.05	9.32	9.24	14.27	14.73
Recycle flow [kscmh]	±0.2	28.7	32.2	27.9	29.2
Reactor feed [kscmh]	±0.2	43.9	47.4	51.8	53.8
Reactor pressure [kPa]	±0.7	2800.0	2800.0	2800.0	2800.0
Reactor level [%]	±0.4	65.0	65.0	65.0	65.0
Reactor temp [°C]	±0.01	124.17	122.90	127.64	128.20
Purge rate [kscmh]	±0.01	0.24	0.21	0.38	0.46
Sep temp [°C]	±0.04	89.71	91.7	71.3	74.1
Sep level [%]	±1.	50.	50.	50.	50.
Sep press [kPa]	±0.8	2724.0	2706.0	2700.	2699.
Sep underflow [m^3/h]	±0.1	24.7	25.2	39.5	40.1
Stripper level [%]	±1.	50.	50.	50.	50.
Stripper press [kPa]	±1.	3321.	3326.	3357.	3365.
Strpr underflow [m^3/h]	±0.2	23.0	22.9	35.0	36.0
Stripper temp [°C]	±0.3	65.6	66.5	48.4	51.5
Steam flow [kg/h]	±1.	5.	5.	7.	7.
Comp. work [kW]	±0.2	349.4	278.9	257.4	263.2
Reac. cool temp. [°C]	±0.02	103.23	102.40	97.20	96.60
Cond. cool temp. [°C]	±0.07	88.40	92.00	69.04	73.50
Feed % A [mol%]	±0.2	33.4	32.2	33.6	36.4
Feed % B [mol%]	±0.1	12.8	14.9	10.3	8.8
Feed % C [mol%]	±0.2	22.5	18.8	22.9	22.4
Feed % D [mol%]	±0.1	6.3	6.0	8.2	8.0
Feed % E [mol%]	±0.3	14.4	16.7	18.4	17.0
Feed % F [mol%]	±0.02	3.85	4.04	3.49	3.88
Purge % A [mol%]	±0.2	34.4	32.7	35.9	40.9
Purge % B [mol%]	±0.1	19.5	21.8	18.9	15.9
Purge % C [mol%]	±0.2	17.8	13.1	17.0	15.7
Purge % D [mol%]	±0.2	0.6	0.9	0.8	0.7
Purge % E [mol%]	±0.1	12.9	16.2	17.3	15.4
Purge % F [mol%]	±0.2	5.3	5.4	5.1	5.7
Purge % G [mol%]	±0.02	6.37	6.62	3.50	3.85
Purge % H [mol%]	±0.05	3.07	3.23	1.59	1.82
Prod % D [mol%]	±0.05	0.01	0.01	0.02	0.02
Prod % E [mol%]	±0.01	0.47	0.58	1.64	1.21
Prod % F [mol%]	±0.01	0.19	0.19	0.47	0.04
Prod % G [mol%]	±0.4	53.9	53.8	53.8	53.4
Prod % H [mol%]	±0.6	43.6	43.9	42.8	43.5

Table 10.2. Steady State Measured Variables for On-Line and Off-Line Optimization of Mode 2 and Mode 5

Measurements	Error	On-line Mode 2 (Duvall)	Off-line Mode 2 (Ricker)	On-line Mode 5 (Duvall)	Off-line Mode 5 (Ricker)
A feed [kscmh]	±0.002	0.304	0.309	0.309	0.325
D feed [kg/h]	±20.	760.	730.	760.	760.
E feed [kg/h]	±20.	8210.	8040.	8210.	8350.
A/C feed [kscmh]	±0.05	8.77	8.55	8.81	8.87
Recycle flow [kscmh]	±0.2	26.7	31.7	31.6	31.3
Reactor feed [kscmh]	±0.2	41.4	46.1	46.3	46.2
Reactor pressure [kPa]	±0.7	2800.0	2800.0	2800.0	2800.0
Reactor level [%]	±0.4	65.0	65.0	65.0	65.0
Reactor temp [°C]	±0.01	125.45	124.20	125.20	124.60
Purge rate [kscmh]	±0.01	0.38	0.36	0.42	0.38
Sep temp [°C]	±0.04	83.80	90.30	91.37	88.90
Sep level [%]	±1.	50.	50.	50.	50.
Sep press [kPa]	±0.8	2727.0	2705.0	2705.0	2705.0
Sep underflow [m^3/h]	±0.1	26.5	26.3	26.3	27.5
Stripper level [%]	±1.	50.	50.	50.	50.
Stripper press [kPa]	±1.	3207.	3327.	3328.	3330.
Strpr underflow [m^3/h]	±0.2	22.2	22.7	23.3	23.6
Stripper temp [°C]	±0.3	59.9	65.4	67.0	63.9
Steam flow [kg/h]	±1.	6.	5.	5.	5.
Comp. work [kW]	±0.2	341.2	274.7	275.5	271.7
Reac. cool temp. [°C]	±0.02	109.30	108.60	109.00	108.50
Cond. cool temp. [°C]	±0.07	80.70	91.60	92.74	89.80
Feed % A [mol%]	±0.2	34.2	34.8	34.5	34.8
Feed % B [mol%]	±0.1	7.6	8.2	7.1	7.9
Feed % C [mol%]	±0.2	23.1	19.4	22.6	19.5
Feed % D [mol%]	±0.1	1.3	1.2	1.2	1.2
Feed % E [mol%]	±0.3	24.5	25.5	23.8	26.0
Feed % F [mol%]	±0.02	5.20	5.60	5.37	5.60
Purge % A [mol%]	±0.2	36.2	36.6	35.9	36.7
Purge % B [mol%]	±0.1	11.5	11.8	10.3	11.5
Purge % C [mol%]	±0.2	19.2	14.6	19.2	14.6
Purge % D [mol%]	±0.2	0.1	0.1	0.1	0.1
Purge % E [mol%]	±0.1	20.2	22.4	20.0	22.9
Purge % F [mol%]	±0.2	7.1	7.4	7.1	7.4
Purge % G [mol%]	±0.02	1.09	1.32	1.39	1.26
Purge % H [mol%]	±0.05	4.70	5.79	6.11	5.51
Prod % D [mol%]	±0.05	0.01	0.00	0.00	0.00
Prod % E [mol%]	±0.01	1.08	0.92	0.73	1.01
Prod % F [mol%]	±0.01	0.37	0.29	0.26	0.32
Prod % G [mol%]	±0.4	11.7	11.7	11.6	11.7
Prod % H [mol%]	±0.6	85.2	85.6	86.1	85.5

Table 10.3. Steady State Measured Variables for On-Line and Off-Line Optimization of Mode 3 and Mode 6

Measurements	Error	On-line Mode 3 (Duvall)	Off-line Mode 3 (Ricker)	On-line Mode 6 (Duvall)	Off-line Mode 6 (Ricker)
A feed [kscmh]	±0.002	0.214	0.194	0.211	0.219
D feed [kg/h]	±20.	5750.	5180.	5750.	5810.
E feed [kg/h]	±20.	770.	700.	780.	790.
A/C feed [kscmh]	±0.05	8.70	7.83	8.71	8.79
Recycle flow [kscmh]	±0.2	27.6	19.7	32.5	20.1
Reactor feed [kscmh]	±0.2	41.5	32.1	46.4	34.0
Reactor pressure [kPa]	±0.7	2750.0	2800.0	2800.0	2800.0
Reactor level [%]	±0.4	65.0	65.0	65.0	65.0
Reactor temp [°C]	±0.01	125.10	121.90	125.31	123.00
Purge rate [kscmh]	±0.01	0.10	0.09	0.11	0.10
Sep temp [°C]	±0.04	100.10	83.40	103.10	80.90
Sep level [%]	±1.	50.	50.	50.	50.
Sep press [kPa]	±0.8	2626.1	2765.0	2707.0	2761.0
Sep underflow [m^3/h]	±0.1	20.7	17.6	20.7	19.6
Stripper level [%]	±1.	50.	50.	50.	50.
Stripper press [kPa]	±1.	3113.	2996.	3315.	3015.
Strpr underflow [m^3/h]	±0.2	20.3	18.0	20.6	20.2
Stripper temp [°C]	±0.3	73.4	62.3	75.6	60.5
Steam flow [kg/h]	±1.	4.	5.	3.	6.
Comp. work [kW]	±0.2	325.2	272.6	284.1	293.2
Reac. cool temp. [°C]	±0.02	102.51	101.90	102.80	100.60
Cond. cool temp. [°C]	±0.07	93.84	45.00	101.51	45.7
Feed % A [mol%]	±0.2	25.8	29.5	26.6	30.0
Feed % B [mol%]	±0.1	27.3	27.7	27.1	26.3
Feed % C [mol%]	±0.2	17.5	18.	18.	18.8
Feed % D [mol%]	±0.1	11.0	12.7	9.7	13.2
Feed % E [mol%]	±0.3	4.2	3.9	3.5	3.9
Feed % F [mol%]	±0.02	2.30	1.29	2.39	1.33
Purge % A [mol%]	±0.2	22.7	27.9	24.3	28.6
Purge % B [mol%]	±0.1	41.0	45.1	38.5	44.4
Purge % C [mol%]	±0.2	10.6	9.2	12.1	9.8
Purge % D [mol%]	±0.2	1.9	2.2	1.4	2.1
Purge % E [mol%]	±0.1	4.5	3.9	3.5	4.0
Purge % F [mol%]	±0.2	3.2	1.8	3.2	1.9
Purge % G [mol%]	±0.02	15.32	9.40	16.12	8.76
Purge % H [mol%]	±0.05	0.86	0.50	0.88	0.46
Prod % D [mol%]	±0.05	0.02	0.03	0.01	0.03
Prod % E [mol%]	±0.01	0.11	0.16	0.07	0.18
Prod % F [mol%]	±0.01	0.06	0.07	0.07	0.08
Prod % G [mol%]	±0.4	89.9	90.1	90.1	90.1
Prod % H [mol%]	±0.6	8.1	8.2	8.2	8.2

Table 10.4. Steady State Manipulated Variables for On-Line and Off-Line Optimization of Mode 1 and Mode 4

Manipulated Variable	Error	On-line Mode 1 (Duvall)	Off-line Mode 1 (Ricker)	On-line Mode 4 (Duvall)	Off-line Mode 4 (Ricker)
D Feed [%]	±0.08	63.40	62.93	98.30	100.00
E Feed [%]	±0.08	53.35	53.14	83.17	86.72
A Feed [%]	±0.1	26.5	26.2	42.5	49.5
A+C Feed [%]	±0.08	61.13	60.56	93.58	96.59
Recycle Valve [%]	±0.08	18.90	1.00	1.00	1.00
Purge Valve [%]	±0.9	27.5	25.8	42.5	48.7
Separator Valve [%]	±0.02	36.77	37.26	60.37	60.96
Stripper Valve [%]	±0.01	46.70	46.44	72.61	74.52
Steam Valve [%]	±0.08	1.00	1.00	1.00	1.00
Reactor Coolant [%]	±0.08	36.43	35.99	58.06	60.79
Condn Coolant [%]	±0.08	12.74	12.43	40.73	35.53
Agitator Speed [%]	±0.08	100.00	100.00	100.00	100.00

Table 10.5. Steady State Manipulated Variables for On-Line and Off-Line Optimization of Mode 2 and Mode 5

Manipulated Variable	Error	On-line Mode 2 (Duvall)	Off-line Mode 2 (Ricker)	On-line Mode 5 (Duvall)	Off-line Mode 5 (Ricker)
D Feed [%]	±0.08	13.02	12.64	12.97	13.10
E Feed [%]	±0.08	98.33	96.22	98.36	100.00
A Feed [%]	±0.1	29.9	30.4	30.3	32.0
A+C Feed [%]	±0.08	57.54	56.09	57.73	58.16
Recycle Valve [%]	±0.08	22.34	1.00	1.00	1.00
Purge Valve [%]	±0.9	45.3	44.4	51.2	47.1
Separator Valve [%]	±0.02	36.64	35.80	35.84	37.42
Stripper Valve [%]	±0.01	43.91	42.87	43.73	44.49
Steam Valve [%]	±0.08	1.00	1.00	1.00	1.00
Reactor Coolant [%]	±0.08	25.80	25.26	25.92	26.07
Condn Coolant [%]	±0.08	16.59	12.91	12.15	14.12
Agitator Speed [%]	±0.08	100.00	100.00	100.00	100.00

Table 10.6. Steady State Manipulated Variables for On-Line and Off-Line Optimization of Mode 3 and Mode 6

Manipulated Variable	Error	On-line Mode 3 (Duvall)	Off-line Mode 3 (Ricker)	On-line Mode 6 (Duvall)	Off-line Mode 6 (Ricker)
D Feed [%]	±0.08	99.0	89.13	99.0	100.00
E Feed [%]	±0.08	9.27	8.38	9.34	9.44
A Feed [%]	±0.1	21.0	19.1	20.8	21.5
A+C Feed [%]	±0.08	57.04	51.37	57.17	57.64
Recycle Valve [%]	±0.08	17.04	77.62	1.00	71.17
Purge Valve [%]	±0.9	13.2	9.5	13.8	10.7
Separator Valve [%]	±0.02	32.99	29.15	32.95	32.69
Stripper Valve [%]	±0.01	43.66	39.43	43.66	44.25
Steam Valve [%]	±0.08	1.00	1.00	1.00	1.00
Reactor Coolant [%]	±0.08	39.78	35.55	39.39	40.54
Condn Coolant [%]	±0.08	8.89	99.00	7.87	99.00
Agitator Speed [%]	±0.08	100.00	100.00	100.00	100.00

Table 10.7. Steady State Operating Costs for On-Line and Off-Line Optimization of Mode 1 and Mode 4

Operating Costs	Error	On-line Mode 1 (Duvall)	Off-line Mode 1 (Ricker)	On-line Mode 4 (Duvall)	Off-line Mode 4 (Ricker)
Purge Losses [$/h]	±5.	79.	74.	118.	142.
Product Losses [$/h]	±1.	22.	25.	106.	87.
Compressor [$/h]	±0.03	18.73	14.95	13.80	14.11
Steam [$/h]	±0.02	0.16	0.15	0.23	0.22
Total Cost [$/h]	±3.	120.	114.	234.	244.
Per Unit Product [¢/kg]	±0.02	0.85	0.81	1.12	1.09

Table 10.8. Steady State Operating Costs for On-Line and Off-Line Optimization of Mode 2 and Mode 5

Operating Costs	Error	On-line Mode 2 (Duvall)	Off-line Mode 2 (Ricker)	On-line Mode 5 (Duvall)	Off-line Mode 5 (Ricker)
Purge Losses [$/h]	±5.	131.	130.	150.	138.
Product Losses [$/h]	±1.	45.	36.	31.	41.
Compressor [$/h]	±0.03	18.29	14.72	14.76	14.56
Steam [$/h]	±0.02	0.18	0.16	0.14	0.16
Total Cost [$/h]	±3.	194.	181.	196.	195.
Per Unit Product [¢/kg]	±0.02	1.35	1.29	1.34	1.33

Table 10.9. Steady State Operating Costs for On-Line and Off-Line Optimization of Mode 3 and Mode 6

Operating Costs	Error	On-line Mode 3 (Duvall)	Off-line Mode 3 (Ricker)	On-line Mode 6 (Duvall)	Off-line Mode 6 (Ricker)
Purge Losses [$/h]	±5.	36.	22.	38.	24.
Product Losses [$/h]	±1.	6.	7.	5.	9.
Compressor [$/h]	±0.03	17.44	14.61	15.54	15.72
Steam [$/h]	±0.02	0.12	0.17	0.11	0.18
Total Cost [$/h]	±3.	58.	43.	59.	49.
Per Unit Product [¢/kg]	±0.02	0.48	0.40	0.47	0.39

the recycle valve (i.e., set to 1%) further reducing the compressor costs. The recycle valve and other steady state process conditions such as reactor temperature seem not to have *a priori* optimal values.

10.2. Case II. Comparison of Operator versus Optimizer

The above results show that the model-based optimization algorithm was able to approach closely the theoretical, optimal operating conditions calculated by Ricker (1995b). However for real life processes, the theoretical, optimal operating conditions are never known because models are rarely exact representations of the process. Models tend to be simplifications of the process which detail the particular process characteristics of interest.

As discussed in the introduction, some criteria must be meet by an on-line optimization routine in order for the optimization to be considered useful. Among the criteria were the following.

1. The model-based optimization has to provide a major benefit in increased production and/or decreased operating costs over the standard operating procedures used in the plant;
2. Disturbances must occur frequently enough for on-line adjustments to be required.

Plant operators, through daily control of the process, know how process setpoints affect production or operating costs. From daily observation of the TE process or a listing of standard operating procedures, the operator would use high reactor pressures and low reactor levels to decrease operating costs and increase production. The operator would also use the maximum agitator speed to increase the reactor cooling capacity. All of these process conditions occur

at an upper or lower process bound specified by standard process operating practices.

The rest of the process conditions (or setpoints for controllers) have arbitrary values for the process operator to set. For example with an allowable operating range of 120 °C to 140 °C for reactor temperature, the operator would probably not choose the correct temperature setpoint for the current process conditions which would minimize operating costs. Also, the operator probably would be using more steam for stripper heating than required which would increase steam costs. These choices and others (as shown later) for plant setpoints affect the maximization of plant production and increase operating costs.

Process disturbances affect the current maximum production rate and profits. At maximum production rates without disturbances in the process, the on-line optimizer would not be required because the process conditions would not change until a product grade change were initiated. Thus, disturbances are used to show the advantages of the on-line optimizer over the operator for maximizing production and profit during daily operation. The remainder of the results below compare profit, operating costs, and maximum production rates for the on-line optimization versus operator process control.

10.2.1. Initial Conditions for Operator Control

The initial process conditions for starting up the TE simulator were based on operator choices for process control. Daily

interaction with the process or a standard operating procedure would help the operator know that following operating conditions tend to increase production and decrease operating costs.

1. Reactor pressure to upper bound of 2800 kPa;
2. Reactor level to lower bound of 65%;
3. Agitator speed to 100%.

Based on the above choices for setpoints for process control, the base case for the TE process was moved to the new process operating conditions using a fixed production rate for all three product grades (i.e., 50/50, 10/90, and 90/10). These three new sets of start-up conditions for the TE process represented the operators best attempt to move the process to operating conditions which would reduce process operating costs while allowing for maximization of production.

10.2.2. Net Profit Function

After running several tests to determine the maximum production rates for Modes 4 to 6 based on the operator process settings and optimizer process settings, the operator based maximum production rates were not the same as the on-line optimization maximum rates. A direct comparison of total operating costs would not be accurate for different production rates. Thus, a new profit equation was used to compare the net profit from operator and on-line optimization control of the process based on different maximum production rates.

$$N_{Profit} = P_{Profit} - C_{Tot} \tag{10.1}$$

Here, Np_{rofit} is the net profit for the process. C_{Tot} is the total operating costs defined in the objective function. P_{Profit} is the product profit based on the following equation.

$$P_{Profit} = F_{11}\left(x_{11G} \cdot C_G + x_{11H} \cdot C_H\right) \tag{10.2}$$

$x_{11,G}$ and $x_{11,H}$ are the mole fractions of G and H in Stream 11. C_G and C_H are the costs of G and H defined in Table 3.5. F_{11} is the molar flow rate of Stream 11 (kgmol/h). The cost data for G and H in Table 3.5 initially applied to the losses of G and H in Stream 9 (i.e. the purge losses). Since G and H are the products, the numbers should closely represent the prices to customers of the products of G and H in Stream 11. Changes in the net profit function represents not only the increase in production but also the decrease in operating costs.

10.2.3. Key Controlled Variables

In *Decentralized Control of the TE Challenge Process*, Ricker (1996) identified five key controlled variables for the TE process which did not have *a priori* optimal values (unlike reactor pressure which should be maintained as high as possible). The key controlled variables have a major impact on process operating costs and process stability.

1. Reactor temperature;

2. %A in the reactor feed;

3. %C in the reactor feed;

4. Recycle valve position;

5. Steam valve position.

The operator would not typically adjust these five variables since no clear optimal setpoint is known. The operator would keep these variables in a standard operating range. However, the optimizer adjusted the setpoints for these variables as part of the optimization routine.

10.2.4. Minimization of Cost for Modes 1 to 3

Using the initial operator start-up conditions for the TE process, the process was operated at a fixed production rate for Modes 1 to 3. The fixed production rates were the same as in the previous section for on-line optimization versus off-line optimization results for Modes 1 to 3. From steady state conditions, the operating costs were determined for operator based control of the process. The on-line optimization operating costs were then compared to the operator operating costs.

Tables 10.10 to 10.12 show a comparison of operating costs and key controlled variables for operator and optimizer based control of the TE process for Modes 1 to 3. For all three modes, the optimizer operating costs are lower because the proper ratio of A and C entered the reactor which minimized purge losses. Steam cost was also lower because the steam was not used. Even though the higher

reactor temperature increased the amount of by-product F in the product stream (Stream 11), the higher reactor temperature yielded higher conversions of the reactants which significantly reduced the amount of E in the product stream. Thus, product costs tended to be lower when the optimizer was used.

10.2.5. Maximization of Production for Modes 4 to 6

Using the initial operator start-up conditions for the TE process, the production rate was increased at 5 hours for Modes 4 to 6 until an operator maximum production rate was established for all three modes. Using the same initial conditions but including the on-line optimizer, the optimized maximum production rate was determined beginning with optimizations at 5 hours.

Table 10.10. Comparison of Operator and Optimizer Operating Costs for Mode 1.

Operating Costs and Key Controlled Variables	Error	Mode 1 (50/50) Optimizer	Mode 1 (50/50) Operator
Purge Losses [$/h]	±5.	79.	88.
Product Losses [$/h]	±1.	22.	26.
Compressor [$/h]	±0.03	18.73	18.82
Steam [$/h]	±0.02	0.16	7.18
Total Cost [$/h]	±3.	120.	140.
Per Unit Product [¢/kg]	±0.02	0.85	0.99
Strpr Underflow [m^3/h]	±0.2	23.0	23.1
Reactor Temp [°C]	±0.01	124.17	120.40
Feed A% [mol %]	±0.2	33.4	32.3
Feed C% [mol %]	±0.2	22.5	26.4
Product D% [mol %]	±0.05	0.01	0.01
Product E% [mol %]	±0.01	0.47	0.68
Product F%[mol %]	±0.01	0.19	0.11
Recycle Valve [%]	±0.08	18.90	22.21
Steam Valve [%]	±0.08	1.00	47.45

Table 10.11. Comparison of Operator and Optimizer Operating Costs for Mode 2.

Operating Costs and Key Controlled Variables	Error	Mode 2 (10/90) Optimizer	Mode 2 (10/90) Operator
Purge Losses [$/h]	±5.	131.	154.
Product Losses [$/h]	±1.	45.	62.
Compressor [$/h]	±0.03	18.29	17.55
Steam [$/h]	±0.02	0.18	8.78
Total Cost [$/h]	±3.	194.	242.
Per Unit Product [¢/kg]	±0.02	1.35	1.77
Strpr Underflow [m^3/h]	±0.2	22.3	22.2
Reactor Temp [°C]	±0.01	125.40	120.54
Feed A% [mol %]	±0.2	34.2	31.7
Feed C% [mol %]	±0.2	23.1	26.7
Product D% [mol %]	±0.05	0.01	0.01
Product E% [mol %]	±0.01	1.08	2.00
Product F%[mol %]	±0.01	0.37	0.20
Recycle Valve [%]	±0.08	22.3	22.21
Steam Valve [%]	±0.08	1.00	47.45

Table 10.12. Comparison of Operator and Optimizer Operating Costs for Mode 3.

Operating Costs and Key Controlled Variables	Error	Mode 3 (90/10) Optimizer	Mode 3 (90/10) Operator
Purge Losses [$/h]	±5.	36.	57.
Product Losses [$/h]	±1.	6.	4.
Compressor [$/h]	±0.03	17.44	20.14
Steam [$/h]	±0.02	0.12	5.15
Total Cost [$/h]	±3.	58.	85.0
Per Unit Product [¢/kg]	±0.02	0.48	0.70
Strpr Underflow [m^3/h]	±0.2	20.3	20.4
Reactor Temp [°C]	±0.01	125.10	120.34
Feed A% [mol %]	±0.2	25.8	32.3
Feed C% [mol %]	±0.2	27.3	26.4
Product D% [mol %]	±0.05	0.02	0.01
Product E% [mol %]	±0.01	0.11	0.06
Product F%[mol %]	±0.01	0.06	0.02
Recycle Valve [%]	±0.08	17.04	22.21
Steam Valve [%]	±0.08	1.00	47.45

Table 10.13 summarizes the advantages of using the on-line optimizer for Modes 4 to 6 to maximize production and profit. Figure 10.1, Figure 10.2, and Figure 10.3 compare the key controlled variables (which varied for operator setpoints) for Modes 4 to 6, respectively, for optimizer control (solid line) and operator control (dashed line).

Table 10.13. Advantages for On-line Optimization Over Operator Control for Modes 4 to 6.

Optimizer versus Operator	Mode 4	Mode 5	Mode 6
Change in Production Rate [m^3/h]	+1.5	+0.4	0.0
Change in Product Profit [$/h]	+500.	+160.	0.
Change in Total Operating Cost [$/h]	-200.	-60.	-26.
Change in Net Profit [$/h]	+700.	+220.	+26.
Change in Net Profit [MM $/yr]	+5.88	+1.85	+0.22

For Modes 4 to 6, the optimal steam valve position setpoint was 1% (i.e., not used). The operator setpoint was around 40% which increased the steam operating costs. Typically, the optimal reactor temperature setpoint was between 125°C to 128 °C which was 6°C higher on average than the operator setpoint. Also, the optimal recycle valve setpoint was 1% (i.e., nearly closed) for all three modes; operator setpoints were 25% to 45%. The compression costs were therefore lower for the optimal operation versus the operator operation.

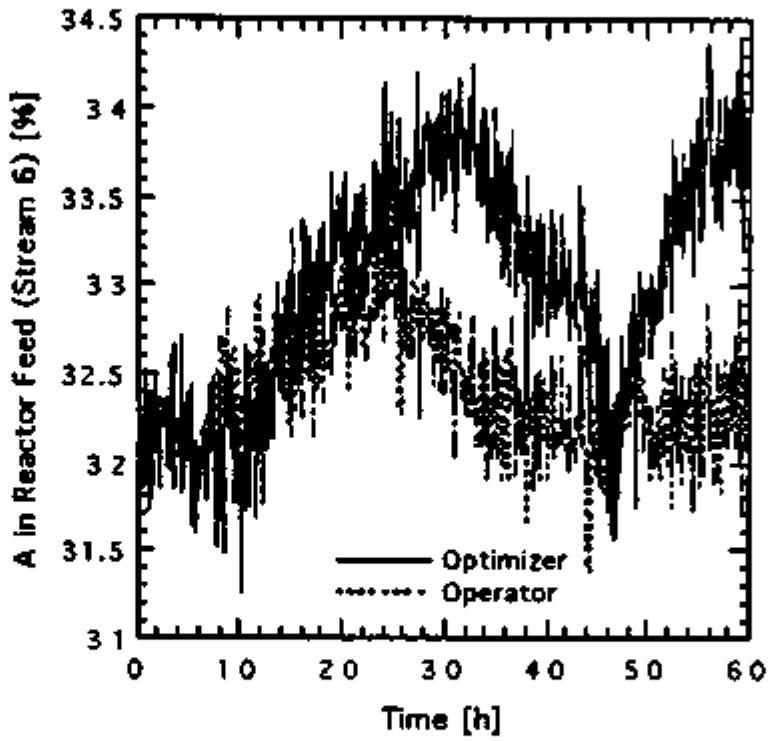

(a)

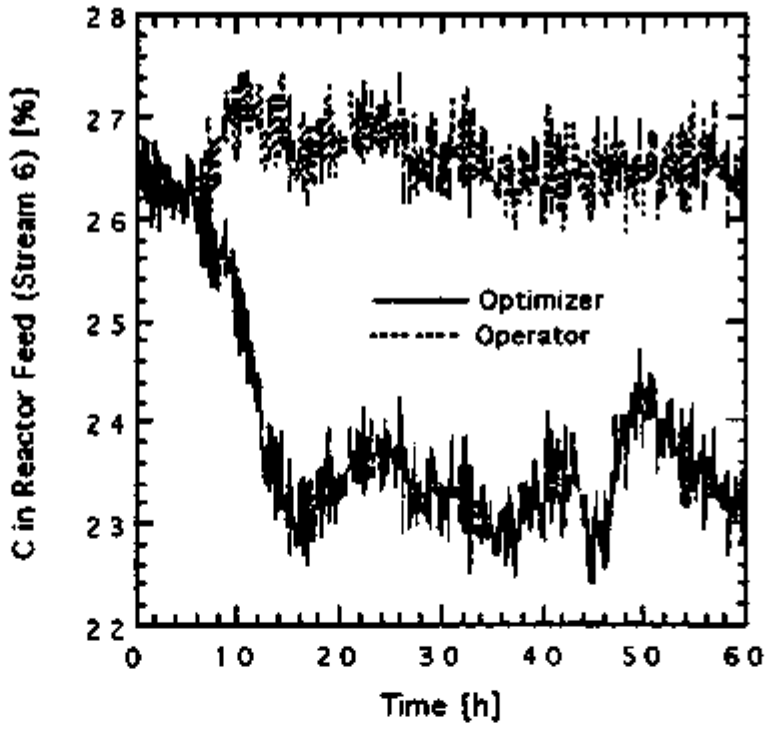

(b)

Figure 10.1. Mode 4 (Maximum Production) for Optimizer Versus Operator. (a) %A in Stream 6. (b) %C in Stream 6.

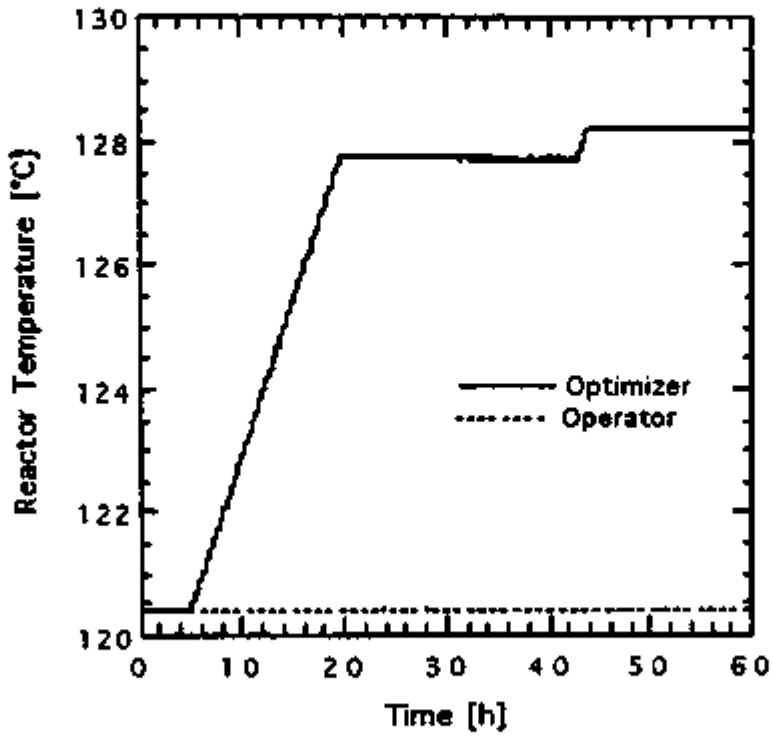

(c)

Figure 10.1. Continued. (c) Reactor Temperature.

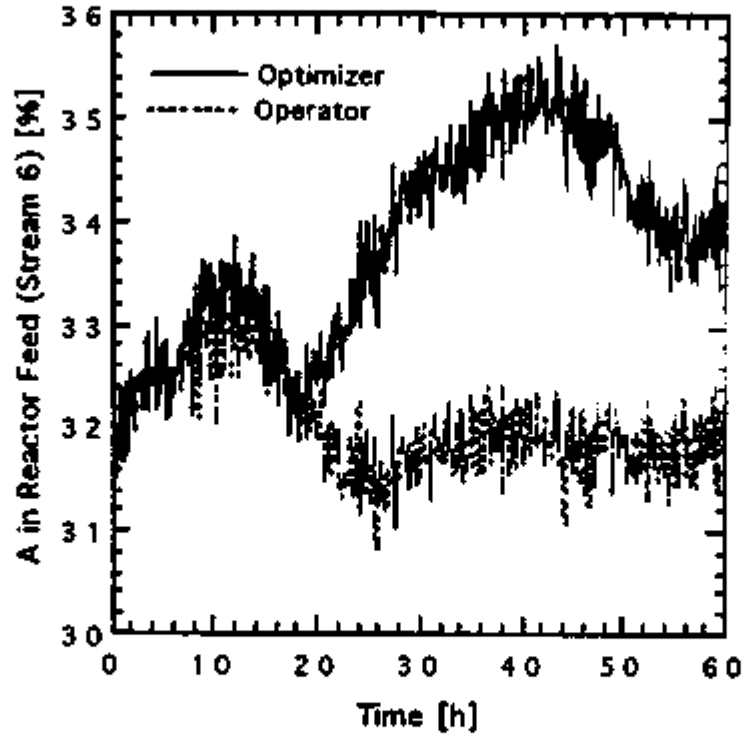

(a)

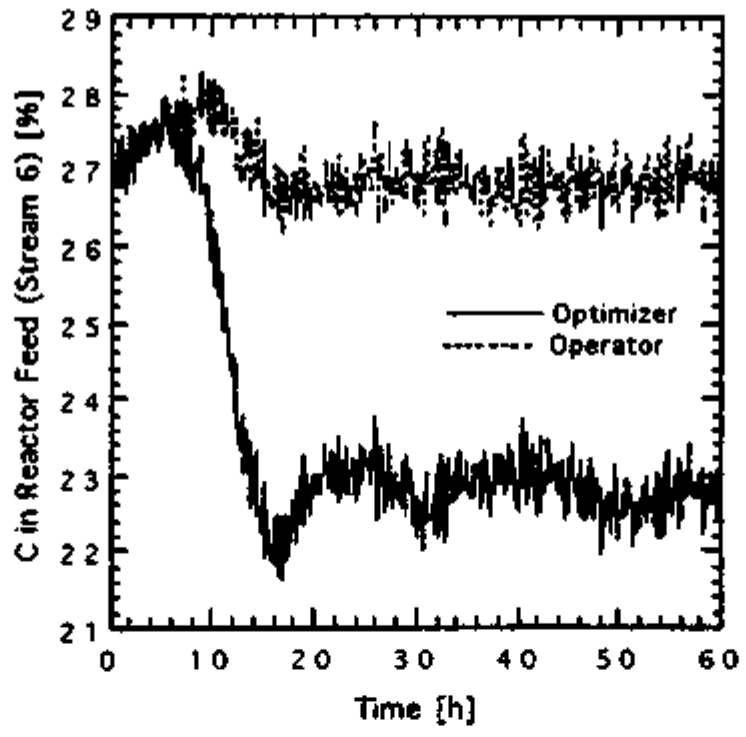

(b)

Figure 10.2. Mode 5 (Maximum Production) for Optimizer Versus Operator. (a) %A in Stream 6. (b) %C in Stream 6.

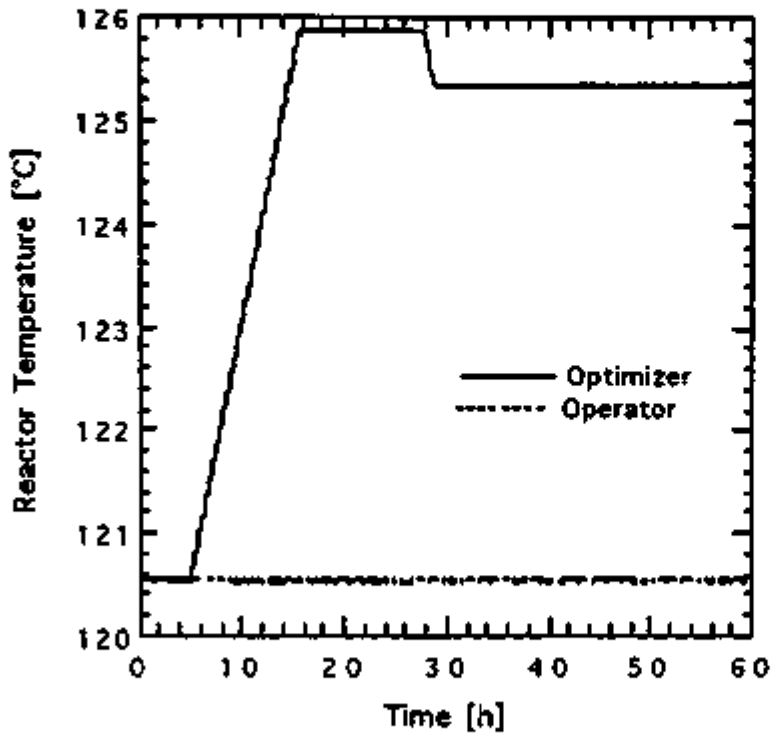

(c)

Figure 10.2. Continued. (c) Reactor Temperature.

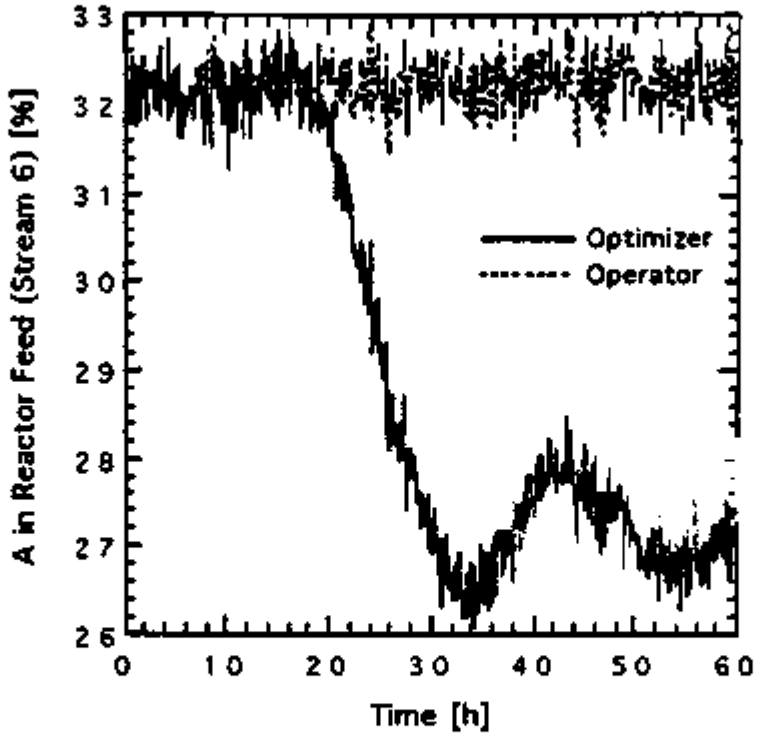

(a)

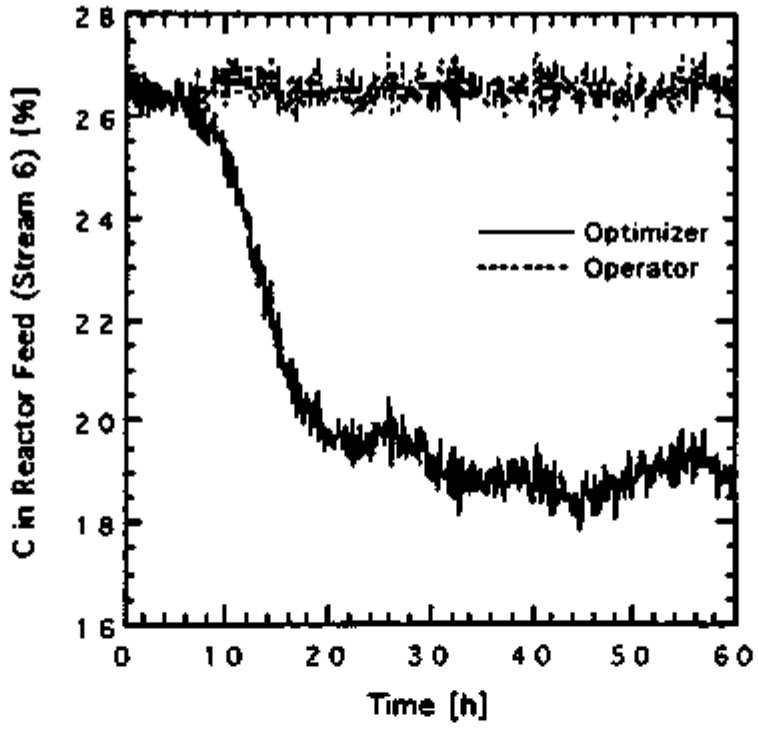

(b)

Figure 10.3. Mode 6 (Maximum Production) for Optimizer Versus Operator. (a) %A in Stream 6. (b) %C in Stream 6.

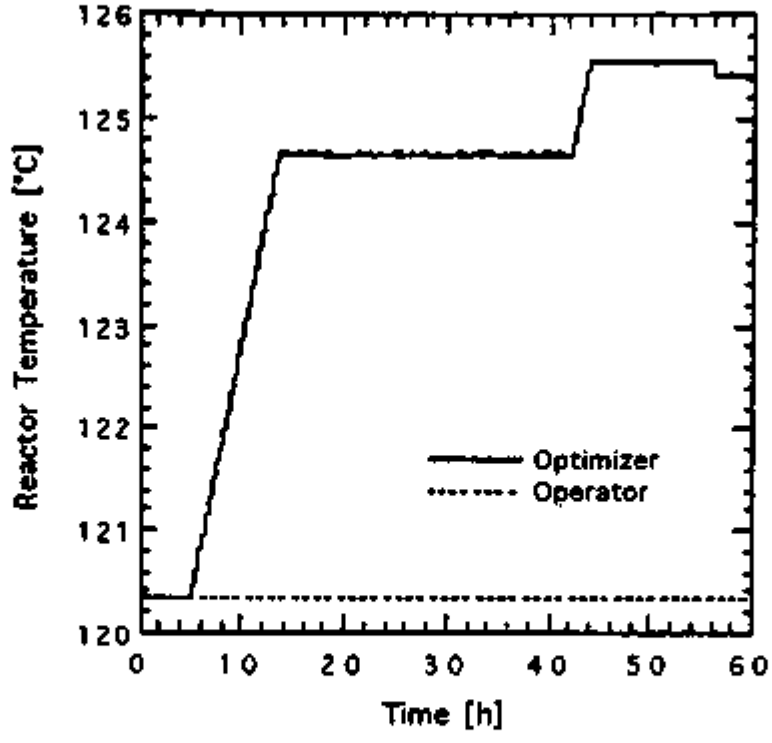

(c)

Figure 10.3. Continued. (c) Reactor Temperature.

For Mode 4 the operator controlled setpoints required the reactor level override (i.e., recycle valve) to be used to maintain the reactor level setpoint. Thus to control the process, the recycle valve setpoint was decreased to about 3%, which was near the optimizer setpoint of 1%. Due to the good process control design on a key control variable, the recycle valve position was automatically placed close to the optimal operating condition setpoint for Mode 4.

For Mode 6, the maximum production rate was the same for both the optimizer and operator control of the process. Thus, the increase in net profit was due to the decrease in purge operating cost, only.

10.2.6. Disturbance Effects on Modes 4 to 6

While some of the disturbances such as Disturbance 6, 8, and 13 described in Table 3.2 tended to increase operating costs for Modes 1 to 3 for both the operator and optimizer control of the process, the optimizer results continually achieved a lower total operating cost when compared to the operator total operating cost. By adjusting the A and C ratio in the reactor feed, adjusting the reactor temperature, and adjusting the recycle valve position, the optimizer was able to minimize costs during disturbances for Modes 1 to 3. However for Modes 4 to 6, disturbances tended to have a greater impact on production rate and net profit.

The previous results showed that the production rate and net profit for Mode 4 would be increased by 5.88 MM $/yr when the optimizer was used. However, disturbances were not used in the above optimization studies. Plants typically operate at maximum production with and without process disturbances so the effect of disturbances on process operation was examined for Modes 4 to 6. Disturbances were used to see if the increases in production rate and net profit would still be maintained, making the on-line optimizer worth implementing. The following results for Mode 4 with disturbances were typical results for Modes 4 to 6.

Only Disturbances 6 and 8 from Table 3.2 had an effect on the maximum production rate and net profit. During all of the other disturbances, the on-line optimizer was able to achieve the production rate and net profit results similiar to Table 10.10.

10.2.6.1. Disturbance 6. Disturbance 6 was the loss of A feed to the reactor. Figure 10.4 shows the effect of Disturbance 6 on total operating cost and key controlled variables for optimizer and operator control. At 5 hours the process was moved towards maximum production for Mode 4 for both the optimizer control and operator control. At 30 hours Disturbance 6 was introduced and remained active for the rest of the simulation. Without Disturbance 6, the process would have moved to the maximum production conditions for Mode 4 discussed in the previous section.

Disturbance 6 resulted in a large reduction in the product rate for both the optimizer and operator control. The production rate was reduced via the high reactor pressure override as the reactor pressure reached 2950 kPa. Thus, production was constrained to about 22.5 m^3/h because component A became the limiting reactant. Normally, D or E was the limiting reactant. With A as the limiting reactant, the optimizer was able to determine new operating conditions which reduced the total operating costs a further 80 $/h when compared to the operator control. Net profit and product profit plots were not provided for this disturbance since production was constrained.

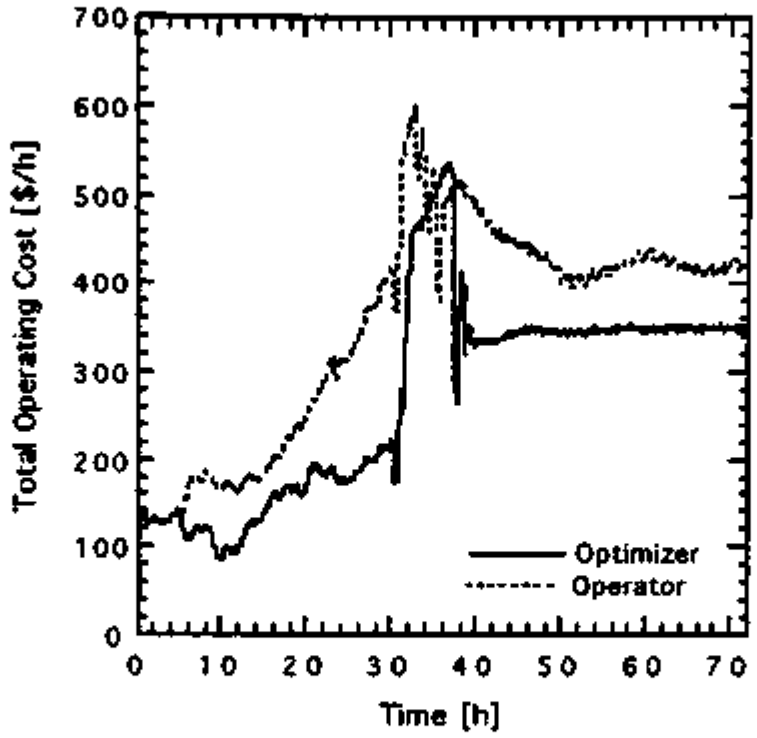

(a)

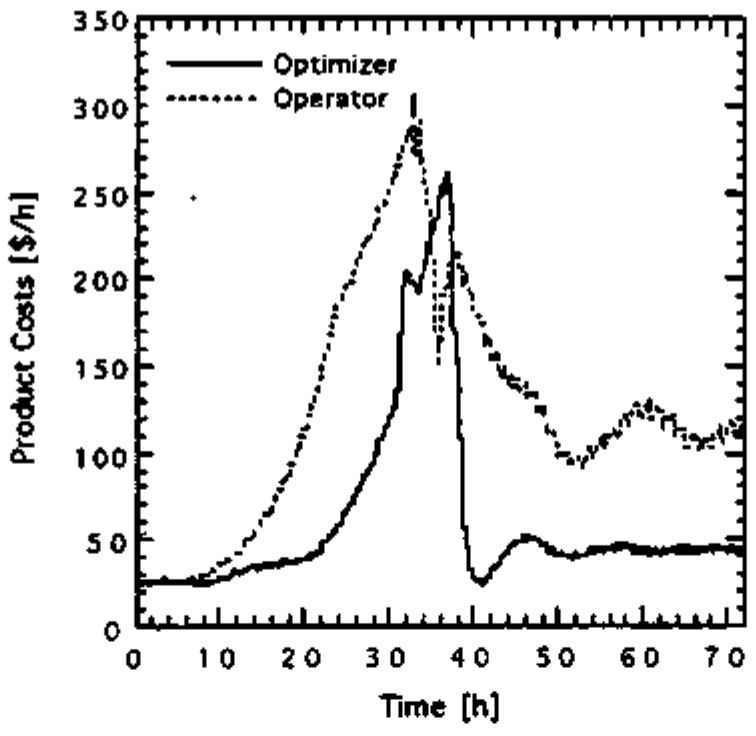

(b)

Figure 10.4. Mode 4 (Maximum Production) with Disturbance 6. (a) Total Operating Cost (b) Product Cost.

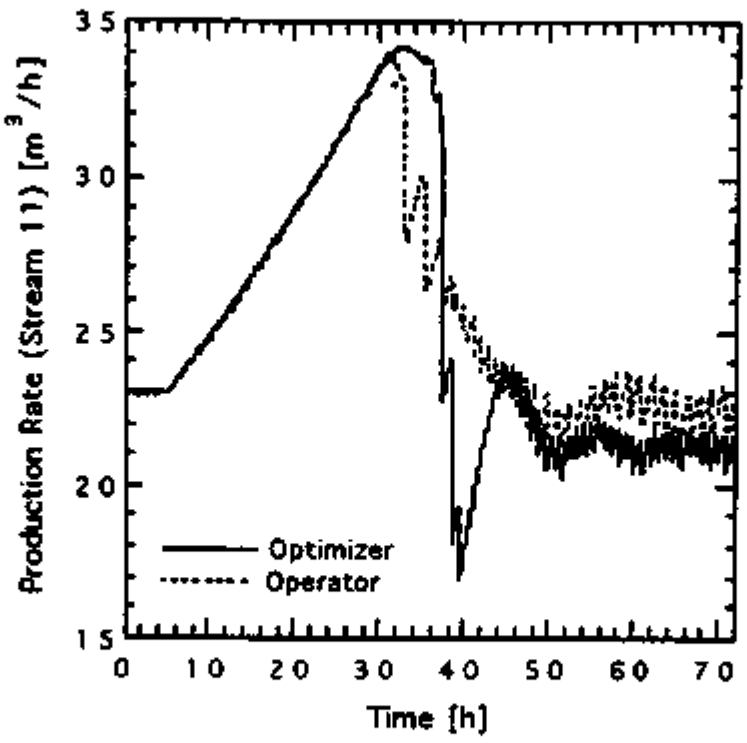

(c)

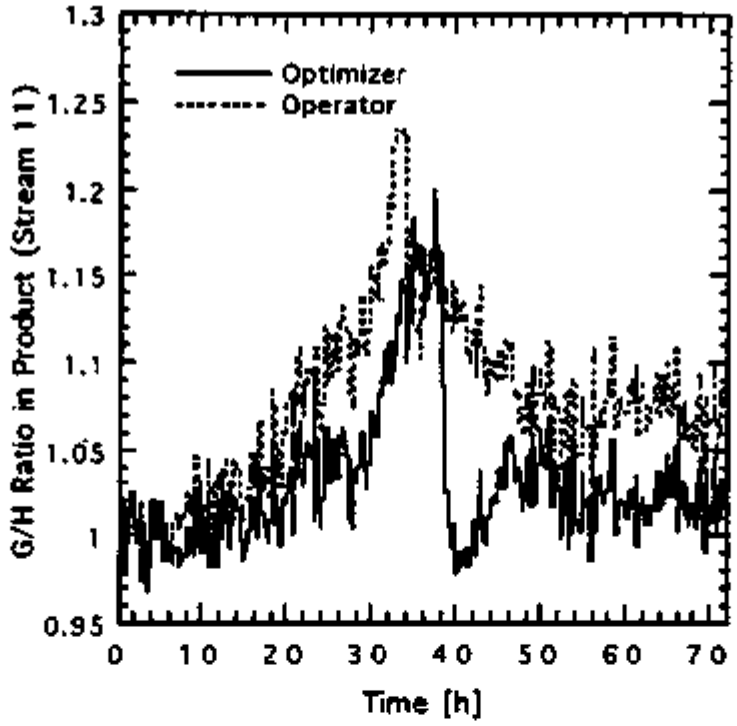

(d)

Figure 10.4. Continued. (c) Production Rate. (d) G/H Ratio in Product.

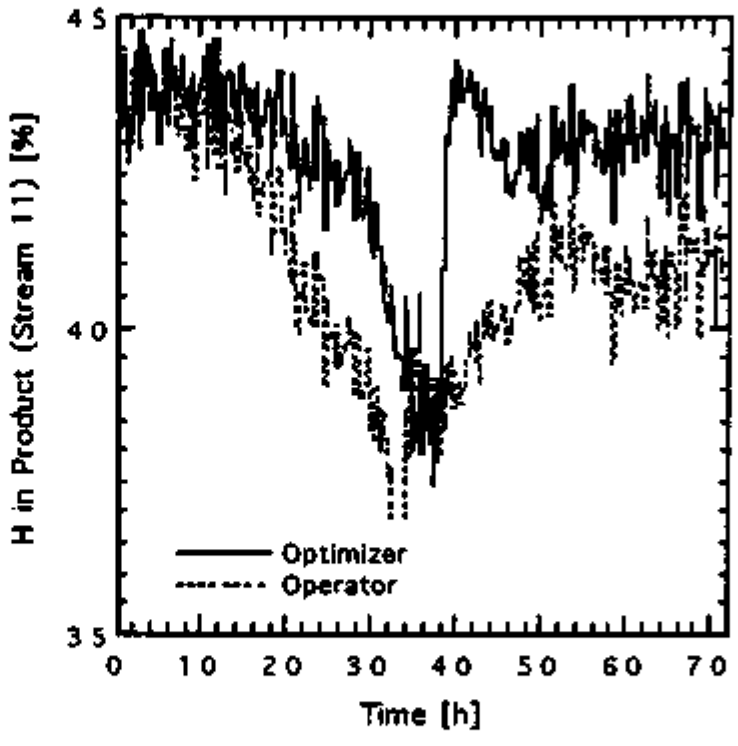

(e)

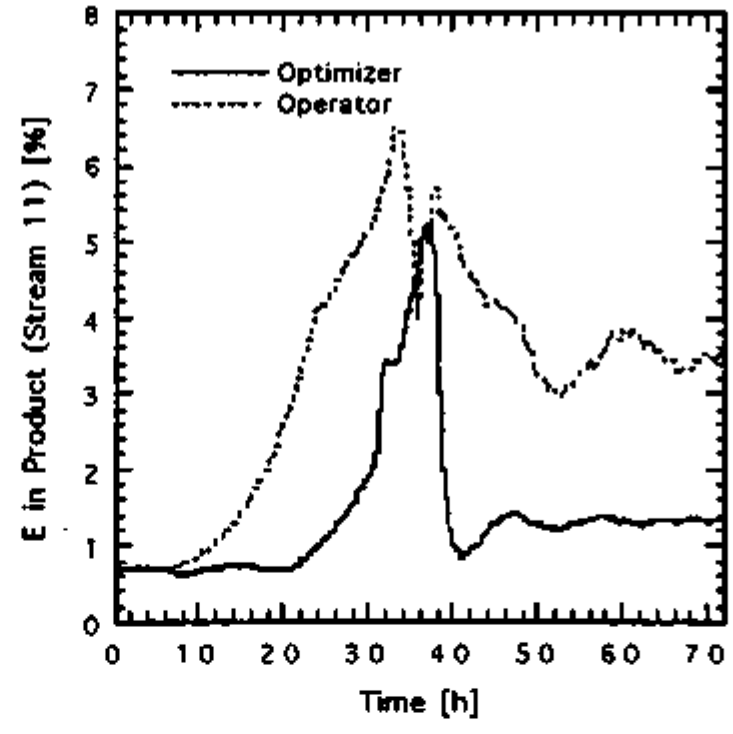

(f)

Figure 10.4. Continued. (e) H in Product. (f) E in Product.

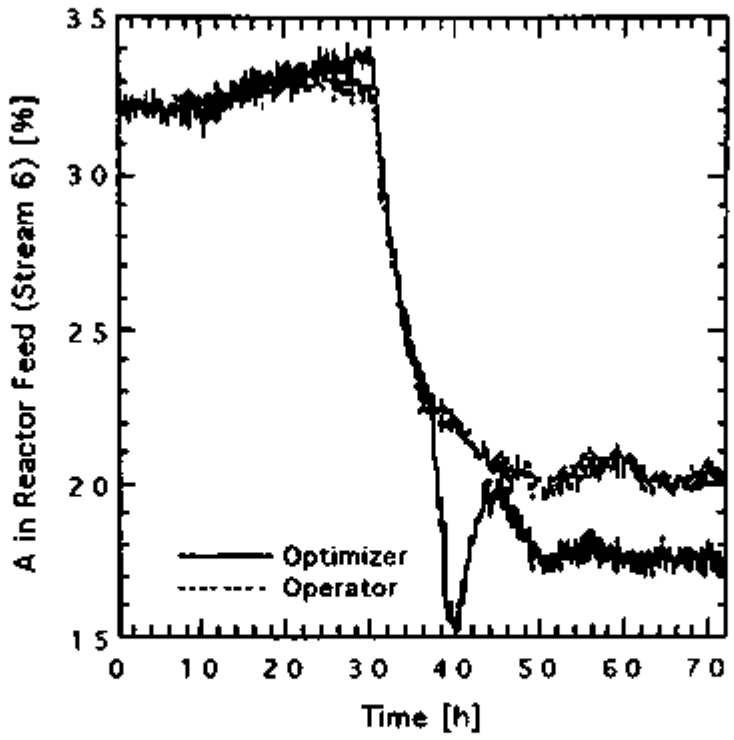

(g)

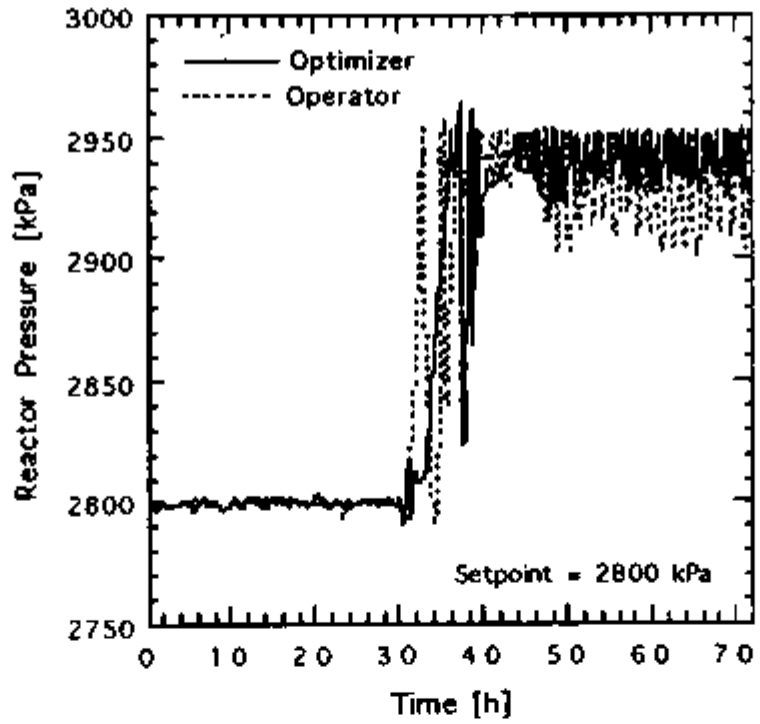

(h)

Figure 10.4. Continued. (g) A in Reactor Feed. (h) Reactor Pressure.

Even though less A was available, the optimizer required a further reduction in the percentage of A in the feed over the operator control to minimize the total operating costs. The steam use was at 1% (i.e., not used) while the recycle valve position was set at about 22% from the optimization. The optimal recycle valve position without disturbances was 1%. The higher compression costs offset the decreased cost of steam use for Disturbance 6.

The operator control seemed to yield more production during the disturbance. However, the G/H ratio was not on target (i.e., 1.00), even 40 hours after the disturbance started, for operator control. While the %G in the product was at setpoint (53.83%), less H and more E were recovered in the product. As a result of the off-specification G/H ratio in the product for operator control, the downstream refining cost would be higher, especially during such a long disturbance.

To correct the problem in the G/H ratio, the operator would need to know that the loss of A feed occurred (i.e., via alarm) and would have to manually adjust the setpoint of %G in the product to maintain the proper G/H ratio in the product. When the disturbance was over, the operator would have to reset the proper %G setpoint again. However, the optimizer automatically corrected process operating conditions to produce the proper G/H ratio without modifying the %G setpoint and lowered the total operating cost simultaneously. While the alarm for A feed loss would still be

required to indicate a feed problem, the operator would not have to make process adjustments to correct the G/H ratio.

10.2.6.2. Disturbance 13. Disturbance 13 was a high frequency drift in the reaction kinetics. Figure 10.5 shows the effect of Disturbance 6 on profit, operating costs, and key controlled variables for optimizer and operator control. At 5 hours the process was moved towards maximum production for Mode 4 for both the optimizer control and operator control. At 30 hours Disturbance 13 was introduced and remained active for the rest of the simulation. Without Disturbance 13, the process would have moved to the maximum production conditions for Mode 4 discussed in the previous section.

Production rate was not constrained for Disturbance 13. However, high reactor pressure caused the reactor pressure override to reduce the production rate under operator control. The override was not required for the chosen optimizer controller setpoints resulting in a higher maximum production rate. The optimizer was also able to decrease the total operating cost by an average of 200 $/h by decreasing the product operating cost. The continual shifts in total operating cost were due to the continual changes in the purge rate to control the reactor pressure at setpoint. With the higher production rate and lower operating cost, the net profit during the disturbance was 700 $/h, on average, higher for optimizer control over the operator control. These values were similar to the optimal results without disturbances in the previous section.

More importantly though, the optimizer maintained the G/H ratio in the product (desired was 1.00) to a better degree than the operator control. Without the on-line optimizer, operator intervention would have been required to maintain the proper G/H ratio in the product. A higher stripper temperature was required to decrease the amount of E and increase the amount of H in the product to maintain the proper G/H ratio. Steam use and cost were reduced but not eliminated by the optimizer. The use of steam combined with a higher reactor temperature (at its upper bound of 130°C) maintained the required higher stripper temperature. Even though more by-product was present in the product stream, the decrease in product cost due to less E in the product was more than enough to offset the product cost increase due to more F in the product.

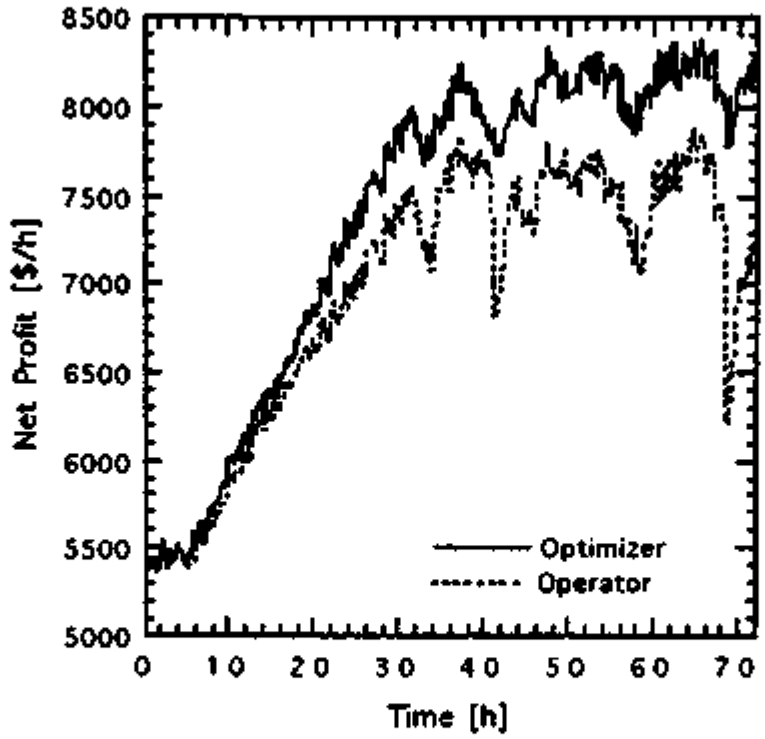

(a)

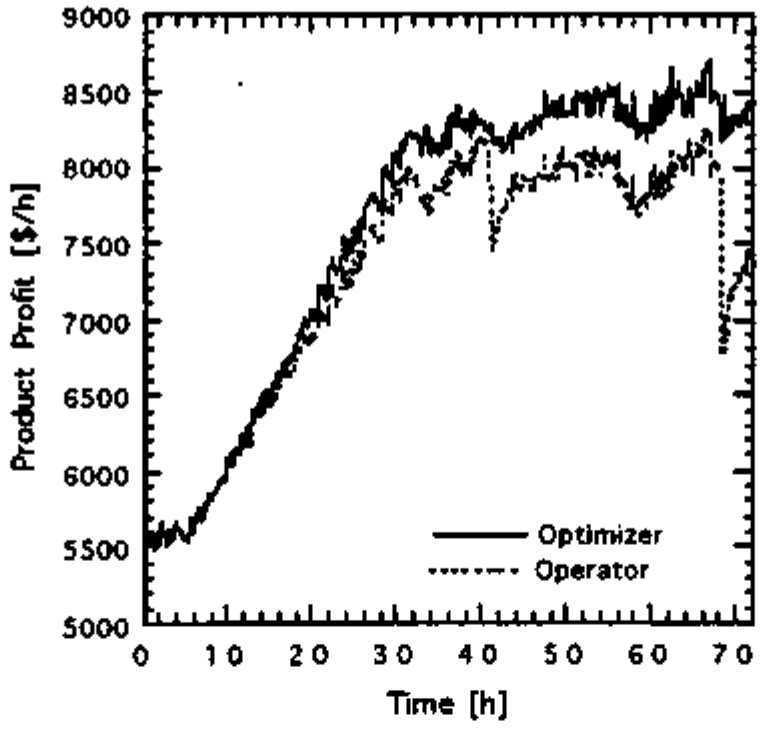

(b)

Figure 10.5. Mode 4 (Maximum Production) with Disturbance 13. (a) Net Profit. (b) Product Profit.

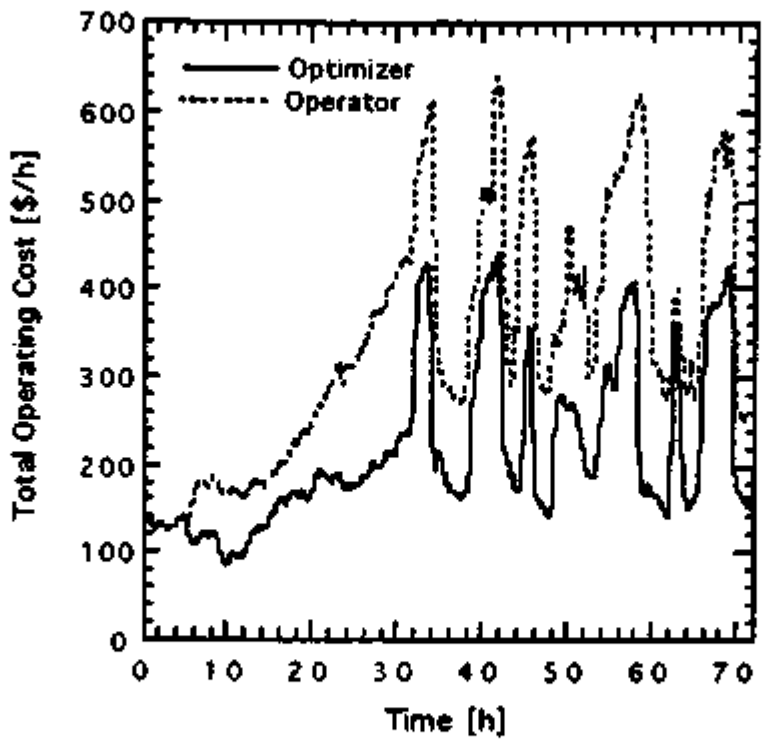

(c)

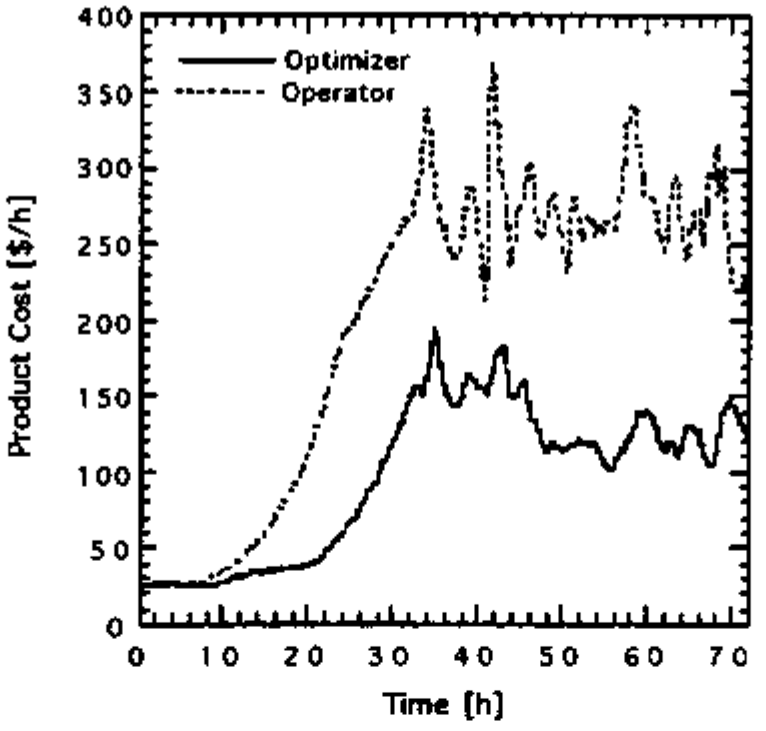

(d)

Figure 10.5. Continued. (c) Total Operating Cost. (d) Product Cost.

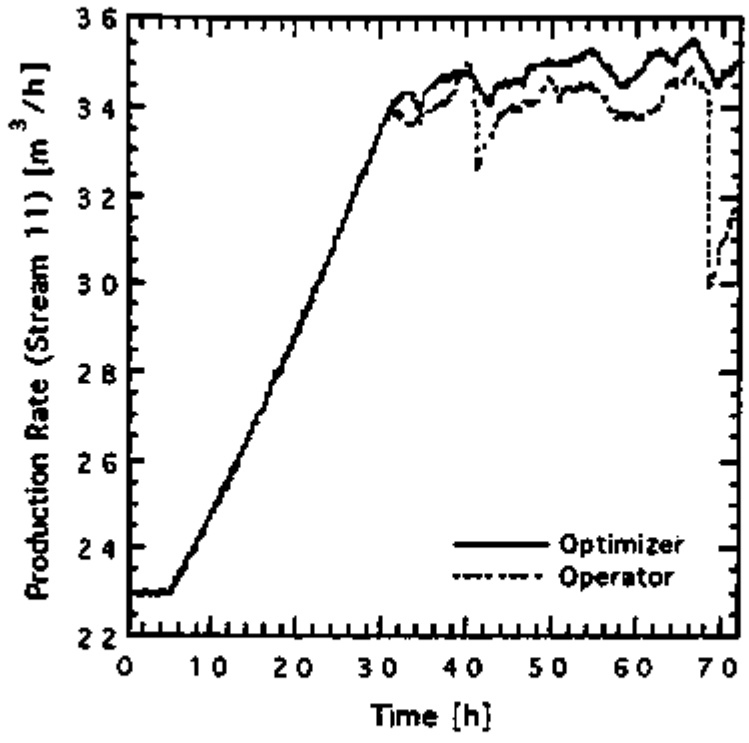

(e)

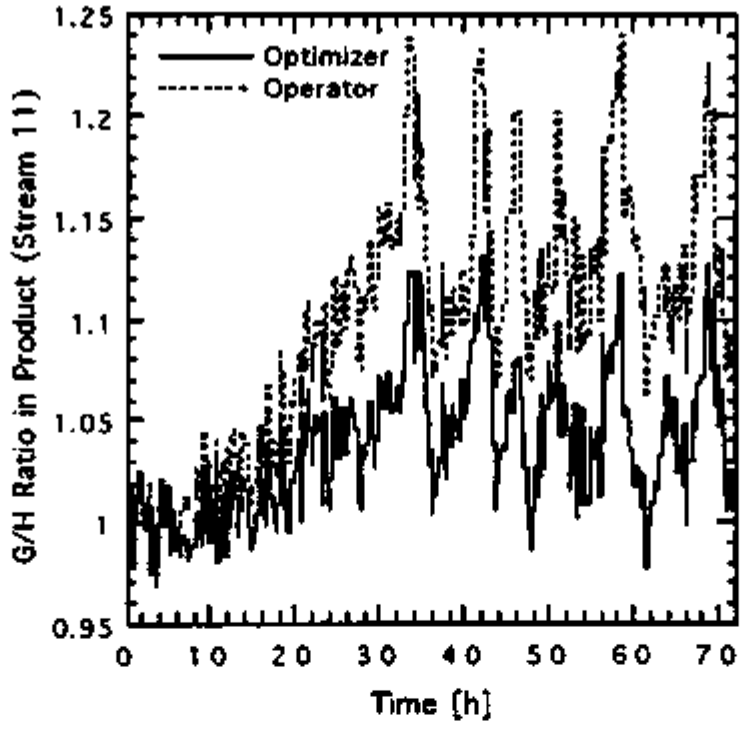

(f)

Figure 10.5. Continued. (e) Production Rate. (f) G/H Ratio in Product.

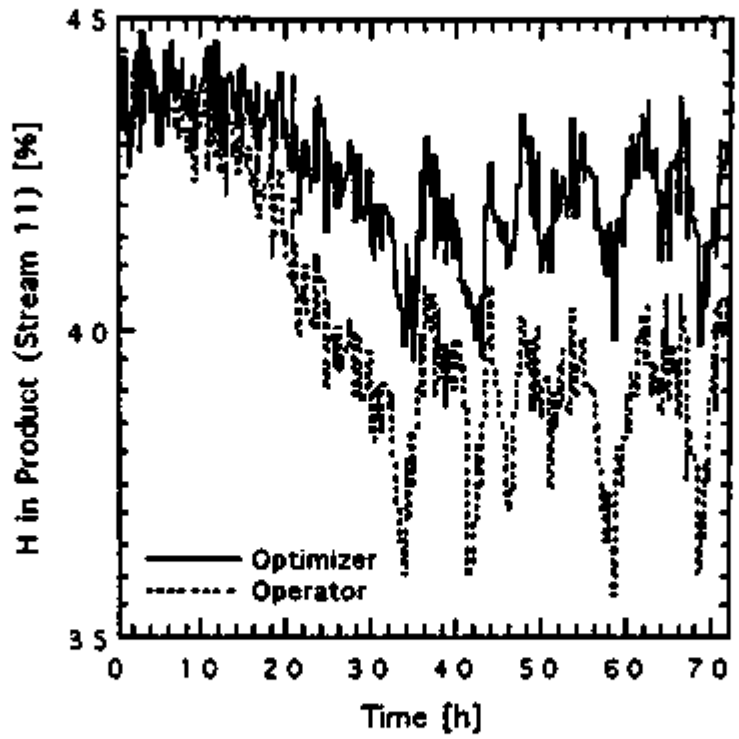

(g)

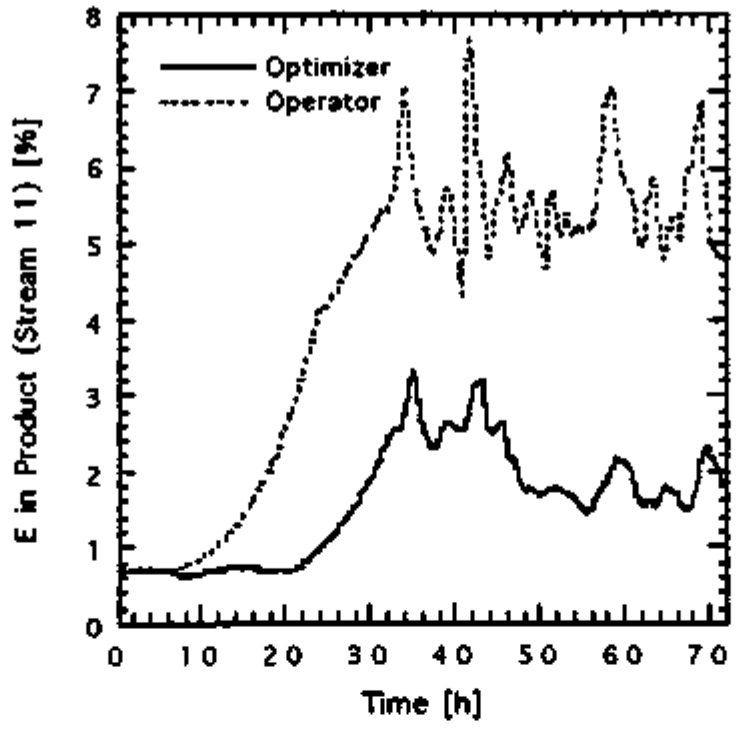

(h)

Figure 10.5. Continued. (g) %H in Product. (h) %E in Product.

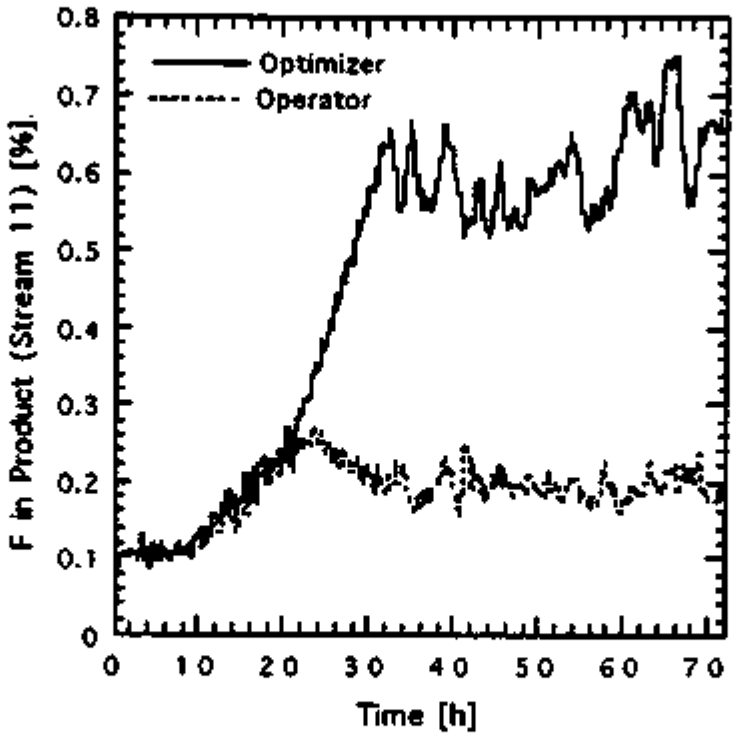

(i)

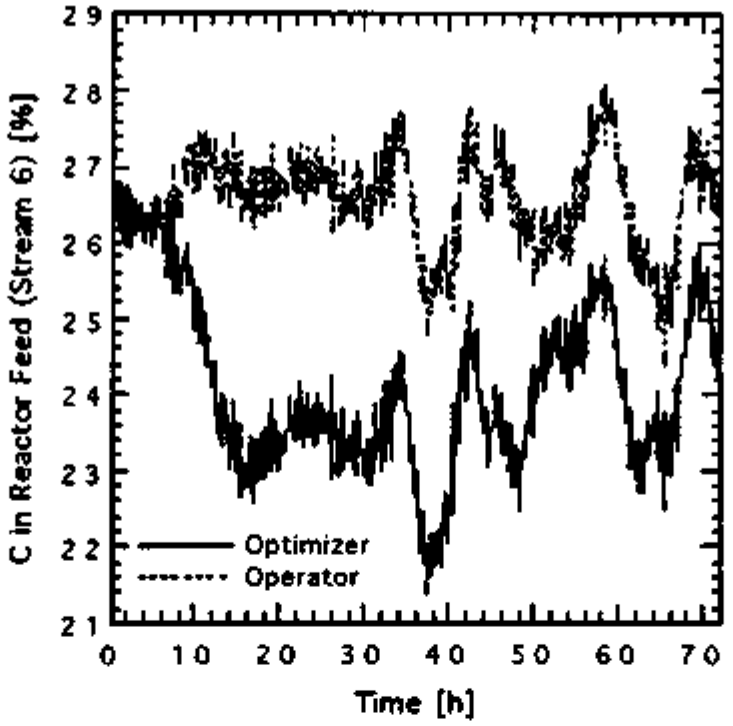

(j)

Figure 10.5. Continued. (i) %F in Product. (j) %C in Reactor Feed.

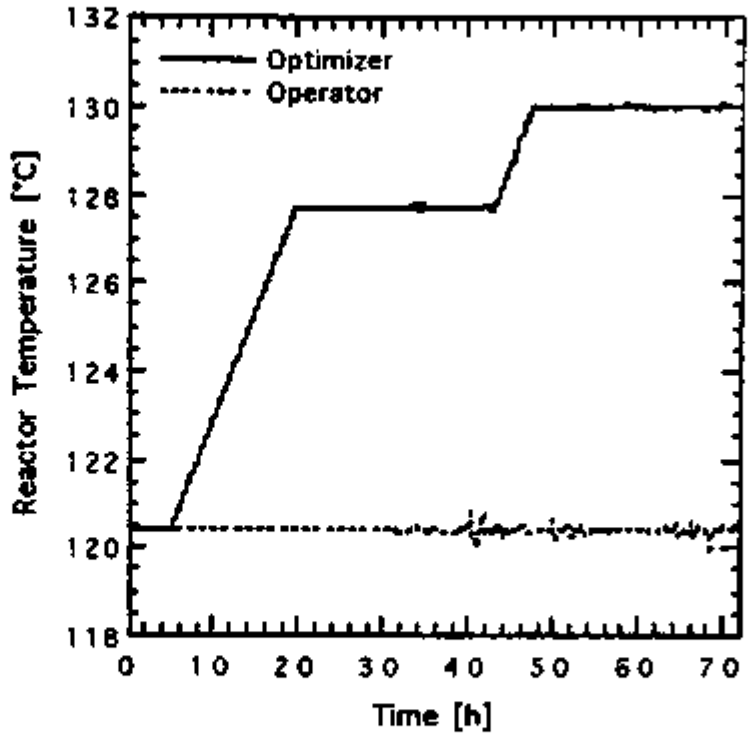

(k)

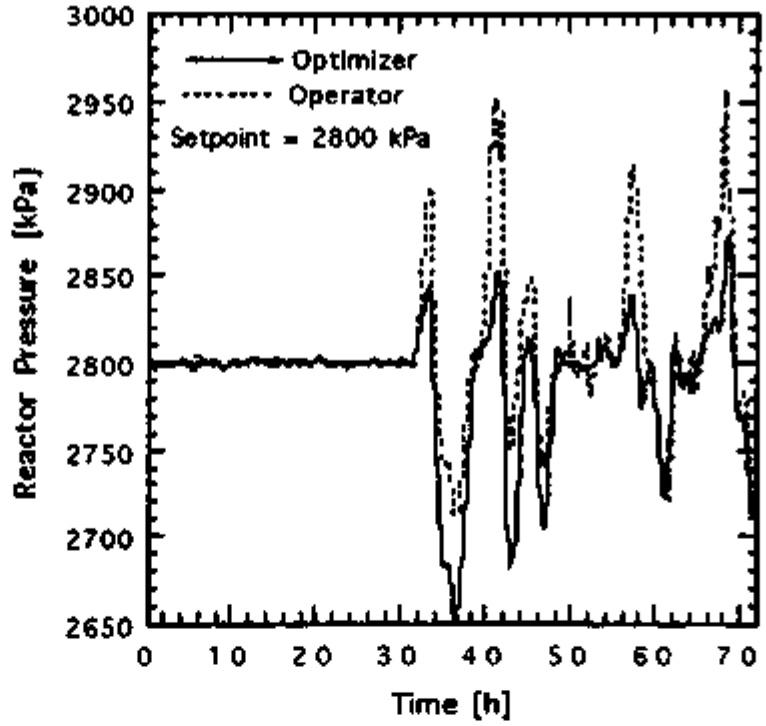

(l)

Figure 10.5. Continued. (k) Reactor Temperature. (l) Reactor Pressure.

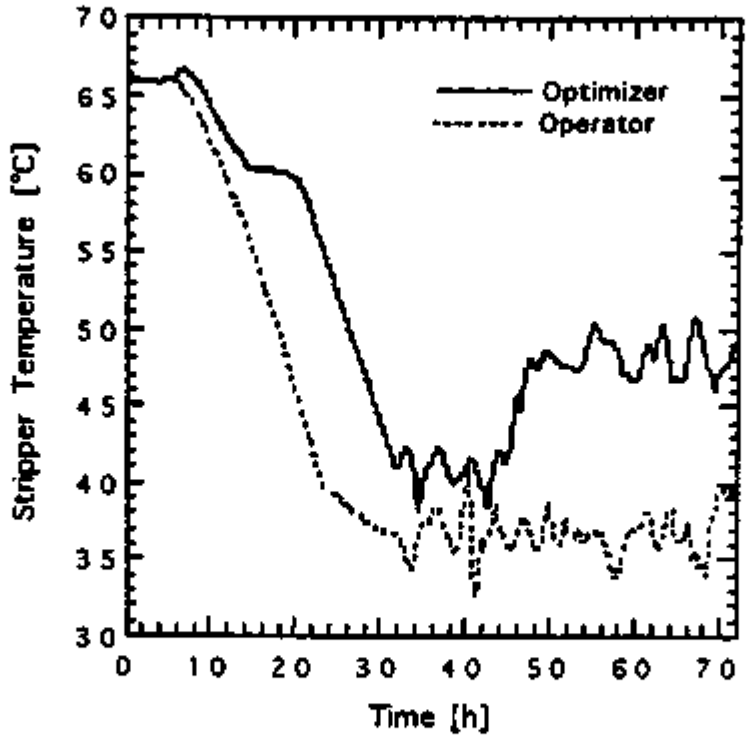

(m)

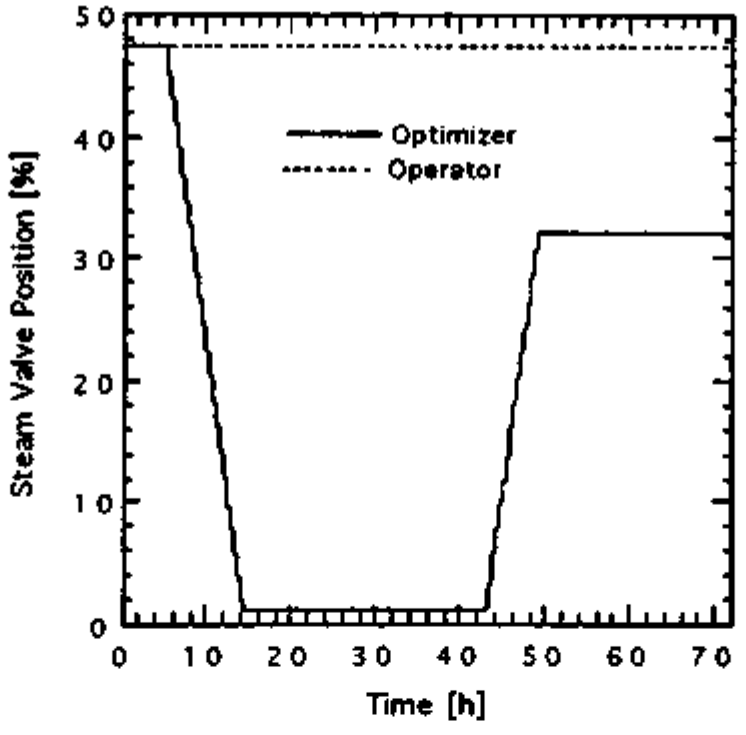

(n)

Figure 10.5. Continued. (m) Stripper Temperature. (n) Steam Valve Position.

CHAPTER 11
CONCLUSIONS AND RECOMMENDATIONS

The scope of this research was to determine the benefits, if any, of using on-line optimization on the TE process. A steady state, model-based, on-line optimization algorithm was developed and implemented to determine the optimal operating conditions for the six modes of operation in the TE process. A successive, quadratic programming algorithm was combined with Singular Value Decomposition to converge the steady state model of the process while determining the optimal operating conditions. A step-size doubling and interval halving method was used to determine the maximum production rates and optimal operating conditions for each product grade without having to move to intermediate product rates.

Even with significant process/model objective gradient gain mismatch (i.e., 25% in gain prediction or less), the model-based optimization was able to approach the optimal operating conditions, which Ricker calculated using full knowledge of the states and derivatives, for the TE process for both fixed and maximum production rates. These results tended to indicate that the objective function is relatively broad and flat, especially around the optimal objective function value.

Through process observation, the operator would be able to determine *a priori* optimal setpoints for certain process variables such as reactor pressure, reactor level, and agitator speed. The

standard operating procedure would include operating at these optimal setpoints. However, other process variables such as %A and %C in the reactor feed, reactor temperature, steam use, and recycle valve position which greatly affect the operating costs and maximum production rate do not have *a priori* optimal setpoints.

Using the on-line optimizer, the optimal setpoints for the current process conditions which reduced operating costs and maximized production were calculated. The use of net profit as a tool for the evaluation of optimizer effectiveness for different production rates was introduced. Net profit, production rate, total operating cost, and key controlled variables were compared for on-line optimization versus operator control of the process.

For normal plant operation at maximum production using the optimizer, steam was not required (i.e., set to 1%). The recycle valve position was usually set at 1% as well. Optimal reactor temperature varied between 125°C to 128°C. The %A and %C setpoints in the reactor feed were also varied, but no clear optimal setpoint can be recommended. As a result of these changes in the process operating conditions, the maximum production rate for Modes 4 and 5 using the optimizer were increased by 1.5 and 0.4 m^3/h resulting in a net profit increase of 700 and 220 \$/h, respectively. The net profit change of 26 \$/h for Mode 6 was due solely to a decrease in total operating cost. While the objective function tended to be broad and flat around the optimal operating conditions, using on-line optimization to determine the setpoints for key process conditions

(i.e., the amount of excess reactants in the reactor feed) further reduced operating costs and increased production rate enough to justify the use of on-line process optimization.

Most disturbances do not affect the maximum production and net profit of the process for Modes 4 to 6. Two disturbances, loss of A feed (#6) and drift in reaction kinetics (#13), resulted in significant changes in the optimal operating setpoints for reactor temperature, steam use, and recycle valve position in order to maximize production rate and net profit while maintaining the desired G/H ratio in the product. Disturbances tended to shift the G/H ratio in the product away from setpoint under operator control. The product grade shift under operator control resulted in higher operating costs and was due primarily to the poor controller setpoint selections that kept the process oeprating in a less stable operating region. For example, the reactor pressure override was required to maintain process control during Disturbance 6 for the operator chosen controller setpoints but not for optimizer chosen controller setpoints. The optimizer correctly adjusted process conditions to maintain the desired G/H ratio during disturbances.

11.1. Recommendations

Use of an on-line optimizer is recommended to minimize the effects of disturbances on G/H product ratio by operating the process in a more stable operating region. More information on the frequency and duration of disturbances is required to further

evaluate the advantages of the on-line optimizer during disturbances. Standard operating procedures should be modified to include increasing reactor temperature between 4°C and 7°C and discontinuing steam use.

Using an optimization algorithm to increase maximum production rates and decrease operating costs is also recommended. The proper amount of %A and %C in the reactor feed was key to determining the optimal operating conditions for all six modes. Due to modeling errors, the optimizer consistently predicted higher setpoints for %A and %C (i.e., higher by 2 to 4 mol%) in the reactor feed than determined by Ricker (1995b) which increased purge costs. These errors should be identified and eliminated to increase the effectiveness of the optimizer.

Currently, 14 hours are required to move between consecutive product grades without violating the variability constraints imposed by Downs and Vogel (1993). Decoupler and process model-based controller implementation could lead to a reduction in the product grade change time while staying within the process variability constraints. The models developed in this research would provide a good starting point for process model based control analysis. The decentralized control scheme suggested by Ricker (1995b) should be modified to control G / H mass ratio in the product instead of %G in product. During some disturbances (i.e., #6 and #13), the product ratio of G/H was moved off specification (i.e., 1.00 for Mode 4) due to a decrease in the amount of H in the product, even though %G in

the product remained at setpoint. Modifications to the decentralized control scheme which control the G/H ratio should minimize the time off specification product is produced.

This research was one of the first attempts at steady state, model-based, on-line optimization of the TE process. The use of net profit as an evaluation tool for different production rates was a new concept introduced. Future research on on-line optimization of the TE process should make similar profit comparisons when determining the effectiveness of an optimization algorithm especially when simplifications in the model-based optimizer are made, or when maximum production rates are different.

REFERENCES

Adebekun K., Output Feedback Control of a Stirred Tank Reactor, *Computers andChemical Engineering* 20, 1017-1021 (1996).

Banerjee A. and Y. Arkun, Control Configuration Design Applied to the Tennessee Eastman Plant-Wide Control Problem, *Computers and Chemical Engineering* 19, 453-480 (1995).

Baughman D. R. and Y. A. Liu, *Neural Networks in Bioprocessing and Chemical Engineering*, Chap. 5, Academic Press, San Diego, CA (1995).

Danckwerts P. V., *Gas-Liquid Reactions*, McGraw-Hill, New York (1970).

Downs J. J. and E. F. Vogel, A Plant-Wide Industrial Process Control Problem, *Computers and Chemical Engineering* 17, 245-255 (1993).

Forbes J. F. and T. E. Marlin, Design Cost: A Systematic Approach to Technology Selection for Model-Based Real-Time Optimization Systems, *Computers and Chemical Engineering* 20, 717-734 (1996).

Froment G. F. and K. B. Bischoff, *Chemical Reactor Analysis and Design*, 2nd ed., John Wiley & Sons, New York (1990).

Gill P.E. et al., *User's Guide for NPSOL: A Fortran Package for Nonlinear Programming*, Technical Report SOL 86-2, Stanford University, CA (1986).

Hines A. L. and R. N. Maddox, *Mass Transfer: Fundamentals and Applications*, Chap. 8, Prentice-Hall, Englewood Cliffs, NJ (1985).

Holland C. D. and Anthony R. G., *Fundamentals of Chemical Reaction Engineering*, Prentice-Hall, Englewood Cliffs, NJ (1989).

Kanadibhotla R. S., *Nonlinear Model Based Control of a Recycle Reactor Process*, Master's Thesis, Department of Chemical Engineering, Texas Tech University, Lubbock, TX (1992).

Kanadibhotla R. S. and J. B. Riggs, Nonlinear Model Based Control of a Recycle Reactor Process, *Computers and Chemical Engineering* 19, 933 - 948 (1995).

Lyman P. R. and C. Georgakis, Plant-Wide Control of the Tennessee Eastman Problem, *Computers and Chemical Engineering* 19, 321-331 (1995).

Marlin T. E. and A. N. Hrymak, Real-Time Operations Optimization of Continuous Processes, Presented at CPC IV in Lake Tahoe, CA (January 1996).

McAvoy T. J. et al., *An Improved Base Control for the Tennessee Eastman Problem*, Presented at the American Control Conference, Seattle, Washington (June 1995).

McAvoy T. J. and N. Ye, Base Control for the Tennessee Eastman Problem, *Computers and Chemical Engineering* 18, 383-413 (1994).

Paulo A. F. et al., Model Predictive Control of a Pilot Plant Reactor with Simulated Exothermic Reaction, *Computers and Chemical Engineering* 20, S769-S774 (1996).

Press W. H. et al., *Numerical Recipes in FORTRAN*, 2nd ed., Chap. 9, Cambridge University Press, Cambridge (1992).

Rahman A. K. M. S. and S. Palanki, On-Line Optimization of Batch Reactors with Two Manipulated Inputs, *Computers and Chemical Engineering* 20, S1023-S1028 (1996).

Ricker N. L., Decentralized Control of the Tennessee Eastman Challenge Process, *Journal of Process Control* 6, 205-221 (1996).

Ricker N. L., Model Predictive Control of a Continuous, Nonlinear, Two-Phase Reactor, *Journal of Process Control* 3, 109-123 (1993).

Ricker N. L. and J. H. Lee, Nonlinear Model Predictive Control of the Tennessee Eastman Challenge Process, *Computers and Chemical Engineering* 19, 961-981 (1995a).

Ricker N. L. and J. H. Lee, Nonlinear Modeling and State Estimation for the Tennessee Eastman Challenge Process, *Computers and Chemical Engineering* 19, 983-1005 (1995b).

Ricker N. L., Optimal Operation and Control of the Tennessee Eastman Industrial Challenge Process, Proceedings from the 2nd International Conference on Industrial Automation, 625-630 (1995a).

Ricker N. L., Optimal Steady-State Operation of the Tennessee Eastman Challenge Process, *Computers and Chemical Engineering* 19, 949-959 (1995b).

Riggs J. B., *An Introduction to Numerical Methods for Chemical Engineers* , 2nd ed., Chap. 6, Texas Tech University Press, Lubbock, TX (1994).

Riggs J. B. and R. R. Rhinehart, *A Review of Nonlinear Approximate Models for Process Control and Optimization*, Presented at the AIChE Annual Meeting, San Francisco, California (1989).

Seborg D. E. et al, *Process Dynamics and Control*, John Wiley and Sons, New York (1989).

Schenker B. and M. Agarwal, Prediction of Infrequently Measurable Quantities in Poorly Modelled Processes, *Journal of Process Control* 5, 329-339 (1995).

Smith J. M. and H. C. Van Ness, *Introduction to Chemical Engineering Thermodynamics*, Chap. 7, McGraw-Hill, New York (1987).

Vinson D. R. et al., Studies in Plant-Wide Controllability Using the Tennessee Eastman Challenge Problem: The Case of Multivariable Control, Presented at the American Control Conference, Seattle, Washington (June 1995).

Yan M. and N. L. Ricker, Multi-Objective Control of the Tennessee Eastman Challenge Process, Presented at the American Control Conference, Seattle, Washington (June 1995).

APPENDIX: STEADY STATE MODEL DATA SETS

Table A.1. Steady State Reactor Model Data

Mode	L_R (%)	T_R (°C)	P_R (kPa)	R_1 (lbmol/hr)	R_2 (lbmol/hr)	R_3 (lbmol/hr)	R_4 (lbmol/hr)
1	75.004	120.4000	2704.9978	252.2012	205.1544	1.1377	5.296×10^{-2}
1	65.0010	120.4010	2600.0037	252.1599	205.2959	1.1666	5.4264×10^{-2}
2	75.003	120.5356	2799.9879	50.3193	370.2599	2.0191	1.0299×10^{-2}
2	75.001	120.5356	2800.0013	49.7239	364.6888	1.9874	1.0171×10^{-2}
3	75.1109	115.001	2705.001	395.0529	36.0412	9.577×10^{-2}	5.674×10^{-2}
3	75.1139	124.995	2600.111	395.5150	36.4127	0.3679	0.1126

Table A.1. Continued

Mode	x_{6A} (%)	x_{6C} (%)	x_{6D} (%)	x_{6E} (%)	F_6 (kscmh)
1	32.1903	26.3849	6.8957	18.8160	42.3576
1	32.1831	26.3804	7.0301	19.0882	41.4931
2	31.8516	26.7561	1.3796	30.0761	41.2432
2	31.8393	26.7453	1.3872	31.6271	40.8709
3	32.2387	26.4681	11.5189	4.2217	45.1975
3	32.2245	26.4598	10.3784	2.8876	41.9791

Table A.2. Steady State Compressor Model Data

Run	T_{Sep} (°C)	P_{Sep} (kPa)	P_{Str} (kPa)	F_8 (kscmh)	v15 (%)	W_{Com} (kW)
1	88.714	2509.352	3095.433	30.425	1.0	265.847
2	80.353	2531.728	2972.961	25.216	25.0	335.633
3	71.385	2544.942	2901.595	21.768	42.764	330.650
4	88.041	2611.697	3215.749	31.807	1.0	275.037
5	79.391	2635.106	3081.103	26.331	25.0	342.925
6	88.805	2756.602	3033.493	22.084	62.333	304.375

Table A.3. Steady State Stripper Model Data

Run	x_{11D} (%)	x_{11E} (%)	x_{11F} (%)	x_{11G} (%)	x_{11H} (%)	T_{Str} (°C)	F_{10} (m^3/h)
1	1.805×10^{-2}	0.845	9.903×10^{-2}	53.742	43.818	65.588	25.160
2	2.196×10^{-2}	1.027	0.111	53.722	43.625	57.951	25.154
3	1.935×10^{-2}	0.905	0.103	53.724	43.754	62.814	25.204
4	1.609×10^{-2}	0.753	9.234×10^{-2}	53.726	40.188	70.340	25.268
5	0.1323	5.5126	0.228	53.735	38.986	42.688	30.682
6	6.568×10^{-3}	0.307	2.944×10^{-2}	53.733	44.344	74.998	23.306

Table A.3. Continued

Run	x10D (%)	x10E (%)	x10F (%)	x10G (%)	x10H (%)	F11 (m^3/hr)	$\frac{F_4}{F_{10}}$
1	0.223	13.782	1.668	47.226	37.100	22.949	1.606
2	0.226	13.878	1.548	47.186	37.162	23.001	1.624
3	0.224	13.822	1.629	47.203	37.124	23.011	1.613
4	0.222	13.702	1.736	47.284	37.055	22.998	1.592
5	0.588	32.157	1.344	38.801	27.744	22.995	1.289
6	0.121	7.471	0.740	51.412	40.2562	22.974	1.796

PERMISSION TO COPY

In presenting this thesis in partial fulfillment of the requirements for a master's degree at Texas Tech University or Texas Tech University Health Sciences Center, I agree that the Library and my major department shall make it freely available for research purposes. Permission to copy this thesis for scholarly purposes may be granted by the Director of the Library or my major professor. It is understood that any copying or publication of this thesis for financial gain shall not be allowed without my further written permission and that any user may be liable for copyright infringement.

Agree (Permission is granted.)

Marshall Wade — 11-7-10

Student's Signature — Date

Disagree (Permission is not granted.)

Student's Signature — Date